CHARACTERIZATION OF P28, A NOVEL ERGIC/*CIS*-GOLGI PROTEIN, REQUIRED FOR GOLGI RIBBON FORMATION

PH MEASUREMENTS IN THE EARLY SECRETORY PATHWAY *IN VIVO*

Inauguraldissertation

zur
Erlangung der Würde eines Doktors der Philosophie
vorgelegt der
Philosophisch-Naturwissenschaftlichen Fakultät
der Universität Basel

von

Eva Jutta Kögler
aus Linz, Oberösterreich

Basel, 2008

Genehmigt von der Philosophisch-Naturwissenschaftlichen Fakultät
auf Antrag von

Prof. Dr. Hans-Peter Hauri and Prof. Dr. Martin Spiess

Basel, den 11. November 2008

Prof. Dr. Eberhard Parlow
(Dekan)

…dedicated to my parents and Lisa

Acknowledgements

I would like to thank Hans-Peter who gave me the opportunity to perform this study in his laboratory. He gave me freedom to develop the projects on my own.

I would like to thank my family and parents for supporting me throughout my studies at the university and during my PhD. Together with Lisa they were always there for me and helped me mentally. Further I would like to thank my grandmother and my uncle Fredi, they spoiled me a lot.

Besides my family, I would like to thank Ivan, who complements and enriches my life.

I am thankful for the nice colleagues and friends I had during the time in the Hauri laboratory.
Sandra, who always stimulates discussions;
Markus, who always cheers up people and with whom one can discuss amicable;
Beat, with whom I discussed a lot about science and also non-scientific stuff during lunch and coffee breaks; Thanks for your friendship.
Houchaima, who always finds a solution;
Veronika, an always helpful person and nice companion on weekends;
Hesso, who brings the Austrian “Schmäh” into the laboratory and is always up to date concerning science.
Karen, who likes the Thai-food as much as I do;
Carine, who reminds me of the optimistic view; every day she brings sunshine into the lab. Especially in the last months she helped and assisted me a lot when I was stressed for my “last” experiments. Thanks for your help and friendship.

Last but not least I am grateful for the support from Vinzenz, who is always there when I need him.

Table of contents

Summary

The secretory pathway of mammalian cells consists of several compartments. Transport between these organelles is accomplished via vesicular carriers or maturation. For non abundant proteins it is thought that transport receptors help the proteins to exit the ER in an effective way. The best characterized mammalian cargo receptor is ERGIC-53, which transports blood coagulation factor V and VIII, cathespin C and Z as well as alpha1-antitrypsin. It localizes to the ER Golgi intermediate compartment (ERGIC) at steady state, but cycles between the organelles of the early secretory pathway. In *S. cerevisiae* Emp24p, a member of the p24 protein family, was revealed to be a cargo receptor for Gas1p and invertase.

I characterized mammalian p28, a γ subfamily member of p24 proteins, which was shown to localize to the ERGIC similar like ERGIC-53. It accumulates therein after Brefeldin A treatment indicating that it cycles. As p24 proteins are known to assemble into complexes I used immunoprecipitation experiments to study the interaction of p28 with other p24 protein members. P28 specifically interacts with p23 and p25. Next, to study the function of the protein, I performed siRNA mediated knockdown experiments. In the absence of p28 the Golgi ribbon is disrupted. However, Golgi ministacks still localize to the perinuclear region. To search for the cause of Golgi fragmentation in p28-depleted cells, I analyzed anterograde and retrograde transport of ts045 VSV-G fusion proteins in p28 knockdown cells. Strikingly, they display normal anterograde as well as retrograde transport. Additionally, the association of COPI coat components with Golgi membranes is thought to be required for compartmentalization. However coatomer redistribution does not seem to be the cause for Golgi fragmentation when p28 is depleted, since I revealed comparable βCOP stainings in control and p28 knockdown cells. Next, I compared my knockdown phenotype with others knowing to result in disruption of Golgi integrity. While knockdowns of ER exit machinery components, SNARE proteins or some tethers give different phenotypes, depletion of GM130 results in a similar phenotype than knocking down p28. Therefore I investigated the distribution of GM130 in p28-depleted cells and assessed an unchanged localization of GM130 to the Golgi. Next, I decided to investigate the Golgi phenotype in more detail. Treating cells with BFA leads to the mergence of Golgi and ER membranes. Subsequent washout of the drug allows the Golgi to reform out of the ER. Lack of p28 rendered the Golgi stacks incompetent to establish a compact ribbon while reforming. Additionally, FRAP experiments revealed that the ministacks are not linked laterally in p28 knockdown cells.

Therefore, I concluded that p28 is besides coatomer, tethers and SNARE proteins, necessary for compact Golgi ribbon formation.

Cargo receptors have to bind their specific cargoes in the ER recruiting them into forming vesicles. These bud off the ER membrane and transport their content to the ERGIC and further to the Golgi. At the ERGIC, *cis*-Golgi the cargo proteins have to be released from their receptors, which then recycle back to the ER. How is binding in the ER and release in post ER compartments accomplished? It was proposed that this process depends on pH. Therefore, I was interested to measured pH along the organelles of the early secretory pathway *in vivo*. I performed pH measurements utilized EGFP as pH sensor *in vivo*. I targeted EGFP to the ER, ERGIC and Golgi to answer the question if there is gradual acidification along these organelles. I adapted a null-point method to estimate pH ranges in the three organelles. In collaboration with the imaging facility of the Friedrich Miescher Institut (FMI, Basel) customized software was developed to analyze data obtained during pH experiments. Especially the small size and mobility of ERGIC structures required sophisticated data processing. Taken together, the pH of the ER (pH 6.9- pH 7.5) is neutral, the Golgi shows acidic pH (pH 6.4- pH 7.0) and the ERGIC (pH 6.5- pH 7.2) revealed an intermediate ER/Golgi pH.

In conclusion, this thesis provides deeper insight into the pH characteristics of the early secretory pathway organelles and shows that the ERGIC protein p28 is required for Golgi integrity.

Introductory remark

The following thesis is devided into two parts. Part I deals with the characterization of p28, whereas part II is about pH measurements in the early secretory pathway *in vivo*.

Part I – Characterization of p28

Introduction

The early secretory pathway

The secretory pathway was originally described in pancreatic exocrine cells in 1964 (Caro and Palade, 1964; Palade, 1975). At that time it was revealed that secretory proteins are transported from the endoplasmic reticulum (ER) through the Golgi to the plasma membrane. Later, the ER Golgi intermediate compartment (ERGIC) was discovered (Schweizer et al., 1990). Overall, the secretory pathway consists of the **ER**, the **ERGIC**, which is unique to higher eukaryotic cells, and the **Golgi** (Figure 1). These membrane-enclosed organelles of the eukaryotic cell represent compartments where different chemical environments can be established and maintained. Thereby it is guaranteed that distinct cellular processes can go on in very close proximity. Several tasks like post-translational modifications, protein-folding, glycosylation, sulfation and disulfide-bond formation are conducted in these organelles. Transport of proteins and lipids in carrier vesicles between these compartments is important to keep the balance between newly synthesized and recycled material (Rothman and Wieland, 1996).

Proteins destined for secretion are first inserted into the endoplasmic reticulum (Blobel and Potter, 1967; Walter and Blobel, 1981). The next station on the avenue is the ERGIC from where proteins can travel in both directions, either they recycle back to the ER or proteins destined for other organelles head anterograde towards the Golgi apparatus (Ben-Tekaya et al., 2005). From there the journey can be continued towards endosomes, secretory granules, lysosomes and the plasma membrane (Figure 1).

Compartments of the early secretory pathway

The **ER** is a reticular membranous network spread throughout the cell. It is pulled towards the periphery by kinesins (Feiguin et al., 1994) and microtubule tips are also implicated in generating the network structure of the ER (Waterman-Storer and Salmon, 1998). The rough ER is decorated with ribosomes for protein synthesis. Proteins are inserted into the ER membrane mainly co-translationally (Caro and Palade, 1964). Other regions of the ER are devoid of ribosomes (Jamieson and Palade, 1967). At these transitional elements or ER exit site COPII-coated vesicles are formed and the itinerary of proteins towards the **ERGIC** and Golgi apparatus starts (Figure 1).

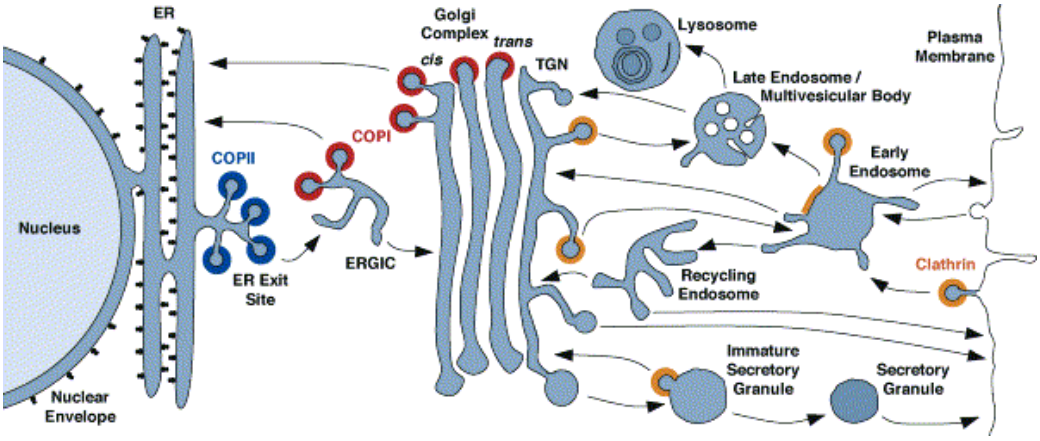

Figure 1: Intracellular transport pathways. Indicated are the compartments of the secretory, lysosomal, and endocytic pathways. Transport steps are indicated by arrows. COPII (blue), COPI (red), and clathrin (orange) coats are depicted. The function of COPII in ER export is widely accepted. Less well understood are the exact functions of COPI at the ERGIC. Reproduced from (Bonifacino and Glick, 2004)

The **ERGIC** consists of vesicular tubular clusters and localizes functionally between the ER and Golgi (Figure 1) (Fan et al., 2003; Saraste and Svensson, 1991; Schweizer et al., 1990; Sesso et al., 1994). The best characterized marker protein of the ERGIC is the cargo receptor protein ERGIC-53 (Lahtinen et al., 1996; Schindler et al., 1993; Schweizer et al., 1988). Immunogold electron microscopy studies revealed ERGIC-53 localization to βCOP-positive structures near the Golgi apparatus and in the cell periphery (Bannykh et al., 1996; Klumperman et al., 1998; Lotti et al., 1992; Martinez-Menarguez et al., 1999; Saraste and Svensson, 1991; Schweizer et al., 1988; Schweizer et al., 1990). Other proteins localizing to the intermediate compartment are Rab1, Rab2, a subset of SNARE proteins (syntaxin 5, rBet1, Sec22), the KDEL receptor and putative cargo receptors like Surf4 and p24 proteins. When cells are treated with the fungal metabolite Brefeldin A (BFA), cycling proteins such as ERGIC-53, KDEL receptor, Surf4 and p24 proteins accumulate in ERGIC membranes (Breuza et al., 2004; Fullekrug et al., 1997; Lippincott-Schwartz et al., 1990; Mitrovic et al., 2008). Another way to accumulate ERGIC proteins is to incubate cells at 15°C. When transport of VSV-G or E1 glycoproteins of Semliki forest virus was studied, the ERGIC was identified to be a 15°C intermediate of the ER-to-Golgi protein transport pathway (Saraste and Kuismanen, 1984; Saraste and Svensson, 1991; Schweizer et al., 1990). There are two models describing the transport from the ER to the Golgi. In the laboratories of Lippincott-Schwartz and Pepperkok a model of VSV-G-GFP-positive pre-Golgi carriers traveling as entities towards the Golgi was proposed (Presley et al., 1997; Stephens and Pepperkok, 2001). After exit of the ER and loosing

COPII the carriers become COPI-positive and travel towards the Golgi (Scales et al., 1997; Shima et al., 1999; Stephens et al., 2000). However, in our laboratory dual color live imaging experiments of secreted RFP and EGFP-ERGIC-53 revealed the ERGIC as a sorting station for anterograde- and retrograde-directed cargo (Ben-Tekaya et al., 2005). EGFP-ERGIC-53-positive elements are long-lived and stationary, showing no net movement towards the Golgi, but they are interconnected by highly mobile elements. These observations rather support a stable compartment model for the ERGIC.

The next station along the secretory pathway is the **Golgi apparatus** (discovered by Camillo Golgi in 1898), which consists of flattened, membrane-enclosed cisternae resembling a crescent-shaped stack located near the microtubule-organizing center in mammalian cells (Alberts, 2002). In contrast, in *S. cerevisiae* cisternae are not stacked. However, the Golgi apparatus has always two faces: a *cis* or entry site and a *trans* or exit site. In mammalian cells the Golgi displays an additional level of order, the compaction of several hundred stacks into a ribbon. This is accomplished by the formation of tubular, lateral bridges between equivalent cisternae (Ladinsky et al., 1999). One major function of the Golgi is the processing of oligosaccharides, added onto glycoproteins in the ER. The outcome is a class of N- and O-linked oligosaccharides and proteoglycans.

It is still under debate if the Golgi matures from *cis* to *trans* side or if there is vesicular transport between Golgi cisternae. There are basically two models that are mainly built up on light and electron microscopy studies. The **cisternal maturation** model was first proposed in 1957 (Figure 2) (Grasse, 1957). It predicts that membranous structures leave the ER and gradually mature into Golgi cisternae. Emphasizing the maturation model Bonfanti found procollagen transversing the Golgi without leaving the lumen of cisternae (Bonfanti et al., 1998). Resident proteins of the Golgi are recycled back in COPI-coated vesicles. In this model anterograde transport would not require vesicles. Utilizing high-resolution morphological techniques Mironov investigated transport carriers emanating next to COPII-positive ERES, which contained procollagen or VSV-G but barely any vesicles were detected (Mironov et al., 2003). This model can explain nicely the transport of large cargo across the Golgi.

On the other hand the **vesicular transport-stable compartment model** proposes vesicle-mediated anterograde and retrograde transport between stable organelles (Figure 2) (Jamieson and Palade, 1966; Jamieson and Palade, 1967). That model arose from studies with radioactive pulse-labeled secretory proteins in guinea pig pancreas slices, which were found in vesicles in the periphery of the Golgi. Using a beautiful *in vitro*-based complementation assay Balch revealed transport between two membrane systems

(Balch et al., 1984). Membranes from mutant CHO cells, lacking GlcNAc transferase, were infected with vesicular stomatitis virus (VSV) and incubated together with membranes from wildtype CHO cells, capable of complex glycosylation, in the presence of cytosol, ATP and protein fractions. Transport was measured by incorporation of radioactively-labeled GlcNAc into VSV-G protein. Those results strongly supported the idea of vesicular transport per se and between Golgi cisternae (Balch et al., 1984). In what direction these vesicles travel was still not answered (retrograde, anterograde or both). Afterwards the identification of the molecular components involved in protein transport (tethers, SNARES, SNAP, NSF) (Balch et al., 1984; Novick et al., 1980; Orci et al., 1986) and the discovery of coats (COPI and COPII) (Barlowe et al., 1994; Orci et al., 1986) further affirmed the existence of vesicular transport.

However, it is still under debate, if COPII-mediated vesicles can transport large cargo like chylomicrons or procollagen (Fromme and Schekman, 2005). Another puzzling point is how COPI vesicles can mediate forward and retrograde transport along the Golgi at the same time.

Recently, a new model was proposed (Patterson et al., 2008). It was found that cargo molecules exit the Golgi exponentially rather than with linear kinetics, implicated by the maturation model. All cargo tested (small, large and transmembrane cargo) show the same behavior. This new model proposes the Golgi stack to be a continuous layer of membranes, in which proteins can equilibrate throughout the structure. Already before, connections between heterogenous cisternae of the Golgi were observed (Marsh et al., 2004; Trucco et al., 2004). Additionally, the new model proposes that proteins partition differentially, probably because of differential distribution of lipids, through the Golgi.

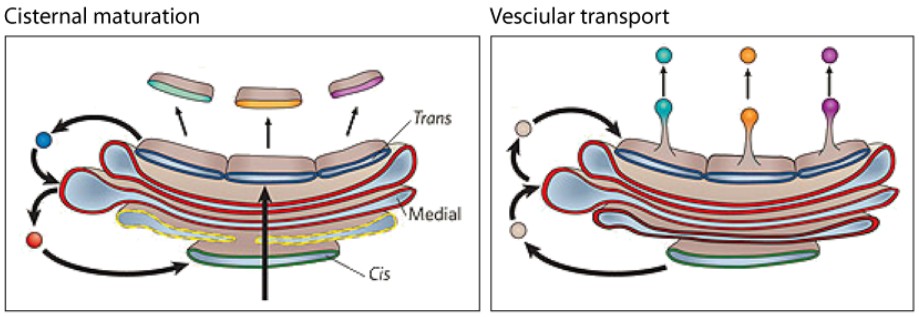

Figure 2: Golgi maturation versus vesicular transport model. In the cisternal maturation model vesicles derived from the ERGIC fuse to form the *cis* cisterna of the Golgi (green). Subsequently this cisterna transforms to the *medial* cisterna (red) (possibly via an intermediate (yellow)). Finally the medial cisterna matures into the *trans* cisterna (blue). The *trans* cisterna is consumed by vesicular transport towards the plasma membrane and endocytic compartments. COPI-coated vesicles recycle resident Golgi proteins at each level. In the vesicular transport model *cis*, *medial* and *trans* cisternae are stable compartments. COPI vesicles deliver cargo between cisternae. At the

trans side of the Golgi vesicles bud off to deliver proteins to distinct destinations. Adapted from (Malhotra and Mayor, 2006)

Vesicular transport

All the transport models involve, at least to some extent vesicles. The machinery of vesicular transport was intensively studied and the process was divided into 4 steps: Budding, transport, tethering and fusion.

Budding

Two classes of coat proteins (COPI and COPII) accomplish budding of vesicles in the early secretory pathway (Figure 1). ER exit of newly synthesized proteins is mediated by COPII-coated vesicles (Barlowe et al., 1994). This coat was identified in *S. cerevisiae* and is evolutionary conserved (Baker et al., 1988; Novick et al., 1981; Schekman, 2002). Starting at the ER, where newly synthesized proteins are either translocated through or integrated into the ER membrane, the **COPII** coat is required to deform the membrane, to capture specific cargo and to generate transport vesicles (Figure 2) (Lee and Miller, 2007; Sato and Nakano, 2007). The minimal machinery to generate COPII-coated vesicles consists of the small G protein of the Ras superfamily Sar1, the heterodimer Sec23/24 and the heterotetramer Sec13/31 (Figure 3 and 6) (Matsuoka et al., 1998). Sar1-GTP is recruited to the membrane via its transmembrane guanine nucleotide exchange factor (GEF) Sec12. Afterwards the Sec23/24 complex is recruited. The Sec24 subunit functions as adaptor to recruit specific cargo into the nascent vesicle. The so-called prebudding complex, consisting of cargo, Sar1 and Sec23/24, is formed at that stage. Subsequently the outer layer of the vesicle coat consisting of Sec13/31 is recruited, which cross-links adjacent prebudding complexes (Stagg et al., 2006). Consequently the membrane is deformed and a 60-80 nm COPII-coated vesicle pinches off (Lee and Miller, 2007). Hydrolysis of GTP leads to disassembly of the coat and exposes the docking and fusion machinery.

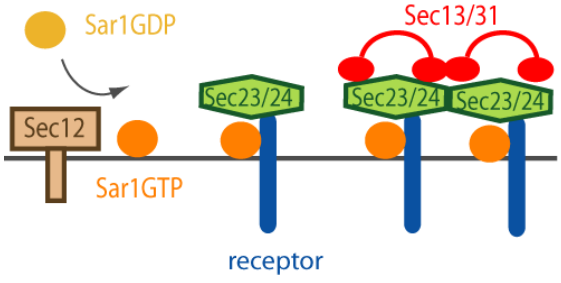

Figure 3: Recruitment of COPII components to the ER membrane. Sar1 is recruited to ER membranes upon binding to its GEF Sec12, which is an integral membrane protein. Thereafter Sar1GTP recruits the heterodimer Sec23/24 to the membrane via binding to Sec23. Cargo molecules are bound by Sec24. Upon this inner layer of the coat the outer layer, consisting of

Sec13/31, is recruited.

The second class of coat protein involved in transport steps in the early secretory pathway is the coatomer complex I (**COPI**). This budding machinery generates vesicles originating from the ERGIC and the Golgi. The COPI coatomer is a complex of seven proteins (α, β, β', γ, δ, ε and ζ) (Kirchhausen, 2000). The initial event of bud formation is the recruitment of ARF1-GTP to the membrane (Figure 4 and 6) (Serafini et al., 1991). This is ensured by interaction with the appropriate GEF. Since ARF1 is implicated in several transport reactions, different GEFs activate ARF1 at distinct locations in the cell. Since ARF1 is myristoylated, it associates with the membrane. Subsequently active ARF1 recruits the assembled coatomer complex to the forming vesicle. Sorting signals in the form of K(X)KXX bind to the α and β' subunit of coatomer (Eugster et al., 2004; Letourneur et al., 1994; Zerangue et al., 2001), whereas the $FFXXBB(X)_n$ of p24 proteins binds to γCOP (Bethune et al., 2006). The rate at which ARF1 hydrolyses GTP depends on the ArfGAP and on coatomer, which are both required for full GTPase activation (Goldberg, 1999).

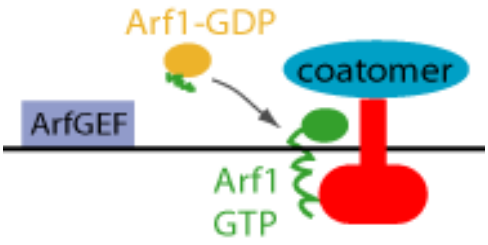

Figure 4: Recruitment of coatomer to membranes. Different ArfGEFs activate ARF1-GDP on cellular membranes. Since ARF1 is myristoylated it associates with the membrane and attracts the pre-assembled coatomer complex from the cytosol. Different sorting motifs were shown to bind to coatomer subunits and therefore ensure the enrichment in COPI-coated vesicles.

Transport

Once a vesicle is pinched off it has to reach its destination. In many instances, transport occurs along microtubules. The motor proteins that are implicated in transport in the early secretory pathway are (+) end-directed kinesins (Lippincott-Schwartz and Cole, 1995; Lippincott-Schwartz et al., 1995) and (–) end-directed dyneins (Vaisberg et al., 1996), which determine directionality of traffic. However, an intact microtubule network is not absolutely required for transport since the disruption with nocodazole does not block secretion but it becomes less directed (Kelly, 1990). Anterograde transport is mediated by dynein (Figure 6) (Burkhardt et al., 1997; Palmer et al., 2005; Presley et al., 1997). Dynactin serves as an adaptor linking dynein with the cargo. The dynactin subunit GFP-$p150^{Glued}$ labels growing tips of microtubules, which track directly through ER exit sites.

At ER exit sites, the dynactin subunit p150^{Glued} interacts with the COPII components Sec23A and Sec24D (Watson et al., 2005).

Permeabilized cells, which overexpress activated Sar1, establish elongated tubules after the addition of cytosol. These show minimal association with dynein (<25%) but clear association with kinesin (>80%) (Aridor et al., 2001). This interaction might be important for ER network generation and kinesin might be there as a remainder of retrograde transport vesicles. The retrograde-directed transport vesicles travel from the Golgi back to the ER via (+) end-directed motor proteins. Kinesin-2 seems to be involved in COPI-dependent retrograde transport (Stauber et al., 2006). Further, injecting anti-kinesin antibodies leads to the inhibition of Golgi to ER transport in contrast to ER to Golgi transport, which is not affected (Lippincott-Schwartz et al., 1995). It was shown that injection of COPI antibodies does inhibit KDEL receptor trafficking, but not the transport of Shiga-toxin and Golgi glycosylation enzymes from the Golgi to the ER (White et al., 1999). Therefore two retrograde transport mechanisms were proposed, one COPI-dependent and the other one Rab6-dependent (Figure 6) (Cosson and Letourneur, 1994; Girod et al., 1999; White et al., 1999).

But what regulates the recruitment of motor proteins to membranes? In terms of retrograde traffic from the Golgi to the ER especially Rab6 was investigated in this context (Figure 6). Fluorescently-labeled Rab6 localizes to transport carriers traveling from the Golgi to the periphery of the cell (White et al., 1999). In a yeast two-hybrid screen Bicaudal-D1 was found as interaction partner of Rab6a (Matanis et al., 2002). Additionally, Bicaudal-D1 is thought to recruit dynein-dynactin to membranes and may function in bidirectional movement together with rabkinesin6, which may drive (+) end-directed movements.

Tethering and fusion

After a vesicle has reached its destination it needs to establish contact with the appropriate acceptor membrane followed by membrane fusion. The machinery enabling this task consists of **Rabs** (Gallwitz et al., 1983; Touchot et al., 1987), **tethers** (Waters and Pfeffer, 1999) and **SNARE proteins** (Sollner et al., 1993; Walch-Solimena et al., 1993). The first step is the contact between two membranes, which is mediated by **tethers**. These are either large extended coiled-coil proteins or multisubunit complexes. Many of the coiled-coil tethers are dimers with a length of 50-300 nm (Sztul and Lupashin, 2006). Tethering proteins in the early secretory pathway important for COPII

vesicle fusion and fusion of vesicles with *cis*-Golgi membranes are **GM130, p115** and **giantin**. Some of the tethers interact with Rab proteins. For instance, Rab1 interacts with p115 (Allan et al., 2000), giantin (Rosing et al., 2007) and GM130 (Barr and Short, 2003; Moyer et al., 2001). GEFs control the site at which the Rabs are activated. The GEF of Rab1 and a tethering complex at the Golgi is transport protein particle I (TRAPPI), which was found to bind to the COPII component Sec23 and therefore ensures the activation and recruitment of p115 into COPII vesicles (Cai et al., 2007; Sacher et al., 1998). P115 is a homodimer with a globular head domain and a coiled-coil region (50 nm), which is implicated in tethering (Waters and Pfeffer, 1999). Depletion or inactivation of p115 leads to a forward transport block of VSV-G and Golgi fragmentation (Alvarez et al., 1999; Puthenveedu and Linstedt, 2004; Sohda et al., 2005). P115 interacts via its N-terminus with either GM130 or giantin. P115 is thought to tether COPII vesicles, which fuse to generate the ERGIC (Figure 5 (1)) (Short et al., 2005). Additionally p115 and GM130 were implicated in ERGIC to *cis*-Golgi tethering (Figure 5 (2)) and finally giantin/p115 and GM130 interactions bridge COPI vesicles to Golgi membranes (Figure 5 (3)) (Short et al., 2005; Sonnichsen et al., 1998; Waters et al., 1992).

Other findings have raised concerns about the tethering model of p115. First, LdlG cells (CHO cells lacking GM130) show normal secretion and Golgi morphology at permissive temperature and second, a p115 mutant lacking the binding domain for GM130/giantin supports traffic. Additionally, knocking down GM130 in HeLa cells does not have an effect on anterograde traffic (Puthenveedu et al., 2006). Another study showed that monomeric SNAREs are necessary to recruit tethers like p115 into forming vesicles, implicating a function of SNAREs upstream of fusion (Allan et al., 2000; Bentley et al., 2006). Recently, knockdown studies of GM130, GRASP65 and GRASP55 led to the hypothesis that these proteins play a role in mediating tethering of tubular connections between equivalent cisternae, which enables Golgi ribbon formation in mammalian cells (Feinstein and Linstedt, 2008; Puthenveedu et al., 2006).

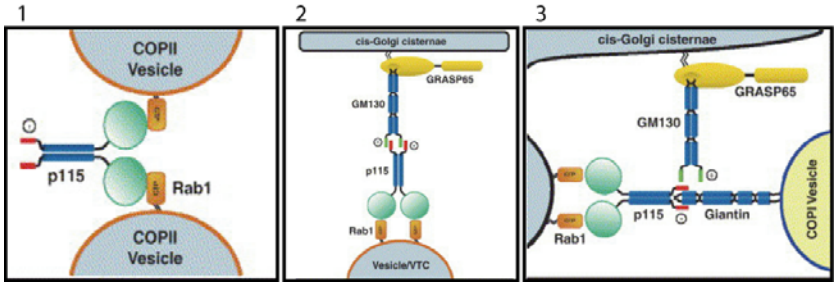

Figure 5: Proteins involved in tethering events in the early secretory pathway. (1) P115 seems to be involved in tethering events mediating homotypic fusion of COPII vesicles. (2) Incoming ERGIC structures may be tethered

to *cis*-Golgi membranes by p115 and GM130, whereas COPI coated vesicles contact *cis*-Golgi membranes via p115, giantin and GM130. Adapted from (Short et al., 2005).

Yet other tethering proteins are **golgin-84** and **CASP** (Bascom et al., 1999; Gillingham et al., 2002). It was shown by an *in vitro* budding assay combined with purification of COPI vesicles that one type of vesicles (golgin-84, CASP positive) contain Golgi enzymes while others (p115 positive) contain p24 proteins (Malsam et al., 2005). The authors propose a model in which golgin-84 functions in intra-Golgi retrograde transport vesicle tethering. However, knockdown studies of golgin-84 in mammalian cells show that depleted cells display reduced anterograde transport of ts045 VSV-G-GFP from ER to the cell surface and they show a fragmented Golgi with reduced size (Diao et al., 2003). A function of golgin-84 in mediating homotypic fusion of neighboring Golgi stacks was proposed.

Another tethering complex is the multisubunit **COG complex** (conserved oligomeric Golgi complex) consisting of eight subunits. It physically interacts with SNAREs (Shestakova et al., 2007) and COPI (Zolov and Lupashin, 2005). Depletion of COG3 in HeLa cells leads to the accumulation of vesicles, the fragmentation of the Golgi ribbon and the perturbation of retrograde traffic of Shiga toxin in these cells (Zolov and Lupashin, 2005). Therefore the COG complex is thought to play a role in intra-Golgi retrograde traffic.

When a vesicle is docked to the right acceptor membrane **SNARE proteins** fulfill their function. These proteins are C-terminally anchored transmembrane proteins with functional N-terminal domains facing the cytosol. There are more than 30 SNAREs known up to date (Hong, 2005). The SNARE hypothesis proposes the docking of membranes via the pairing of a "v-SNARE" on the vesicle membrane with "t-SNAREs" on the target membrane (Figure 6) (Rothman, 1994). V- and t-SNAREs generate a stable four-helix bundle, in which one α-helix is contributed by the monomeric v-SNARE, whereas three α-helices are contributed by the oligomeric t-SNARE (Fasshauer et al., 1997; Sutton et al., 1998). The hypothesis fits with the localization of SNARE proteins to different intracellular compartments. Therefore the function of SNAREs is to bring membranes close together so that they can fuse and on the other hand they add another level of specificity. Subsequently the SNAREs are recycled by disassembly of the SNARE complex mediated by α-SNAP (soluble NSF attachment protein) and NSF (N-ethylmaleimide sensitive fusion protein).

Taken together Rabs, tethers and the SNARE machinery collaborate to ensure fusion of membranes at the correct time and place.

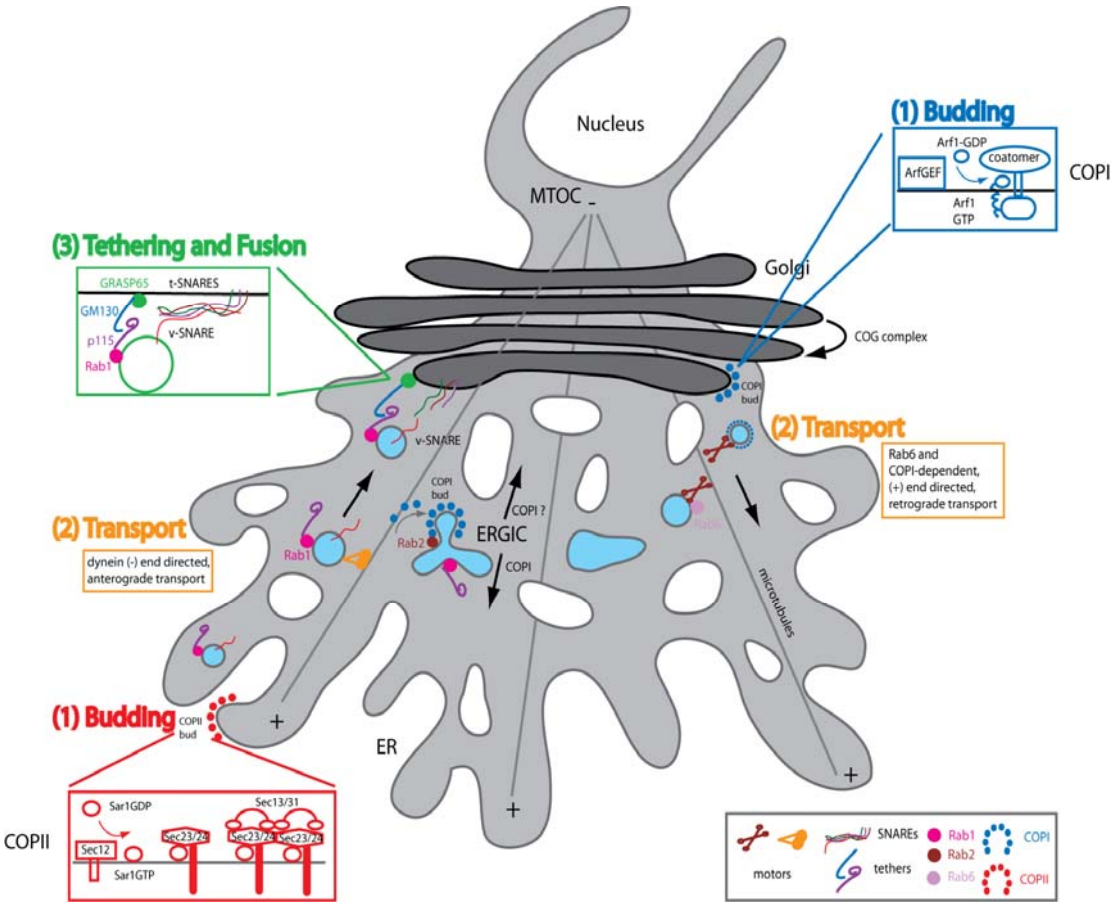

Figure 6: Summary of the transport steps in the early secretory pathway. From ER membranes COPII-coated vesicles bud off containing cargo proteins (1). Rabs, tethers and SNAREs are incorporated into COPII-coated vesicles. After homotypic or heterotypic fusion they form the ERGIC. Transport vesicles heading towards the Golgi travel along microtubules using the motor protein dynein (2). At the Golgi apparatus tethers on both donor and acceptor membranes establish the first contact between the lipid bilayers (3). Subsequently fusion is mediated by SNARE proteins (3). From the Golgi COPI-coated vesicles bud off and head retrograde towards the ER (1). For retrograde transport COPI-dependent and Rab6-dependent transport routes were reported (2).

ER exit models

The content of transport vesicles are cargo proteins, which constitute only a few percent of the ER-localized proteins. There are two models proposed, how secretory proteins are separated from components of the ER (Warren and Mellman, 1999). First, the **bulk flow model**, where proteins leave the ER independent of any export signal, just depending on their abundance. Retention signals on ER resident proteins would keep them in the ER and retrieval signals would ensure the recycling of escaped ER proteins (Wieland et al.,

1987). This was shown by adding small membrane-permeable peptides to cells. They localize to the ER, from where they are transported to the Golgi without bearing any export signal. Since these peptides contain an attachment sites for N-glycosylation, their transport to the Golgi can be followed. Finally they are secreted into the extracellular space. The model proposes that cargo proteins move out of the ER by default at concentrations prevailing in the ER lumen and do not require export signals. The second model, termed **receptor-mediated export**, predicts the existence of signals on cargo proteins, which ensure selective incorporation into budding COPII vesicles (Baines and Zhang, 2007; Kuehn and Schekman, 1997). The Sec24 subunit of the COPII coat was shown to interact with transmembrane cargo proteins through three distinct cargo-binding sites (Miller et al., 2002; Miller et al., 2003; Mossessova et al., 2003). In mammalian cells the existence of different Sec24 isoforms increases the diversity of COPII vesicles (Wendeler et al., 2007b). Escaped ER-resident proteins are retrieved by a salvage process. Some of these proteins contain a canonical di-lysine signal (KKXX or KXKXX) in their cytoplasmic tail, which binds directly COPI at the Golgi complex (Cosson and Letourneur, 1994; Letourneur et al., 1994). Soluble proteins often bear a KDEL signal, which mediates the interaction with the KDEL receptor in the Golgi (Hardwick et al., 1990; Semenza et al., 1990). After binding to the ligand the receptor oligomerizes, is phosphorylated and recycles back to the ER, where the ER protein is released (Cabrera et al., 2003).

Cargo receptors in Saccharomyces cerevisiae

The receptor-mediated export is particularly appropriate for minor proteins. Some specific cargo receptors were already identified. Most of the cargo receptors known are yeast proteins. Erv29p was identified as cargo receptor of pro-α-factor (Belden and Barlowe, 2001). When deleted from cells it specifically inhibits pro-α-factor transport. A hydrophobic signal (Ile-Leu-Val) sequence motif mediates binding to the receptor (Otte and Barlowe, 2004). This motif is functional even when transferred onto other proteins (e.g.: Kar2p). Another cargo receptor is Emp24p, a member of the p24 family (cargoes: Gas1p and invertase).

Cargo receptors in mammals

A well-defined cargo receptor in mammalian cells is ERGIC-53. It is required for the efficient secretion of blood coagulation factors V and VIII (Nichols et al., 1998). Other cargo proteins are cathepsin C, cathepsin Z and alpha1-antitrypsin (Appenzeller et al., 1999; Nyfeler et al., 2008; Vollenweider et al., 1998).

Putative cargo receptors are the p24 proteins based on findings in yeast (Muniz et al., 2000), whereas no cargo protein has been found so far in mammalian cells.

ER exit motifs of transport receptors

ERGIC-53 contains a di-phenylalanine (FF) motif in the cytoplasmic tail, which ensures ER exit in an oligomeric form (Kappeler et al., 1997). Similar di-hyrophobic signals are found in many transmembrane cargo proteins including the p24 family, Erv41p and Erv46p. An arginine-leucine motif at the C-terminus of GAT1 (GABA transporter 1) was found to bind specifically only Sec24D (Farhan et al., 2007). Another motif is the di-acidic ER exit motif, which was first identified on the VSV-G protein and was later also found on CFTR, lysosomal acid phosphatase (Nishimura and Balch, 1997; Nishimura et al., 1999), potassium channels (Ma et al., 2001) and the yeast proteins Sys1p (Votsmeier and Gallwitz, 2001) and Gap1p (Malkus et al., 2002). Further, a C-terminal valine residue (-1 position) was shown to interact with the COPII coat in a position-dependent, context-independent manner *in vitro* (Nufer et al., 2002; Paulhe et al., 2004; Wendeler et al., 2007b). Taken together, aromatic signal (FF, YY, FY, YF, FX or YX), di-hydrophobic signal (LL, II), valine at position -1, and di-acidic signals can mediate ER export.

p24 proteins

The cargo receptor Emp24p in yeast is a member of the p24 proteins. There are eight family members in yeast, five in *C.elegans*, seven in *Drosopohila* and at least six in mammals. These are type I single transmembrane proteins, with a size ranging from 23-27 kDa. They all share a common domain arrangement. Following an N-terminal signal sequence they contain a GOLD domain, a β-strand rich domain (typically 90-150 amino acids long), which stands for Golgi dynamics (Anantharaman and Aravind, 2002) and they comprise a coiled-coil domain which is thought to mediate protein protein interactions amongst family members (Emery et al., 2000). Finally they contain a single

transmembrane domain and a short cytoplasmic tail, which contains binding motifs for COPII and COPI (Dominguez et al., 1998; Fiedler and Rothman, 1997; Fiedler et al., 1996). Several studies revealed p24 proteins to form hetero-oligomeric complexes (Fullekrug et al., 1999; Gommel et al., 1999; Jenne et al., 2002).

p25 – an α subfamily member

Multisequence alignment revealed four p24 subfamilies (Dominguez et al., 1998; Smith and Smith, 1990). The first member of the p24 family of proteins cloned and characterized was p25, a calnexin-interacting protein isolated from dog microsomes (Wada et al., 1991). P25 belongs to the α subfamily and contains a single N-glycosylation site. In electron microscopy p25 is detected mainly in the ER and to some extent in the *cis*-Golgi network (Dominguez et al., 1998). Dominguez et al. performed binding studies *in vitro* with immobilized synthetic peptides of p24 proteins and HeLa cytosol. They found COPII binding for all tails (p23, p24, p25, p26 and gp27), whereas p23, p25 and after longer exposure p24 also bind to coatomer. Amino acid substitution experiments revealed that COPII binding is attenuated when the FF signal was mutated to AA but unaffected when changing downstream sequences. In contrast, mutating FF to AA only slightly affect coatomer binding (contradictory to Sohn et al., 1996). However, mutating FF and KK together completely abolishes coatomer binding. Overexpressed p25SS (di-lysine signal mutated) targets to the ER, Golgi, plasma membrane and endosomes and pulls other overexpressed p24 members out of the early secretory pathway (Emery et al., 2003). Moreover, cells overexpressing p25SS accumulate large amounts of cholesterol in the perinuclear region suggesting p25SS-rich membrane domains to exclude cholesterol. This assumption is strengthened by the fact that p25SS distributes in specialized domains on the plasma membrane, which are devoid of the transferrin receptor, rafts and cholesterol.

Recently, p25 was shown to be important for coatomer recruitment onto Golgi membranes *in vivo* (Mitrovic et al., 2008). Depletion of p25 from mammalian cells leads to the partial redistribution of βCOP from the Golgi and fragments the Golgi apparatus into ministacks. Further, p25 is involved in ER targeting of the protein tyrosine phosphatase TC48, which is implicated in cell growth, mitogenesis, motility, cell-cell interaction, signal transduction, gene expression and metabolism (Gupta and Swarup, 2006).

p24- a β subfamily member

Emp24p was cloned and characterized in *S. cerevisiae* (Schimmoller et al., 1995). Already before, the protein was isolated from partially purified endosomal fractions in yeast (Singer-Kruger et al., 1993). A deletion strain revealed transport delay in a subset of proteins (Gas1p and invertase) and a defect in retention of Kar2p (BiP) (Schimmoller et al., 1995). Crosslinking studies revealed that Gas1p can be cross-linked with Emp24p and Erv25p (Muniz et al., 2000). In vesicle budding reactions Emp24p was found in budded vesicles together with SNARE proteins indicating a role of Emp24p in COPII vesicle formation (Schimmoller et al., 1995). Concurrently, Rothman and coworkers purified ^{35}S- labeled Golgi membranes from CHO cells and incubated them with cytosol and GTPγS to generate COPI vesicles (Stamnes et al., 1995). P24 was found in these COPI vesicles. Supporting these data, a deletion strain in yeast displays reduced number of vesicles. In a double deletion strain of emp24 and sec18-1, a fusion mutant that accumulates large number of vesicles, the accumulation of vesicles is substantially attenuated. Accordingly, the authors proposed a function of p24 in vesicle budding. Taken together p24 was found in COPII- as well as COPI-coated vesicles. Another study identified Emp24p amongst other p24 family proteins as a suppressor of mutations in the Sec13 protein (leads to transport blocks). Therefore it was concluded that p24 proteins negatively regulate COPII vesicle generation in yeast (Elrod-Erickson et al., 1996).

In search for interaction partners of p24, several proteins were found: ArfGAP, GRASP proteins and PAR-2. FRET and peptide binding studies demonstrated p24 to interact with ArfGAP (Majoul et al., 2001; Lanoix et al., 2001). The unique RR motif of p24 inhibits coatomer-dependent hydrolysis on ARF1 (Goldberg et al., 2000). Furthermore, p24 interacts with GRASP65 and GRASP55 depending on the two terminal valines (Barr et al., 2001). The mutation of this residue leads to the mislocalization of p24 to the plasma membrane, suggesting GRASP proteins to play a role in keeping p24 in the early secretory pathway.

Interaction of p24 with PAR-2 regulates signal- and ARF1-dependent trafficking of the receptor from the Golgi to the plasma membrane and therefore regulates the life-cycle of PAR-2 (Luo et al., 2007).

p23 – a δ subfamily member

Blum et al. isolated p23 and p24 from mammalian microsomal membranes (Blum et al., 1996). Concurrently, Belden et al. investigated Erv25p in *S. cerevisiae* (Belden and Barlowe, 1996). Erv25p and Emp24p were shown to interact with each other as

demonstrated by cross-linking, and they depend on each other for stability. Both deletion strains show reduced transport of Gas1p and invertase (Schimmoller et al., 1995).

In mammalian cells, p23 was isolated from *in vitro* Golgi-derived COPI vesicles of CHO cells (Sohn et al., 1996). Immobilized synthetic p23 tails bind to COPI from total lysates. Immunofluorescence analysis revealed p23 localizing to the perinuclear Golgi region and electron microscopy showed its localization to COPI vesicles and Golgi membranes. The enrichment of p23 in COPI vesicles led the authors to speculate that p23 is a coatomer receptor. In fact p23 binds to the γCOP subunit of coatomer (Harter and Wieland, 1998). Photocrosslinking studies revealed that a di-lysine retrieval motif shares a common binding site with the noncanonical di-lysine motif in the p23 tail. Transport vesicles are only generated in the presence of membrane cargo proteins containing a KKXX motif or putative cargo receptors of the p24 family *in vitro* (Bremser et al., 1999). When p23 tails are incubated with coatomer and subsequently centrifuged, aggregation of coatomer is observed (Reinhard et al., 1999). This is not the case in the presence of Wbp1p (containing a canonical KKXX motif). With limited proteolysis experiments it was shown that in the presence of p23 tails, coatomer is more stable indicating a conformational change of the coat upon binding to p23 tails. Therefore p23 might play a role in the machinery of COPI vesicle generation. This hypothesis was strengthened when p23 was found to be a receptor for ARF1 (Gommel et al., 2001).

In contrast to Wieland's study, Gruenberg and coworkers investigated the localization of p23 and did not find it in COPI vesicles in BHK cells (Rojo et al., 1997). They claim p23 not to be important for COPI recruitment to membranes. Microinjection of p23 antibodies leads to the inhibition of transport of VSV-G protein and they propose segregation and transport function for p23 in the early secretory pathway.

Nickel et al. constructed CD8-p23 fusion proteins and investigated the cycling of p23 in the early secretory pathway (Nickel et al., 1997). They focused on the transmembrane domain and tail of p23 to study retrieval of the protein. A fusion construct consisting of the lumenal domain of CD8 and the transmembrane domain and tail of p23 results in mainly ER localization of the chimaeric protein, indicating the importance of the lumenal part of p23 in Golgi localization. However, the fusion protein receives post-ER modifications indicating a retrieval function of the tail. Indeed, when the KK or FF signal in the tail is mutated to SS and AA, respectively, the protein localizes to the Golgi and retrieval is impaired.

Another study investigated the localization and trafficking of p23 and p24 in CHO cells (Blum et al., 1999). The authors performed live imaging experiments with GFP

tagged p24 proteins and found them localizing to the Golgi and in peripheral punctate structures. The latter exhibit microtubule-dependent movement, which is controlled by trimeric G-proteins. Strong overexpression of p24-GFP leads to Golgi fragmentation and redistribution of ERGIC-53 to the ER.

A study using overexpressed myc-p23 showed that p23 does not have an effect on anterograde or retrograde traffic, but it induces ER-derived tubules (Rojo et al., 2000). Highly overexpressing cells show even a fragmentation of the Golgi apparatus. These observations raised the idea that p23 could have morphogenic function. A similar effect on the Golgi was observed in p23 knockout mice (Denzel et al., 2000). Heterozygous mice exhibit structural changes of the Golgi (dilated saccules), where the number of vacuoles surrounding the Golgi appears to be increased. Further these mice show reduced levels of p25 and other members, whereas the respective mRNA levels are indistinguishable.

Recently, some interacting proteins of p23 were found. In a yeast-two hybrid screen with chimaerins, p23 was revealed as interacting protein. Chimaerins are Rac-GAPs and therefore accelerate GTP hydrolysis of Rac, which leads to the down regulation of Rac (Wang and Kazanietz, 2002). Phorbol esters promote chimaerin to translocate from the cytosol to the Golgi. This association is thought to be mediated by p23.

Additionally, p23 was found to be a component of the presenilin complex, which modulates γ-secretase activity in an *in vitro* assay (Chen et al., 2006). The γ-secretase cleaves the amyloid precursor protein (APP), which leads to the secretion of the β-amyloid (Aβ) product. The secretion of this cleavage product is increased in p23 siRNA depleted cells. Other substrates of the secretase are not affected in terms of maturation, glycosylation or trafficking. Additionally, increased biosynthetic stability and maturation, cell surface accumulation of the amyloid precursor protein and increased secretion of soluble APP has been reported (Vetrivel et al., 2007).

Another p23 interacting protein is the tyrosine phosphatase TC48 (Gupta and Swarup, 2006). However the function of p23-TC48 interaction is unclear.

p26, gp27 and tp24 - γ subfamily members

The first γ subfamily members were cloned by Emery and Gayle (Emery et al., 2000; Gayle et al., 1996). P26 and tp24 both localize to the Golgi apparatus in different cell lines. After BFA treatment p26, gp27 and tp24 do not redistribute to the ER but rather show accumulation in spotty structures throughout the cytosol, suggesting their localization to the intermediate compartment (Emery et al., 2000; Fullekrug et al., 1999).

A complex consisting of p23, p24, p25 and gp27 was isolated by IP and 2 D gel electrophoresis (Fullekrug et al., 1999). So far there is nothing known about the function of these subfamily members.

p24 proteins in Drosophila melanogaster

P24 proteins (*éclair* (p25) and *baiser* (p23)) affect the development of dorsal structures in *Drosophila melanogaster* embryos. Mutant female flies do not lay eggs and males show reduced fertility. It is thought that these proteins are necessary for the activity of the maternally expressed Tkv receptor (TGF-β receptor, type I receptor) during early embryogenesis (Bartoszewski et al., 2004). If p24 proteins are necessary for Tkv packaging into COPII vesicles or if they play a role in folding or the posttranslational modification of Tkv is not known. Like *éclair* and *baiser*, the p24 member *logjam* is also essential for oviposition in flies (Boltz et al., 2007). In a screen for mutants in female reproductive behavior *logjam* was identified to have an oviposition phenotype (Carney and Taylor, 2003). This γ subfamily member localizes to punctate structures and colocalizes with ERGIC-53 (Boltz et al., 2007). Tissue-specific expression of *logjam* in the central nervous system in *logjam*-deficient flies rescues the egg-laying phenotype. Thus, *logjam* is not essential for egg development but rather needed in the central nervous system to ensure egg laying. Some of the p24 proteins were found to have developmental, tissue-specific and sex-specific expression patterns (Boltz et al., 2007).

p24 proteins in Xenopus laevis

A study on induced proopiomelanocortin (POMC) transport in *Xenopus laevis* revealed that a subset of p24 proteins are upregulated in intermediate pituitary cells (Holthuis et al., 1995). These melanotrope cells synthesize vast amounts of POMC when toads are shifted from a white to a black background. The Xp24δ_2 protein localizes to Golgi-membrane fractions in inactive cells, whereas in black background adapted cells the protein redistributes to pre-Golgi and ER-containing fractions. Thus, p24δ_2 in *Xenopus* redistributes depending on the biosynthetic activity of the cell (Kuiper et al., 2001). Direct interaction of the p24 family member and the prohormone was not detected.

Transgenic expression of GFP-tagged p24 proteins in toads reduces endogenous p24 protein levels and has an effect on processing of POMC, leads to higher levels of APP, induces Golgi fragmentation, large spherical electron-dense structures or increases

sulfation of POMC (Strating et al., 2007). Therefore in *Xenopus* overexpressing distinct p24 subfamily members leads to disparate phenotypes.

p24 proteins in Caenorhabditis elegans

P24 proteins were also studied in *C. elegans*. Mutations in *Sel-9* (p24, Sel= suppressor/enhancer of lin-12) elevate the activity of lin-12 (notch2) and glp-1 (notch3), mutations altering the extracellular domains of LIN-12 and GLP-1 (Wen and Greenwald, 1999). This suggests that p24 in *C. elegans* regulates the transport of LIN-12 and GLP-1 to the cell surface. Therefore *C. elegans* p24 seems to have a quality control function. In contrast, in mammalian cells the transport and cleavage of notch was investigated in a p23 knockdown background and was seen to be unaffected (Chen et al., 2006).

p24 proteins in plants

Unlike mammalian p24 proteins, plant p24 members all contain a conserved di-lysine (-3, -4 position from the C-terminus) and di-aromatic (YF, -7, -8 position from the C-terminus) motif. Both, ARF1 and coatomer bind to *At*p24 (*Arabidopsis thaliana* p24) immobilized tails (Contreras et al., 2004). Like for mammalian p23 is was shown that ARF1-GDP is bound preferentially. The KK motif is sufficient for binding of ARF1 and COPI. Additionally, COPII binding to *At*p24 tails is mediated by the di-aromatic motif (Contreras et al., 2004). COPI strongly competes with Sec23 binding and only after COPI depletion COPII binding is observed. Overexpression of *At*p24 revealed that, *At*p24 localizes to the ER and mutants revealed that the di-lysine motif is sufficient for correct localization (Langhans et al., 2008). When the di-lysine motif is mutated, the protein is not retained in the ER but transported to the prevacuolar compartment (PVC). Therefore p24 proteins in plants show steady state localization to the ER, bind COPII, COPI, ARF1 and are efficiently retrieved from later compartments by interaction of the di-lysine with COPI.

Proposed functions of p24 proteins

Although the precise function of this protein family is not known, various studies implicate several roles related to vesicular transport. A function in the early secretory pathway is indicated already by their localization in the ER, ERGIC and *cis*-Golgi (Blum et al., 1999; Denzel et al., 2000; Emery et al., 2000; Gommel et al., 1999; Mitrovic et al.,

2008; Rojo et al., 2000; Rojo et al., 1997; Sohn et al., 1996). P24 proteins may form **specialized membrane domains**. For instance, p25-induced domains on the plasma membrane exclude cholesterol (Emery et al., 2003). Moreover p23 is known to induce tubule-like structures in the ER and fragments the Golgi when overexpressed (Rojo et al., 2000). The same is true for strongly overexpressed p24, which redistributes ERGIC-53 to the ER and fragments the Golgi (Blum et al., 1999).

P24 proteins are enriched in COPI vesicles in yeast and mammalian cells, supporting the action of p24 proteins in **COPI vesicle formation** and **retrograde transport** (Bremser et al., 1999; Dominguez et al., 1998; Gommel et al., 2001; Harter and Wieland, 1998; Reinhard et al., 1999; Sohn et al., 1996; Stamnes et al., 1995). In yeast Kar2p is not efficiently retained in p24 deleted strains indicating a role in retrograde traffic (Aguilera-Romero et al., 2008; Marzioch et al., 1999; Springer et al., 2000). Additionally, the retrieval of TC48 depends on the interaction with p25, which seems to recycle TC48 back to the ER (Gupta and Swarup, 2006). Binding studies show that p24 tails bind to coatomer in mammals and plants *in vitro* (Bethune et al., 2006; Contreras et al., 2004). Recently it was shown that p25 and other cargo receptors participate in βCOP recruitment to the Golgi *in vivo* (Mitrovic et al., 2008). This is in agreement with yeast data, where p24 members are involved in the formation of COPI vesicles from the Golgi apparatus (Aguilera-Romero et al., 2008). Further, ARF1-GDP and ArfGAP are interacting proteins of p24 proteins in yeast, mammals and plants (Aguilera-Romero et al., 2008; Contreras et al., 2004; Gommel et al., 2001; Majoul et al., 2001). Undoubtedly, several studies support p24 proteins in governing retrograde traffic in the early secretory pathway. Ultimately, a model was proposed, where p24 proteins are thought to generate priming complexes by recruiting ARF1-GDP and coatomer to membranes, serving as **ARF1 and coatomer receptors** (Figure 7) (Gommel et al., 2001; Springer et al., 1999). Afterwards p24 inhibits GTP hydrolysis ensuring coatomer to remain on the membrane (Lanoix et al., 2001). The presence of cargo proteins promotes polymerization of the coat leading to vesicle formation and budding (Reinhard et al., 1999). Furthermore, p23 tails induce a conformational change in coatomer upon binding (Reinhard et al., 1999). This process involves the cytoplasmic tails of p24 proteins, whereas the lumenal part of p24 proteins may bind cargo**.** In yeast the GPI-anchored protein Gas1p and invertase interact with Emp24p (Muniz et al., 2000).

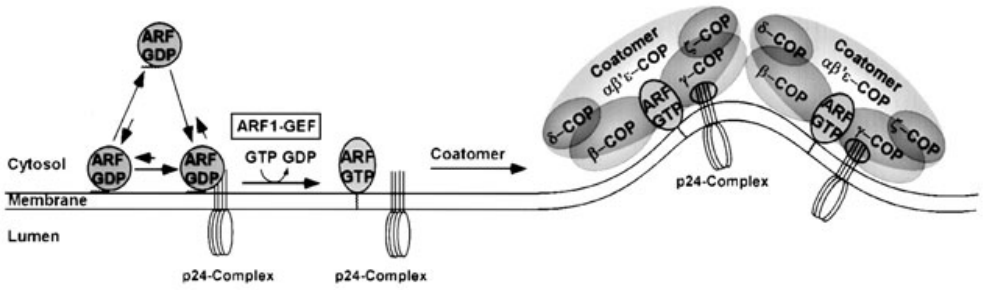

Figure 7: ARF1- and coatomer-receptor function of p24 proteins. Soluble ARF1-GDP binds to membrane phospholipids at low affinity. Upon binding to a p23-oligomer this interaction is stabilized. P23 binds preferentially ARF1-GDP. After GDP has been exchanged for GTP on ARF1 it is released from p23. Coatomer is recruited from the cytosol and binds to ARF1-GTP and p23. P23 tails were even implicated in changing the conformation of coatomer, which might lead to coat polymerization and vesicle formation (Reinhard et al., 1999). Reproduced from (Gommel et al., 2001).

Aim of the project

Characterization of p28, a novel ERGIC/*cis*-Golgi protein, required for Golgi ribbon formation

P28 was initially found by mass spectrometry in ERGIC membranes isolated from HepG2 cells after BFA treatment (Breuza et al., 2004). We studied p28 in more detail, since we were interested in the function of this γ subfamily member of the putative p24 cargo receptors in mammalian cells. To this end we performed localization studies, immunoprecipitations, knockdowns and transport assays. Surprisingly the knockdown of p28 in mammalian cells led to fragmentation of the Golgi ribbon. Only few components are currently known to mediate Golgi ribbon formation including coats and tethering proteins. To pin down the cause of Golgi fragmentation in p28-depleted cells we first compared our knockdown phenotype with others already known to lead to Golgi ministack formation and second, we decided to describe the phenotype as detailed as possible with Golgi reformation and fluorescence recovery after photobleaching (FRAP) experiments.

p28, a novel ERGIC/*cis*-Golgi protein, required for Golgi ribbon formation

Koegler E[1], Bonnon C[1], Waldmaier L[2], Mitrovic S[1], BenTekaya H[1] , Halbeisen R, and Hauri HP[1]*

[1]Biozentrum, University of Basel, CH-4056 Basel Switzerland

[2]Institute of Biochemistry and Genetics, University of Basel, CH-4058 Basel Switzerland

*Corresponding author:
Biozentrum, University of Basel
Klingelbergstrasse 50/70
4056 Basel, Switzerland

Phone +41 61 267 2222
Fax +41 61 267 2208
E-mail Hans-Peter.Hauri@unibas.ch

Abstract

The mammalian Golgi apparatus consists of individual cisternae that are stacked in a polarized manner to form the compact zones of the Golgi. Several stacks are linked into a compact ribbon via highly dynamic lateral bridges in non-compact zones. Little is known about the proteins involved in maintaining the Golgi structure. Here we have characterized p28, a new γ subfamily member of the p24 membrane proteins. P28 localized to ERGIC and *cis*-Golgi in human HeLa and HepG2 cells and was enriched in the ERGIC after Brefeldin A treatment, indicating that p28 is a cycling protein. Immunoprecipitations revealed p28 to interact with a subset of other p24 proteins. Depletion of p28 by siRNA led to a striking fragmentation of the Golgi without affecting the localization of microtubules, coatomer or tethers such as GM130. At the ultrastructural level the Golgi fragments appeared as ministacks with apparently unchanged *cis-trans* morphology, but not linked to a ribbon. Golgi reformation studies after BFA washout and FRAP experiments revealed that the lack of p28 prevented the formation of a Golgi ribbon. We conclude that the formation of a Golgi ribbon requires p28 in addition to tethers, coatomer and SNAREs.

Introduction

Protein transport through the secretory pathway is initiated at the endoplasmic reticulum, where secretory proteins are concentrated into coat protein (COP) II-coated buds (Aridor et al., 1995; Zeuschner et al., 2006). After scission these vesicles accumulate as tubulo-vesicular clusters (ER Golgi intermediate compartment (ERGIC)) in the vicinity of ER exit sites (Appenzeller-Herzog and Hauri, 2006; Bonifacino and Glick, 2004). From the ERGIC cargo proteins are transported further to the Golgi apparatus in pleiomorphic, coatomer-coated (COPI) structures (Ben-Tekaya et al., 2005). Additionally, COPI-coated transport vesicles function in recycling of membrane proteins and lipids from the ERGIC and *cis*-Golgi back to the ER. For retrograde transport coatomer binds to canonical di-lysine signals (K(X)KXX) in the cytoplasmic tails of proteins (Cosson and Letourneur, 1994; Letourneur et al., 1994) or in the case of the KDEL receptor to the phosphorylated and oligomerized protein (Cabrera et al., 2003).

The Golgi apparatus is a multi-compartment organelle of high complexity. It consists of up to 7 individual cisternae, which are stacked and polarized in compact zones of the Golgi. Golgi stacks possess a *cis* or entry side and a *trans* or exit side. Several stacks are linked into a compact ribbon via highly dynamic, tubular bridges in non-compact zones (Ladinsky et al., 1999). These bridging tubules emanate from Golgi rims. A balance of anterograde and retrograde vesicular traffic maintains the Golgi higher order architecture. Moreover, golgins such as GM130, p115, GRASP55, GRASP65, and golgin-84, form a matrix important for shaping and organizing Golgi cisternae. These proteins localize to the cytosolic side of the Golgi and transport vesicles, where their long coiled-coil domains function in tethering (Barroso et al., 1995; Diao et al., 2003; Puthenveedu et al., 2006; Puthenveedu and Linstedt, 2004; Short et al., 2001).

During mitosis the Golgi disassembles in two steps (Lucocq and Warren, 1987). First it fragments into ministacks. Thereafter, for the second step of disassembly two different mechanisms, still under debate, were proposed: either vesiculation or mergence of the Golgi with the ER. Experimentally fusion of the Golgi with the ER can be induced by Brefeldin A (BFA) (Lippincott-Schwartz et al., 1989). Brefeldin A leads to the redistribution of coatomer from membranes and the formation of Golgi-tubules that fuse with the ER. Under this condition, non-matrix Golgi proteins redistribute to the ER, whereas matrix proteins accumulate in the ERGIC (Nakamura et al., 1995). After washout of BFA the Golgi reforms in a multi-step process (Altan-Bonnet et al., 2004; Puri and Linstedt, 2003). Golgi nucleation is initiated from GM130/gp27 associated structures.

GM130 and gp27 both localize to the ERGIC rather than the ER after BFA treatment. Onto these structures other Golgi components (e.g.: Golgi enzymes) follow while the Golgi reassembles (Kasap et al., 2004). Gp27 belongs to a family of transmembrane proteins, termed p24, conserved from fungi to mammalian cells. Their precise function remains unclear and controversial but different functions were postulated. First, yeast mutants of p24 proteins display delayed transport of a subset of proteins, what accounts them as cargo receptors, but so far there has been no cargo found in mammalian cells (Schimmoller et al., 1995). Furthermore, these proteins are constituents of COPII- and COPI-coated vesicles (Schimmoller et al., 1995; Stamnes et al., 1995). Second, particularly p23 and p25 seem to be COPI-coat protein receptors revealed by *in vitro* binding studies (Bethune et al., 2006; Dominguez et al., 1998; Emery et al., 2000; Fiedler et al., 1996; Goldberg, 2000; Gommel et al., 2001; Harter and Wieland, 1998; Sohn et al., 1996). Supporting *in vitro* data, recently in mammalian p25 knockdown cells it was shown that p25 controls βCOP recruitment to membranes and therefore helps to maintain the architecture of ERGIC and Golgi (Mitrovic et al., 2008). Importantly, p24 proteins are type I transmembrane proteins, which all share the same topology. The lumenal part contains a coiled-coil domain for oligomerization (Emery et al., 2003; Cuifo et al., 2000), a GOLD domain (Anantharaman and Aravind, 2002), a single transmembrane domain and a short cytoplasmic tail. The GOLD domain is thought to potentially mediate interactions with cargo proteins. The cytoplasmic tails contain a $FFXXBB(X)_n$ ($n \geq 2$) motif (Bethune et al., 2006). The di-phenylalanine motif functions in COPII binding (Dominguez et al., 1998), whereas for COPI binding both the FF and di-lysine motif are required (Bethune et al., 2006; Fiedler et al., 1996; Goldberg, 2000; Sohn et al., 1996). So far all the family members were localized to ERGIC and *cis*-Golgi membranes, but they generate opposing concentration gradients along these organelles (Jenne et al., 2002). Thus, they likely function in the ERGIC or *cis*-Golgi.

In the present study, we have characterized a new γ subfamily member of the p24 protein family in human cells. We found it localizing to the ERGIC/*cis*-Golgi similarly to other p24 proteins. Depleting cells of p28 led to fragmentation of the Golgi ribbon. The ministacks were still localized perinuclear, but they lost their lateral linkage. Based on Golgi reformation studies after BFA washout we propose p28 to be required for the formation of lateral connections between equivalent cisternae during Golgi assembly.

Material and Methods

Antibodies

The following antibodies were used: mouse mAb G1-93 against human ERGIC-53 (Schweizer et al., 1988), mouse mAb A1-182 against BAP31 (Klumperman et al., 1998) (ALX-804-602; Alexis, Lausen, Switzerland), mouse mAb G1-133 against giantin (Linstedt and Hauri, 1993) (ALX-804-600-C100; Alexis, Lausen, Switzerland), mouse mAb MAD anti-βCOP (Pepperkok et al., 1993), mouse mAb 1A2 against α-tubulin (kindly provided by Karl Matter, University CollegeLondon, United Kingdom), mouse mAb HA.11 (Bapco), mouse mAb 9E10 against the myc epitope, rabbit pAb against p23, p24 and p25 (Jenne et al., 2002) (kind gifts from F. Wieland, University of Heidelberg, Germany), antibodies against GM130 (Barroso et al., 1995; Nelson et al., 1998) (kind gift from D.S. Nelson, University of Alabama Medical School, Birmingham), mouse anti-GFP (Roche), mouse anti-VSVG antibody (I-14, kind gift from A. Helenius, ETH Zurich); Polyclonal antibodies against the cytosolic C-terminal tail of p28 were raised in rabbits #2095 and #2096 by immunizing them (Sigma-Genosys) with the peptide MLKSLFEDKRKSRT corresponding to amino acids 216-229 of the C-terminal tail of p28. The 2096 terminal antiserum (ter2096) was used for Western blotting (1:1000) affinity-purified, concentrated and subsequently used for immunofluorescence (IF) microscopy (1:1000 for visualizing endogenous p28, 1:8000 for visualizing only overexpressed p28). Affinity purifications were carried out with the synthetic peptide CMLKSLFEDKRKSRT (Sigma-Genosys), which corresponds to the immunization peptide covalently coupled to Affigel 10 beads (Biorad) according to the manufacturer. As secondary antibodies Alexa 488-, Alexa 568- (Molecular Probes Europe BV, Leiden, Netherlands) and horseradish peroxidase-coupled antibodies (Jackson Immuno Research Inc.) were used. HRP-coupled goat-anti-mouse or goat-anti-rabbit (Jackson ImmunoResearch) were used as secondary antibodies for Western blotting.

Cell culture, transfections and siRNA

HepG2 cells (ATCC) were grown in MEM supplemented with 10% fetal bovine serum. Fugene6 (Roche) was used for transient transfections. For co-expression studies total 0.5 μg DNA was used per well (12 well plates). 24 h later, the cells were processed for immunofluorescence and imaged with a 40x objective on a Leica TCS NT confocal laser-scanning microscope. HiPerfect (Qiagen) was used for siRNA (5nM) transfections. Three

days after siRNA-transfections cells were processed for immunofluorescence or lysates were prepared (50 mM TrisHCl pH 7.4 at 4°C, 150 mM NaCl, 1% NP40). SiRNA oligonucleotides against p28 were designed according to Ambion, Inc. 2004. A p28 mRNA secondary structure prediction was carried out using the mfold-server (Zuker, 2003). Windows of 200 nucleotide lengths were shifted along the target sequence at a step width of 100 nucleotides and of each window, the five lowest energy structures were calculated and secondary structure elements were compared in terms of conservation. The synthesis of small interfering RNA duplexes with an additional two base 3' (TT) overhang on each the sense and the antisense strand was done by Eurogentec (Liege, Belgium). The target sequence was 5`-AATATGGGAGAACAGGCACAA-3` (siRNA382, Eurogentech: Liege, Belgium). Two other siRNAs targeting p28 were tested and also reduced p28 protein levels, but to a lesser extent. All of them led the Golgi fragmentation phenotype in HeLa and HepG2 cells. Nonsilencing control siRNA was purchased from Qiagen (Basel, Switzerland).

Recombinant DNA

P28 was cloned from RNA preparations of HepG2 cells, which where lysed in peqAgold RNA solution (peqLab, Erlangen, Germany) and homogenized by passing them several times through an RNAase free pipette. The RNA was phase separated, incubated 5 min at room temperature and chloroform was added. Phases were separated by centrifugations (15 min at 4°C; 12.000G). Reverse transcription was performed with the Omniscript®Reverse Transcription Kit (Qiagen) (forward primer: GGAATTCAG CAGGGATGGGCGA; reverse primer: GCTCTAGATGTTACGTACTCTAGTTTGGA G). PCR reactions were performed using a DNA polymerase mix with Pfu or Pwu (Roche Diagnostics and Promega, Madison, WI, USA) to amplify p28 (primers for sequence overlap PCR of HA-p28: forward primer 1: GGAATTCAGCAGGGATGGGCGA, reverse primer 1: AGTCTGGAACGTCGTAAGGATAGAGGGAAGGTGTGAAGCCGGC; forward primer 2: ACGACGTTCCAGACTATGCTGATAGCGACTTCACCTTTACCCTTC, reverse primer 2: GCTCTAGATGTTACGTACTCTAGTTTGGAG); Constructs of tagged p24 proteins were described already earlier (Emery et al., 2000). The first 61 amino acids of β1,4-galacosyltransferase were cloned into the pEGFP-N1 vector (Clontech) to obtain a fluorescent Golgi marker for FRAP experiments. The following primers were used for DNA amplifications: 5' CTGATAGATCTATGAGGCTTCGGGAGC 3' (containing a *BglII* site) and 5'

AGGCGGAATTCTGAGCTGCAGCGGTGTGGAGAC 3' (containing an *EcoRI* site). Accession numbers for phylogentic analysis were (h: human, mm: *mus musculus*, ce: *C.elegans*): mm_p24gamma (GI: 12852381), h_CGI-100 (p28) (GI: 4929669), mm_T1/ST2 (GI:1223892), h_T1/ST2 (GI:1223890), ce_p24gamma (GI: 3878371), mm_p24gamma3 (GI: 12835786), h_p24B (GI: 4583677), mm_p24gamma2 (GI: 38083572), h_CGI-109 (GI: 4929687), ce_p24gamma2 (GI: 2773205), mm_Tm21 (GI: 31980851), h_Tm21 (GI: 1359886), ce_p24delta (GI: 3877300), mm_gp25L2 (GI: 37590162), h_gp25L2 (GI: 996057), ce_p24alpha (GI: 4008413), mm_p24A (GI: 5931557), h_p24A (GI: 19683999) and ce_p24beta (GI: 2275635) were used as sequences.

Immunofluorescence

Cells were fixed with 3% paraformaldehyde and permeabilized with 0.1% saponin or 0.2% Triton X-100 in 10 mM glycine PBS (solution 1). Non-specific binding was blocked by 1 h incubation in solution 1. Cells were then incubated with primary antibodies diluted in solution 1 for 1 h followed by appropriate secondary antibodies for 1 h (solution 2). After several washings in 0.1% saponin in PBS (solution 2), the cells were embedded in Mowiol 4-88 (Calbiochem) supplemented with 1.3 mg/ml DABCO (Sigma-Aldrich). Primary antibodies were detected with affinity-purified Alexa®Fluor either goat anti-mouse or goat anti-rabbit (Molecular Probes). Images were obtained using a Leica TCS NT confocal laser-scanning microscope (63× 1.32 NA or a 100× 1.4 NA lens, a pinhole diameter of 1 Airy unit, and 488 nm laser excitation for GFP and 568 nm for Alexa568).

Immunoblotting

Cells were lysed for 1 h at 4°C in 50mM Tris HCl pH 7.4 at 4°C, 150 mM NaCl, 1% Triton X-100 supplemented with protease inhibitors. Lysates were centrifuged at 20.000G for 30 min at 4°C. Afterwards 50 μg of protein were subjected to SDS-PAGE, proteins were transferred to nitrocellulose membranes and immunoblotted sequentially with primary and secondary antibodies in 5% milk PBS or 0.05% Tween20 in PBS, respectively. Secondary antibodies were visualized with ChemiGlow West Chemiluminescence Substrate (Alpha Innotech). For quantifications AlphaEase software (version 5.5; AlphaInnotech) was used.

Immunoprecipitations

HepG2 cells were tranfected with tagged p24 proteins, 48 h later lysates were prepared. Cells from a 10 cm plate were scratched in 2 ml lysis buffer (50 mM Tris-HCl pH 7.4 at

4°C, 150 mM NaCl, 0.5% NP-40) supplemented with protease inhibitors. After spinning at 100.000G at 4°C for 1 h, lysates were added to antibodies coupled to protein G-sepharose. Beads were washed four times with lysis buffer, once with wash buffer 1 (50 mM Tris-HCl pH 7.4 at 4°C, 150 mM NaCl) and once with wash buffer 2 (50 mM Tris-HCl pH 7.4 at 4°C). Afterwards immune complexes were eluted with 1 x Laemmli buffer without DTT and loaded onto 18% SDS-polyacrylamide-gels.

Transmission electron microscopy

HepG2 cells were treated with either control or p28 siRNA, fixed with 3% paraformaldehyde, 0.5% glutaraldehyde in 10 mM PBS pH 7.4. After washing with PBS cells were post-fixed in 1% osmium tetroxide. Afterwards samples were dehydrated, embedded in Epon 812 resin (Fluka, Buchs, Switzerland) and sections were stained with 6% uranyl and lead acetate. Samples were analyzed with an EM912 Omega EFTEM electron microscope (LEO Electron microscopy, Oberkochen, Germany).

Metabolic labeling

HeLa cells were deprived of L-methionine for 20 min, pulsed for 10 min with 100 µCi ^{35}S-methionine (Perkin Elmer, Wellesley, MA, USA) and chased for the indicated times in HeLa culture medium containing 10mM L-methionine. At the end of the chase, the medium was collected and centrifuged for 10 min at 10.000G to remove cell debris. For the 0 min chase time cells of parallel cultures were homogenized in PBS by passing them 10x through a 25G needle. 5 µl aliquots of homogenate and media were TCA precipitated and radioactivity was measured by scintillation counting. Total protein secretion into the medium was normalized to the total counts in cell homogenates at 0 min chase.

VSV-G-GFP pulse-chase

Shortly before transfection, HeLa cells were seeded in 6 cm plates. Knockdowns were done using HiPerfect transfection reagent (Qiagen). SiRNAs at a final concentration of 5nM in 100µl of serum-free DMEM were incubated during 15 min at room temperature and then transfection complexes were added drop-wise onto the cells. After 48 h, the cells were transfected with ts045 VSV-G-GFP (kind gift from Kai Simons, MPI Dresden). 24 h later, the cells were pulsed with 100 µCi ^{35}S-methionine and ^{35}S-cysteine (Easytag TM express protein labeling mix, Perkin Elmer, Switzerland) for 10 min and chased in the presence of unlabeled methionine in excess for 40 min and immunoprecipitated with anti-GFP antibody. After Endo H digestion (Wendeler et al., 2007a), proteins were separated by SDS-PAGE, visualized by

autoradiography, and quantified by phosphor imaging using ImageQuantTM software (Molecular Dynamics, Sunyvale, CA, USA).

VSV-G-GFP immunofluorescence-based transport assay

HepG2 cells were transfected with control or p28 siRNA. Two days later they were transfected with ts045 VSV-G-GFP and incubated at 40°C over night. The following day the cells were shifted to 32°C for 20, 40 or 60 min. Subsequently the cells were stained with anti-VSV-G antibody, which recognizes a lumenal antigen, on ice. Washed with cold MEM and fixed at RT with 3%PFA. A secondary anti mouse-antibody coupled with Alexa568 was used. For each time point 15 cells were analyzed in three independent experiments and surface to total VSV-G-GFP fluorescence was calculated using ImageJ 1.40 software.

VSV-G-KDEL receptor based retrograde transport assay

HeLa cells were transfected with control or p28 siRNA. One day later they were transfected with a ts045 VSV-G-KDELreceptor construct (kind gift from V. Hsu, Harvard University) (Cole et al., 1998). The day after, cells were shifted for 12 h to 32°C. Finally, three days after siRNA transfection cells were either fixed or shifted for an additional hour to 40°C before fixation with 3%PFA. Immunofluorescence stainings were performed using mouse anti-myc and rabbit anti-p28 antibody. A secondary anti mouse-antibody coupled with Alexa568 and anti-rabbit coupled with Alexa488 were used. In three independent experiments on average 87 cells per condition were analyzed for ER or Golgi localization of VSV-G-KDELreceptor.

BFA washout and Golgi reformation assay

HeLa cells were treated with control and p28 siRNA and three days later they were exposed to 5µg/ml Brefeldin A (Sigma) for 40 min. Subsequently cells on coverslips were washed extensively with medium and PBS and put into new 12 well plates. After 120 min of recovery the cells were fixed with 3% PFA, permeabilized with 0.1% saponine and stained for giantin and p28. The reformed Golgi was categorized into compact or fragmented (quantifications in more than 100 cells per experiment in three independent experiments).

Fluorescence recovery after photobleaching

HeLa cells were transfected with 5 nM siRNAs followed the day after by transfection (Fugene 6, Roche) with GalT-EGFP plasmid DNA. Two days later cells were used for FRAP experiments on a LeicaSP5 microscopy at 37°C (63x objective, 1.4 NA). A region

of interest was bleached with 100% laser power for 2 frames and afterwards fluorescence recovery was monitored for 20 frames every 3 sec and than for 20 frames every 6 sec. Quantifications were performed using ImageJ software. The fluorescence intensity in the bleached region was normalized to an unbleached region in the vicinity. Finally the values were normalized to the prebleached intensity. Mean fluorescence recovery from 10 cells out of 3 independent experiments was calculated.

Results

A new γ subfamily member of the p24 proteins cycling in the early secretory pathway

During a screen to discover new ERGIC proteins, we identified p28 by mass spectrometry in ERGIC fractions prepared from BFA-treated HepG2 cells (Breuza et al., 2004). P28 was also found in a comparative screen, searching for proteins conserved from *C. elegans* to humans (Lai et al., 2000). It is encoded by the gene TMED5, which is located on chromosome 1 at locus 1pter-q31.3. The sequence of the cloned cDNA from p28 predicts a protein of 229 amino acids. After cleavage of the 23 amino acid signal sequence p28 has a predicted molecular weight of 23.5 kDa (ExPASy Compute pI/MW, 2005). It shares the common domain structures with other p24 proteins, consisting of GOLD domain, coiled-coil domain, a single transmembrane domain and a short cytoplasmic tail (Figure 1A). Phylogenetic analysis assigned p28 to the γ subfamily of p24 proteins (Figure 1C). Unlike the γ subfamily member gp27 (Fullekrug et al., 1999) it does not contain any predicted N-glycosylation sites (NetNGlyc 1.0). Alignments of p28 orthologs from human, yeast, worm and mouse revealed identical and similar amino acids (Figure 1B). Especially the position and length of the transmembrane domain is highly conserved. The highly conserved FF after the transmembrane domain is not as conserved in p28 (LF) and there is no classical ER retrieval motif (Figure 1B).

To characterize endogenous p28, we prepared polyclonal antibodies. Rabbits were immunized with a peptide containing the 12 C-terminal amino acids of p28. Anti-p28 antiserum recognized a band between 20 and 25 kDa on Western blots from HepG2 lysates (Supplemental Figure S1 lane 1). To test for its specificity we overexpressed myc-p23, HA-p24 and myc-p25. These family members were not detected by the p28 antibody (Supplemental Figure S1 lane 2, 3 and 4).

With immunofluorescence we determined the subcellular distribution of p28 in HepG2 cells by using the affinity purified antibody. P28 localized to the perinuclear region in addition to dotted structures distributed in the periphery of the cell (Figure 2A). The staining in the perinuclear region partially colocalized with the Golgi marker giantin (Figure 2A). P28-positive structures showed partial colocalization with the ERGIC marker ERGIC-53 (Figure 2B). Next, we investigated the effect of BFA on the localization of p28. BFA is known to accumulate rapidly cycling proteins in the ERGIC (Lippincott-Schwartz et al., 1990). In BFA-treated HepG2 cells p28 accumulated in

punctate structures in the cytoplasm colocalizing with ERGIC-53 (Figure 2B). Thus, p28 is a γ subfamily member of the p24 proteins, which localizes to the ERGIC, *cis*-Golgi and cycles in the early secretory pathway.

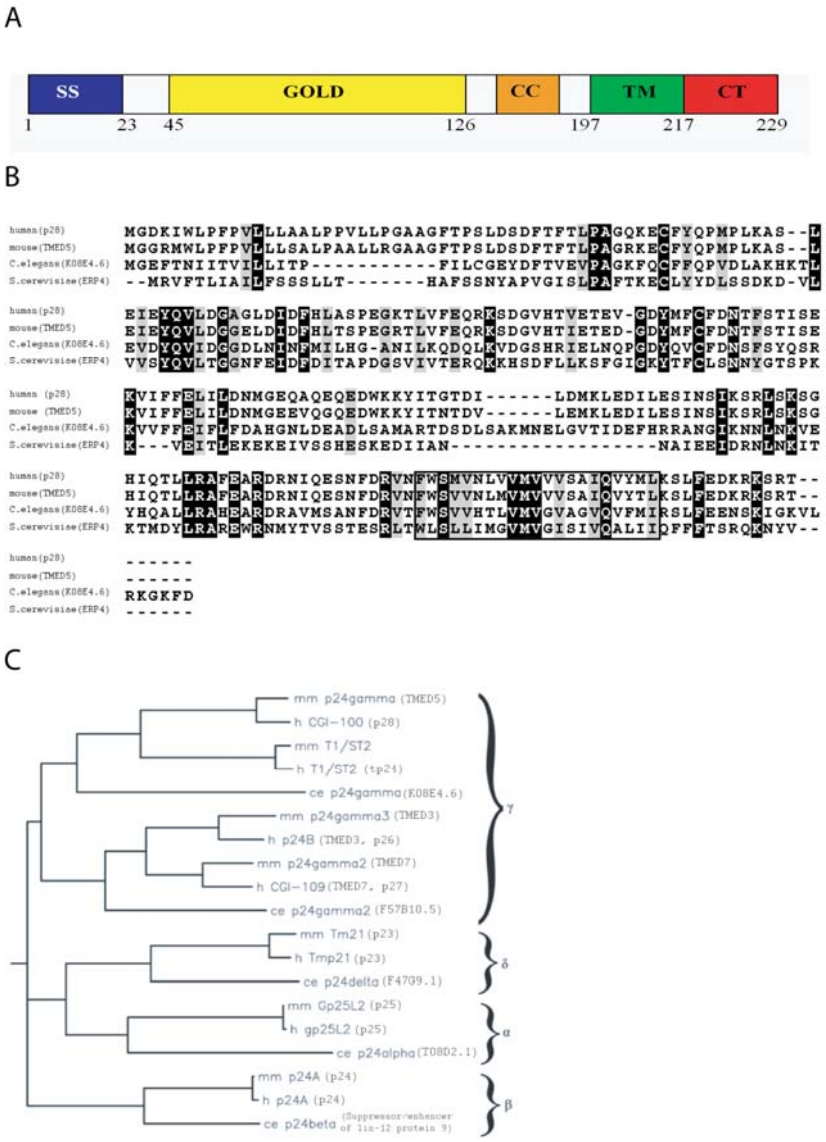

Figure 1: P28 a new γ subfamily member of p24 proteins. (A) P28 is a 229 amino acid protein. Similar to other p24 proteins, p28 consists of a 23 amino acid signal sequence, a GOLD domain (81 amino acids), a coiled-coil domain (CC), a single transmembrane domain (21 amino acids, TM) and a 12 amino acid cytoplasmic tail (CT). (B) Alignment of p28 orthologs from mouse, human, *C.elegans* and *S. cerevisiae*. There is a conserved phenylalanine at position -9 and a single lysine at -4 in human p28. Conserved residues are shaded in black, similar ones in grey. The putative transmembrane domain is indicated by a box, which showed constant length and positioning, and was deduced by TMMH prediction program. (C) Phylogenetic analysis and tree drawing was performed with clustalW program (Biology workbench interface http://workbench.Sdsc.edu/) and revealed p28 as γ subfamily member of the p24 proteins. Other protein names are indicated in parentheses. TMED stands for transmembrane emp24-domain containing protein. h: human, mm: *mus musculus*, ce: *Coenorhabditis elegans*.

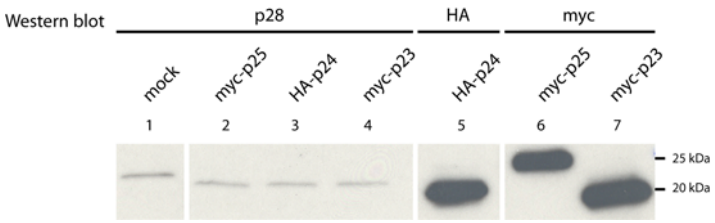

Supplemental Figure S1: The p28 antiserum recognizes specifically p28. HepG2 cells were either mock transfected (lane 1) or transfected with myc-p23 (lane 4 and 7), HA-p24 (lane 3 and 5) or myc-p25 (lane 2 and 6) and 48 h later lysates were prepared and analyzed by SDS-PAGE and Western blotting with p28 (lane 1 to 4), HA (lane 5) or myc (lane 6 and 7) antibodies. The p28 antiserum specifically recognized a band at about 23.5 kDa and did not detect other p24 proteins.

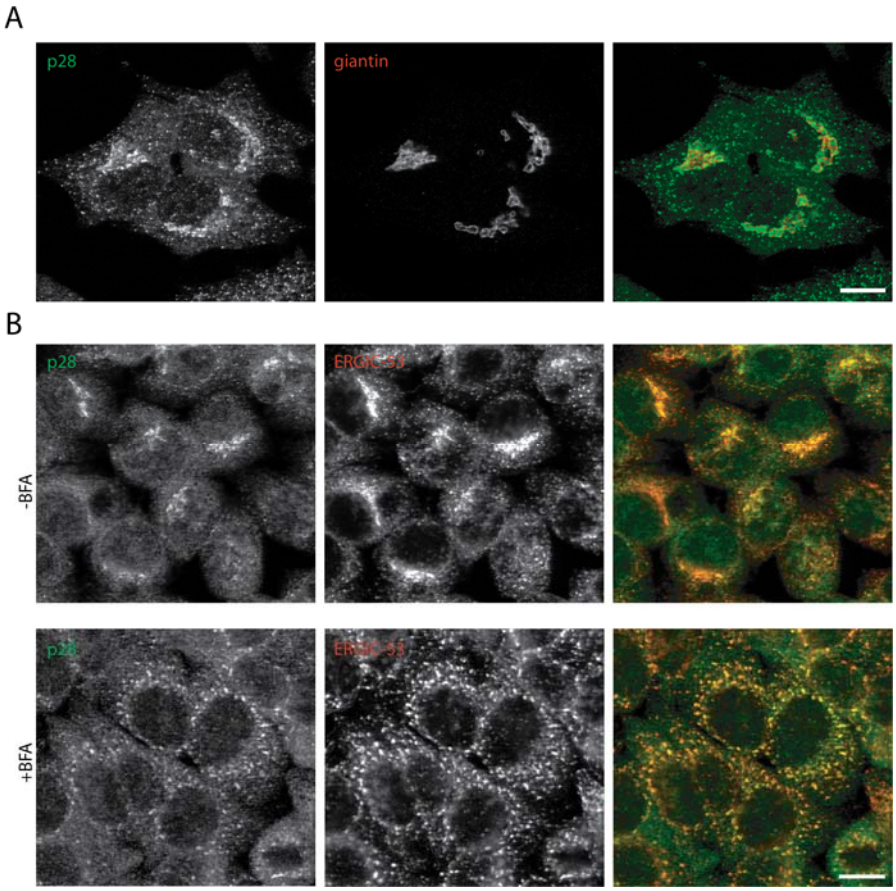

Figure 2: p28 localizes to the ERGIC, *cis*-Golgi. Double-immunofluorescence stainings on HepG2 cells were performed and analyzed by confocal microscopy using antibodies against p28, giantin and ERGIC-53. (A) p28 and giantin colocalized in the perinuclear Golgi region. (B) Additionally, p28 stained peripheral punctate structures showing colocalization with the ERGIC marker ERGIC-53. After treating cells for 90 min without (-BFA) or with (+BFA) 10 µg/ml BFA, p28 and ERGIC-53 both accumulated in ERGIC clusters. Bars, 10 µm.

Exogenous p28 requires p23 for correct localization

P24 proteins build up concentration gradients from ER to Golgi (Jenne et al., 2002). They all localize to the ERGIC and *cis*-Golgi but to different extents. Exogenous p24 proteins require co-expression of other family members for export from the ER (Dominguez et al., 1998; Emery et al., 2000; Fullekrug et al., 1999). Therefore we determined whether coupled transport together with other p24 members is required for export of p28 from the ER. To mainly detect overexpressed protein we highly diluted the affinity purified p28 antibody. Under these conditions only transfected cells showed staining for p28. We quantified the number of cells showing localization of the overexpressed protein to the ER, ERGIC or to ER-derived membranous structures. Overexpressed p28 localized in about 80% of the cells to the ER (Figure 3A). However, in about 20% of low expressing cells p28 was localizing to the ERGIC (Figure 3A). Localization of overexpressed p24 proteins to the ER is a general effect, because also myc-p23, myc-p25 and HA-p24 localized there in HepG2 cells (data not shown). This indicates the importance of the correct proportion between p24 proteins for proper targeting and cycling of these proteins. Interestingly, when p28 was overexpressed in combination with myc-p23 we observed in more than 60% of the cells localization of p28 to punctate structures, reminiscent of ERGIC localization (Figure 3A and B top panel). Surprisingly, whereas tagged p28 reached the ERGIC myc-p23 showed an ER pattern.

Since the coiled-coil domain of p24 proteins has been shown to mediate interactions between family members (Ciufo and Boyd, 2000; Emery et al., 2003), we generated myc-p23 lacking the coiled-coil domain (myc-p23Δcc). Co-expressing this protein together with p28 we tested for its potential to rescue p28 localization. ERGIC, *cis*-Golgi localization was prevented when myc-p23 lacking the coiled-coil domain was co-expressed with p28, supporting the notion that the coiled-coil domain of p24 proteins mediates interaction with other family members (Figure 3A and B bottom panel). We suggest that p23 is needed to render p28 ER exit competent. If there is less p23 than p28 present in the cells, then p23 would be a limiting factor for ER exit of p28. Supporting this, p23 and p25 were shown to exist in fivefold lower concentrations than p24 and p27 in HeLa cells (Jenne et al., 2002). The combined expression of HA-p24 and p28 did not result in enhanced ER export of p28 indicating the independence of p28 localization from p24 (Figure 3A). Co-expression with p25 did not result in enhanced ER export of p28 either, but rather led to the induction of tubular membranous ER structures, already observed in overexpression studies of other p24 proteins (Gommel et al., 1999; Rojo et al., 2000). When p28 was overexpressed in combination with p24 and p25 almost 100%

of the cells showed p28 in the ER, compared to 80% in p28 transfected cells alone (Figure 3A). This suggests that overexpressed HA-p24 and myc-p25 sequester endogenous p23 and therefore enhance ER localization of p28. Taken together, we conclude that at least p23 is necessary for correct targeting of exogenous p28 in HepG2 cells.

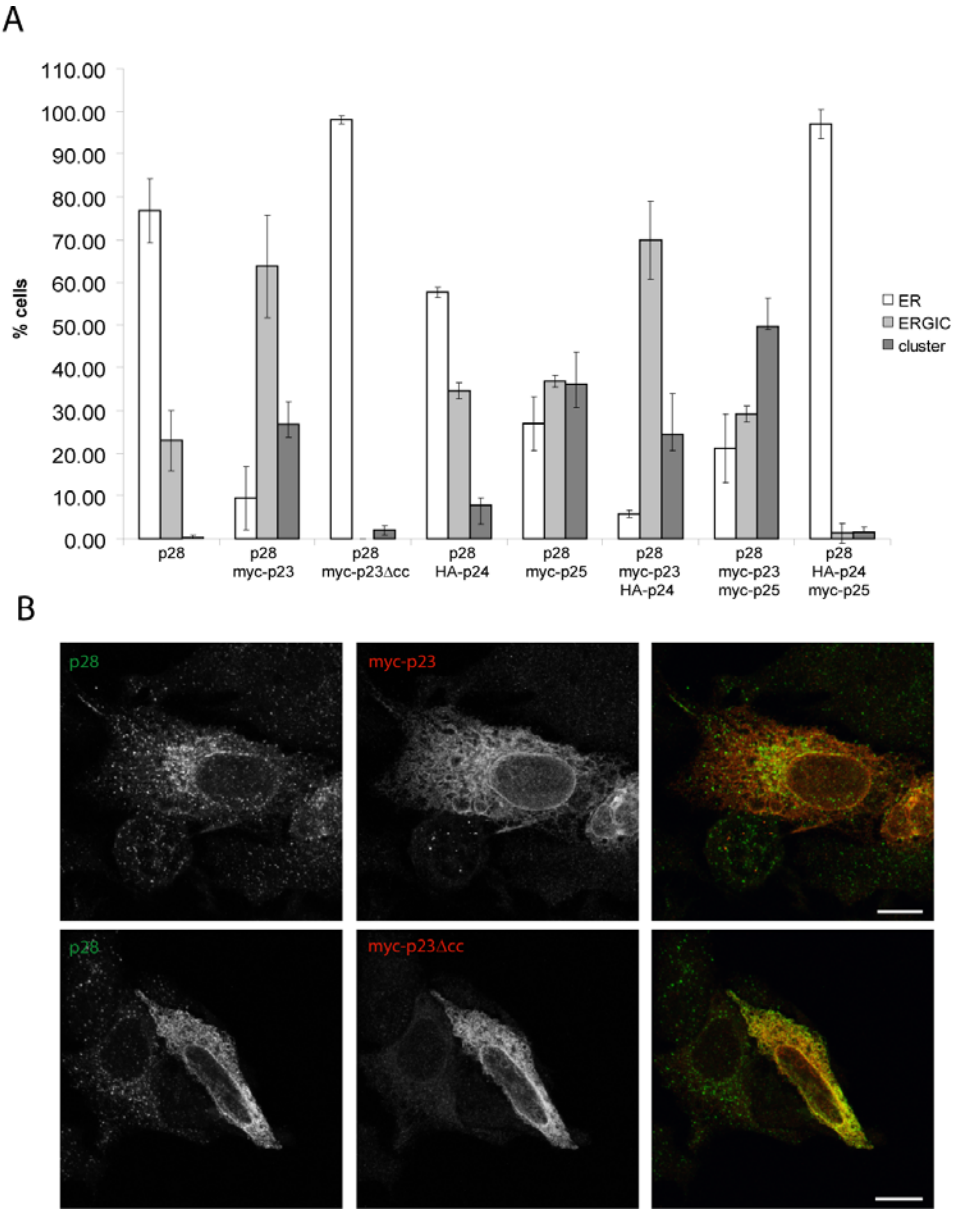

Figure 3: ER exit of p28 is aided by p23. (A) HepG2 cells were transfected either with p28 alone or together with myc-p23, myc-p23Δcc, HA-p24 and myc-p25 in double and triple transfections as indicated. Cells were subjected to immunofluorescence using anti-p28 antibody in combination with HA and myc antibodies. P28 localization to the ER, ERGIC, or ER-derived clusters was quantified in 3 independent experiments. Results are mean values ± SD. Overexpressing p28 alone led to an ER localization of the protein in almost 80% of the cells. When overexpressed together with myc-p23 more than 60% of the cells showed p28 leaving the ER. However, deleting the coiled-coil domain of p23 (myc-p23Δcc) inhibits the rescuing effect. Combined overexpression of p28 and HA-p24 did not enhance ER exit of p28 significantly. Overexpression of myc-p25 massively induced membrane clusters. Triple transfection of p28, myc-p23 and HA-p24 did not really boost the ER exit of p28.

Expressing p28 together with HA-p24 and myc-p25 led to an almost complete block of p28 in the ER indicating a sequestering effect. (B) Double transfected HepG2 cells with p28 and myc-p23 or myc-p23Δcc. Cells were subjected for immunofluorescence using antibodies against p28 and myc. P28 and myc-p23 co-expressing HepG2 cells show p28 localization to punctate structures and accumulations in the Golgi region, reminiscent of ERGIC localization. However, in p28 and myc-p23Δcc co-expressing HepG2 cells p28 remained in the ER, indicating the requirement of the p23 coiled-coil domain to aid p28 ER exit. Bars, 10 μm.

Interaction of HA-p28 with p24 family members

These results raised the question of whether p28 interacts with other p24 proteins. Previous studies implicate these proteins to form dimeric or oligomeric complexes consisting of different subfamily members (Gommel et al., 1999; Jenne et al., 2002; Marzioch et al., 1999). Since the antibody raised against p28 was unable to immunoprecipitate endogenous p28, myc- and HA-tagged protein was studied in transfected HeLa cells. HeLa cells were transfected with tagged p24 proteins in different combinations and lysates were prepared 48 h later. Immunoprecipitations were performed with antibodies directed against myc and HA bound to protein G-Sepharose. Bound immune complexes were eluted, and analyzed by SDS-PAGE followed by Western blotting using antibodies directed against myc and HA. Immunoprecipitation of myc-p23 co-precipitated HA-p28 (Figure 4A lane 2 and 5). However, when the coiled-coil domain of myc-p23 was deleted (myc-p23Δcc), they did not interact with each other any more (Figure 4B lane 2 and 5). Also an interaction between myc-p25 and HA-p28 was observed (Figure 4C lane 2 and 5). However, HA-p24 did not pull down myc-p28 in either direction (Figure 4D lane 2 and 5 and data not shown).

Based on these co-immunoprecipitation studies we conclude that HA-p28 forms hetero-oligomeric complexes with myc-p23 and myc-p25. Since deletion of the coiled-coil domain in p23 resulted in loss of interaction we propose that the interaction most probably is mediated via the coiled-coil domain of p24 proteins. These results support the myc-p23-dependent localization of p28 to the ERGIC shown with co-expression studies (Figure 3).

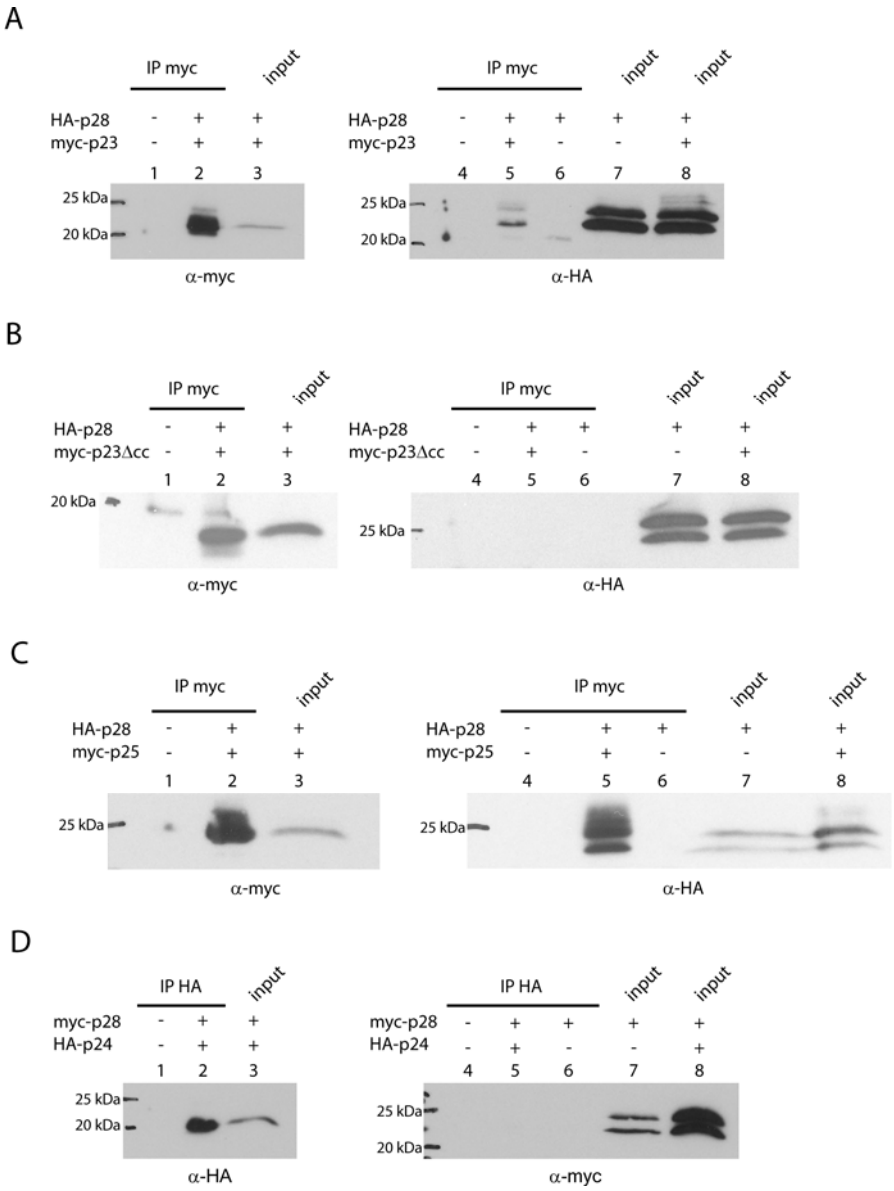

Figure 4: HA-p28 interacts with myc-p23 and myc-p25. HeLa cells were transfected with tagged p24 proteins as indicated. 48 h later lysates were prepared and subjected to immunoprecipitations (IP) with the indicated antibodies. Immunocomplexes were analyzed on 18% SDS-polyacrylamide gels and by Western blotting (antibodies indicated below the blots). (A) Myc-p23 immunoprecipitation led to the detection of HA-p28 (lane 2 and 5). HA-p28 did not bind unspecifically to protein G-sepharose coated with myc antibody (lane 6) and antibody light chain bands were not present since elution was performed with non-reducing sample buffer and without boiling (lane 1 and 4). (B) The interaction between HA-p28 and myc-p23 was prevented when the coiled-coil domain of p23 was deleted (lane 5). (C) Further there was an interaction with myc-p25 observed (lane 5). (D) An interaction between HA-p24 and myc-p28 was not detected in either direction. P28, which lacks a potential N-glycosylation site, appears as a double band presumably because of a proteolytic cleavage event. Input, 30% (lanes 3, 7 and 8).

Interdependence of p28 with other p24 proteins

Hitherto it was shown by depletion studies in yeast and mammalian cells that p24 family members are interdependent (Denzel et al., 2000; Marzioch et al., 1999). Depletion of one member can affect the stability of another family member. We next tested this dependency using siRNA-based silencing of p28 in mammalian cells. Analysis of siRNA-treated HepG2 cells was performed 3 days after transfections with 3 different siRNAs (data not shown). At this time point, there was a significant reduction at the protein level and cells retained their normal appearance (Figure 5A). Immunoblotting after depletion of p28 by siRNA oligonucleotides revealed that the knockdown efficiency was about 80% in HepG2 cells (Figure 5B). We analyzed the protein levels of other p24 proteins in p28 knockdown cells. Treating cells with p28 siRNA efficiently decreased p28 protein levels but also p23 and p25 were slightly reduced in HepG2 cells, 30% and 15% respectively (Figure 5B). The most affected family member was p23, reinforcing the interconnection of p28 and p23. P25 is glycosylated and appears as a double band in Western blotting (Figure 5A). In p28-depleted cells the high mannose band lost intensity. This implicates that the new synthesis of p25 was affected or the protein became instable and was subsequently degraded. The complex glycosylated protein band did not change in intensity. Similarly, in heterozygous p23 mice p25 protein levels are 30% reduced in liver, kidney and MEFs, whereas the mRNA level of p25 is not affected (Denzel et al., 2000). These results show that there is interdependence of p24 proteins in mammalian cells.

Immunoprecipitations studies together with the correct targeting of overexpressed p28 in the presence of enhanced p23 and the observation that p23 levels are reduced in p28-depleted cells and led us to hypothesize that these two proteins act in concert.

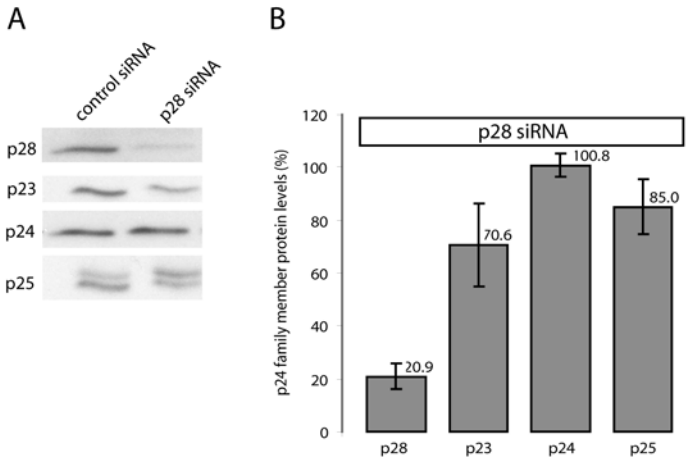

Figure 5: Interdependence of p24 proteins. HepG2 cells were knocked down for p28 and cell lysates were subjected to Western blotting with antibodies against p28, p23, p24 and p25. Lanes were loaded with equal amounts of lysate. (A) Knocking down p28 affects the protein levels of p28, p23 and p25, whereas p24 protein levels were not reduced. (B) Quantification of (A) from 3 independent experiments in HepG2 cells. P24 family member protein levels were normalized to control siRNA treated samples. In p28-silenced cells p23 protein level was 30% reduced. P25 protein level was less affected (15%) and p24 was not affected at all under these conditions. Given are relative protein levels in percent ± SD quantified from 3 independent experiments.

Depletion of p28 perturbs Golgi integrity

In search of the function of p28 we depleted HepG2 cells of p28 and investigated them in more detail. After transfection with p28 siRNA the punctate ERGIC and perinuclear staining of p28 was abolished in essentially all of the cells in immunofluorescence (Figure 6A). The endoplasmic reticulum marker BAP31 stained a reticular and spread ER network throughout the cell in p28-depleted and control HepG2 cells (Figure 6A). Recently, we published that silencing of p25 in HeLa cells leads to a reduced number of ERGIC structures and destabilizes the ERGIC (Mitrovic et al., 2008). Staining for the ERGIC marker ERGIC-53 revealed punctate structures in the cytoplasm and an accumulation in the perinuclear region comparable to control cells (Figure 6B). However in the same cells, we visualized the Golgi with an antibody against the membrane-anchored coiled-coil protein giantin and obtained a scattered Golgi staining (Figure 6B). Several Golgi fragments were detected in p28 knockdown cells. P28 siRNA treatment did not substantially alter the juxtanuclear Golgi localization but rather fragmented the Golgi. Since disruption of microtubules with nocodazole leads to Golgi fragmentation into ministacks we stained for α-tubulin in p28-depleted HepG2 cells (Supplemental Figure S2) (Cole et al., 1996). Like in control siRNA treated cells the arrangement of microtubules was not affected in p28-depleted HepG2 cells. As mentioned above we recently published the p25 knockdown, which results in Golgi fragmentation like in p28-depleted cells (Mitrovic et al., 2008). However, in contrast to p25-depleted cells, where βCOP is dissociated from fragmented Golgi elements (Mitrovic et al., 2008), we visualized prominent βCOP signals on the fragmented Golgi (Figure 7A). This indicates a different mechanism of Golgi fragmentation in p25 and p28 knockdown cells.

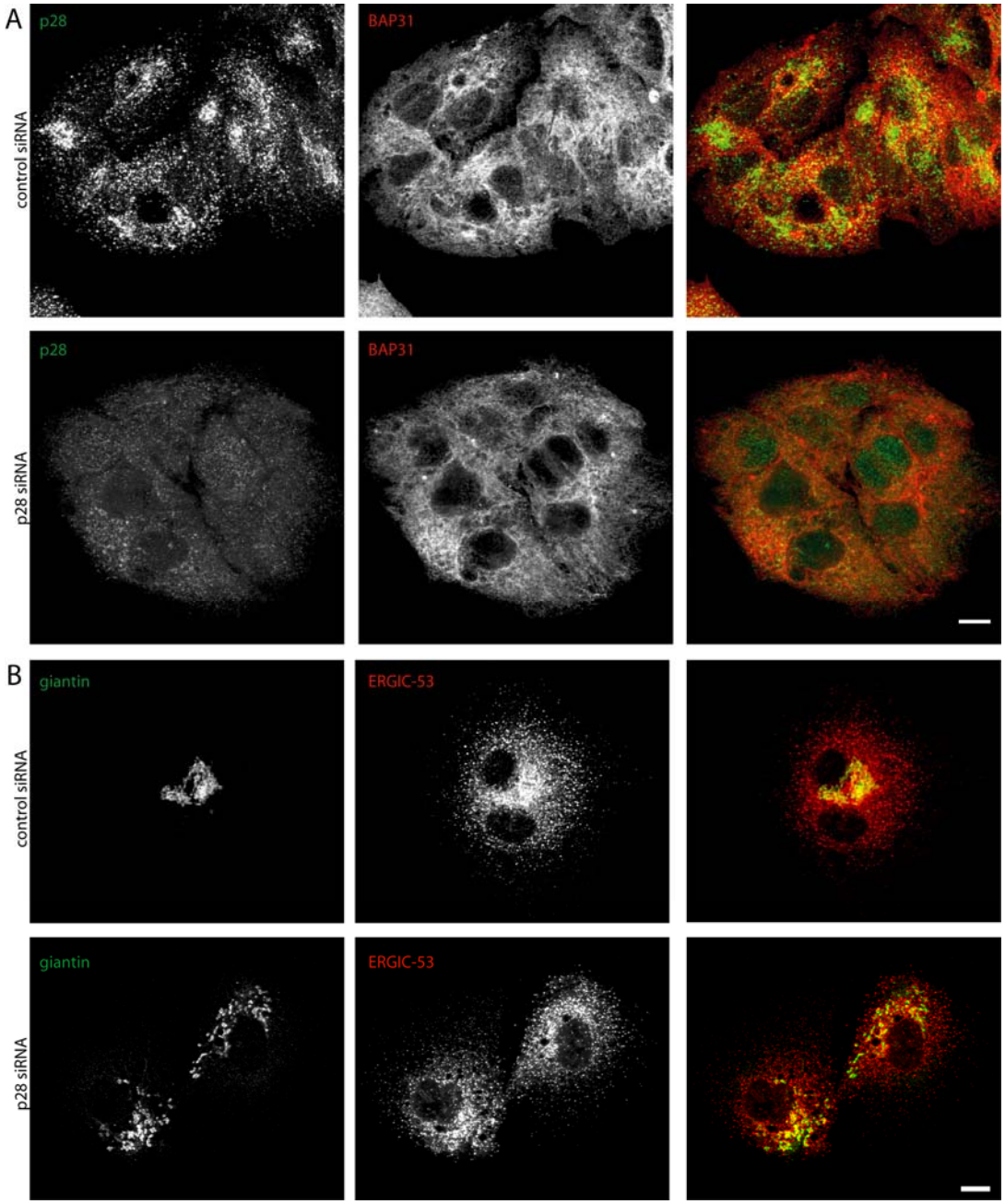

Figure 6: Knockdown of p28 perturbs Golgi organization. HepG2 cells were transfected with control or p28 siRNA as indicated, 3 days after transfection they were processed for immunofluorescence and stained with p28 and BAP31 (A) or ERGIC-53 and giantin (B) antibodies. (A) Control siRNA treated cells showed a reticular staining of the ER with BAP31. Likewise the BAP31 staining revealed no morphological changes of the ER in p28-depleted cells. Knockdown of p28 efficiently reduced the staining for p28 in immunofluorescence. (B) Staining for the Golgi protein giantin revealed a compact perinuclear Golgi in control siRNA transfected cells, whereas in p28 siRNA-treated cells the Golgi was fragmented. Stainings for the ERGIC marker ERGIC-53 indicated no obvious changes in number, size or distribution of ERGIC-53 in p28-silenced HepG2 cells. Bars, 10 μm.

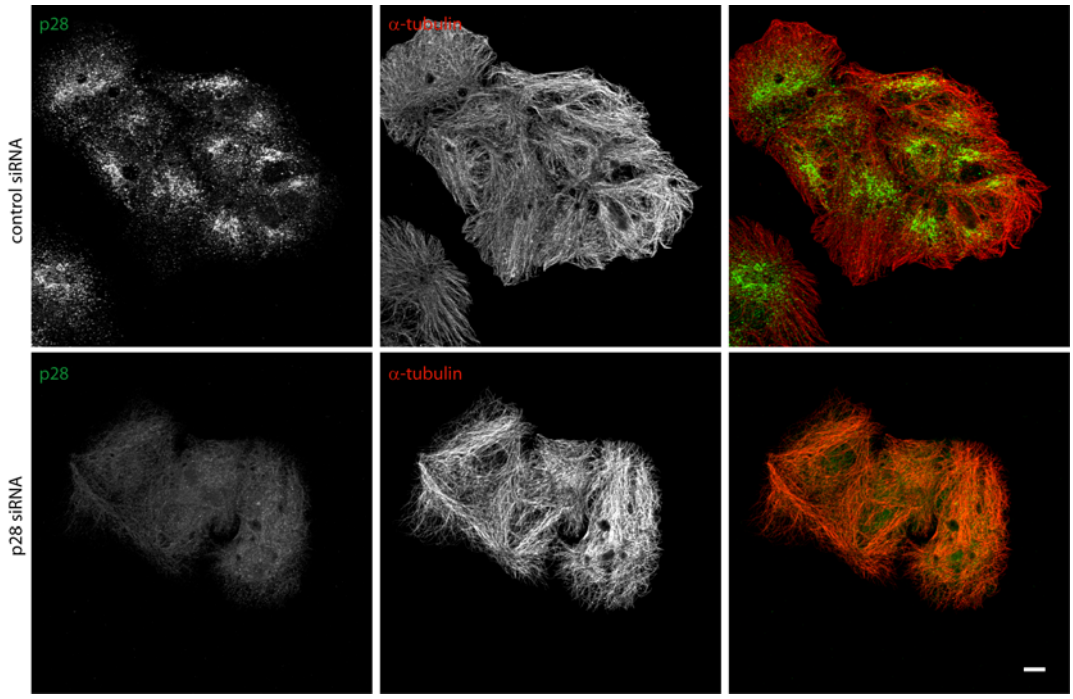

Supplemental Figure S2: The microtubule-network is normal in p28-depleted cells. HepG2 cells were transfected with control or p28 siRNA and 3 days later subjected to immunofluorescence using p28 and α-tubulin antibody. Like in control siRNA tranfected cells the α-tubulin staining was unchanged in p28-depleted cells. Bar, 10 μm.

To characterize the Golgi-phenotype in p28 knockdown cells in more detail we utilized transmission electron microscopy. In control cells the Golgi consisted of colinear units of Golgi stacks (Figure 7 B). Even both control and p28-depleted cells exhibited flattened and stacked cisternae these did not coalign with one another in p28 knockdown cells (Figure 7 B). Normal stacking of the cisternae in p28-depleted cells suggests normal *cis-trans* topology. Overall, ER and ERGIC are not changed in morphology and coatomer remains associated with the Golgi in p28-silenced cells. Nevertheless, lack of p28 fragments the Golgi into ministacks, which remain close to the nucleus.

Secretory transport is p28-independent

One possible cause of Golgi fragmentation is an imbalance in anterograde traffic. Previous studies have shown that, anterograde transport is affected after depletion of the tethering protein p115 (Puthenveedu and Linstedt, 2004), the ER exit component Sec16 (Watson et al., 2006) or the GTPase Sar1 (Ye et al., 2007). Since p24 proteins are putative cargo receptors and were found to be constituents of COPII-coated vesicles we investigated whether anterograde transport defects are the cause of Golgi fragmentation in p28-depleted HepG2 and HeLa cells (Schimmoller et al., 1995).

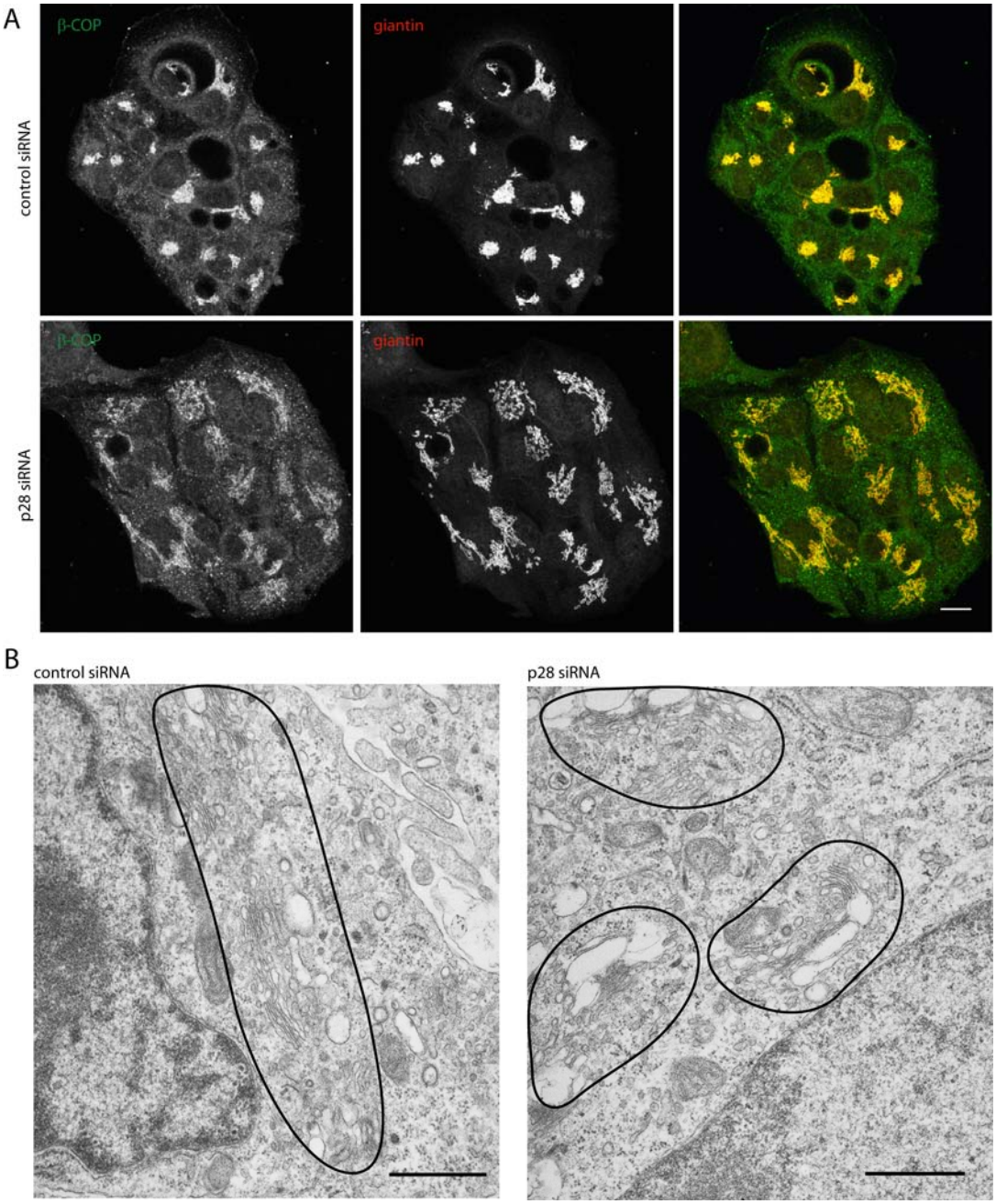

Figure 7: P28 knockdown does not redistribute βCOP, but induces Golgi ministacks. (A) HepG2 cells were either treated with control or p28 siRNA and 3 days after transfection cells were subjected for immunofluorescence using giantin and βCOP antibodies. The βCOP subunit of the COPI coat was still associated with Golgi membranes in p28-depleted cells. Bars, 10 μm. (B) HepG2 cells were either treated with control (left) or p28 (right) siRNA and embedded in Epon and subjected to transmission electron microscopy 3 days after knockdown. Cells were 16.000 times magnified and the Golgi apparatus was imaged. Golgi stacks are highlighted. Whereas in control cells (left) a single Golgi ribbon was detected, p28-depleted cells exhibit several Golgi ministacks (right). Bars, 0.91 μm.

Therefore we measured secretory transport using the temperature sensitive mutant of vesicular stomatitis virus glycoprotein tagged with GFP (ts045 VSV-G-GFP) in p28 knockdown HepG2 cells. Incubation at the restrictive temperature leads to the accumulation of the protein in the endoplasmic reticulum. Shifting to 32°C releases the ER-block of the temperature-sensitive mutant protein and leads to the transport of the glycoprotein to the plasma membrane. In both control and p28 knockdown HepG2 cells the ratio of surface VSV-G to total VSV-G was calculated. Quantifications at multiple timepoints indicate the successive transport of VSV-G-GFP from the ER, through the Golgi to the plasma membrane in both control and p28 siRNA transfected HepG2 cells (Figure 8A). The dynamics of transport along the organelles of the early secretory pathway were comparable in control and p28 siRNA transfected cells. Under both conditions HepG2 cells showed prominent VSV-G staining on the plasma membrane after 60 min of chase (Figure 8B). Additionally, since p24 proteins were implicated to function in the early steps of transport, we investigated ER to Golgi transport in more detail in p28-silenced HeLa cells. Therefore we performed radioactive pulse-chase experiments using VSV-G-GFP. VSV-G-GFP is complex glycosylated in the Golgi and therefore the transport from the ER to the *medial* Golgi can be analyzed by pulse-chase experiments combined with Endo H digestions of the chased protein. The half-maximal conversion of Endo H-sensitive to Endo H-resistant protein of VSV-G-GFP is about 40 min. Both in control and p28-depleted HeLa cells about 45% of VSV-G-GFP was Endo H-resistant at 40 min after chase indicating normal anterograde transport from ER to *medial* Golgi in p28 knockdown cells (Figure 8C). Moreover, we monitored total secretion of ^{35}S-methionine-labeled proteins in HepG2 cells. Three days after knockdown the amount of secreted proteins was unchanged in p28 knockdown cells compared to control siRNA treated HeLa cells (Figure 8D).

Taken together, we tested ER to Golgi as well as Golgi to plasma membrane transport of VSV-G-GFP in p28 knockdown cells. Neither of these transport steps was perturbed in p28-depleted cells. Forward traffic through the disrupted Golgi was identical to that observed through a compact Golgi in control cells. These results render it very unlikely that impaired protein transport caused the Golgi disruption phenotype in p28-depleted cells.

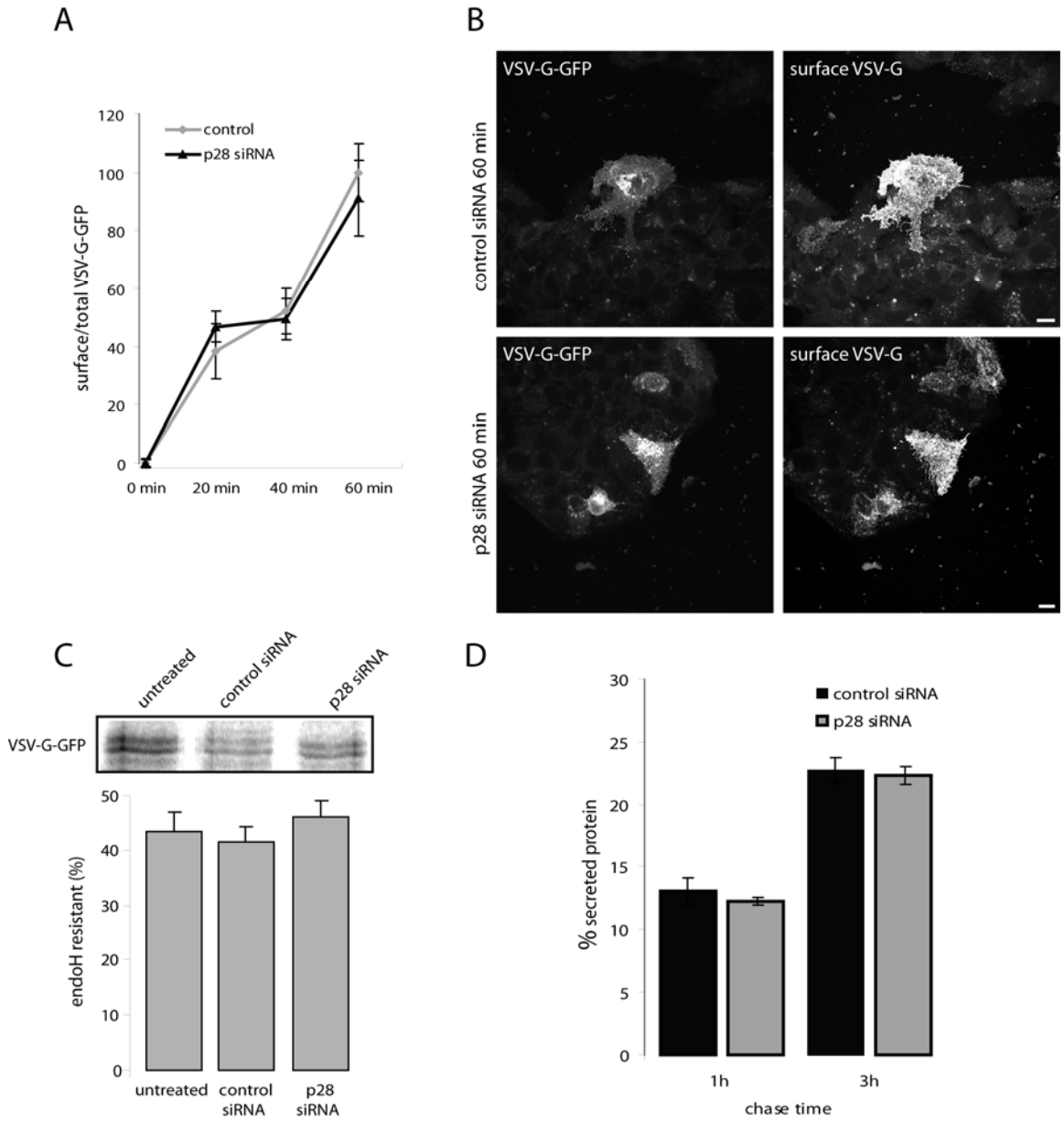

Figure 8: Secretory transport is p28-independent. Anterograde traffic of VSV-G-GFP from the ER to the plasma membrane in control and p28-depleted HepG2 and HeLa cells was investigated. (A) HepG2 cells were treated with control or p28 siRNA, 2 days later transfected with ts045 VSV-G-GFP and put at 40°C. The day after, cells were subjected to immunofluorescence using antibodies against VSV-G. Transport of ts045 VSV-G-GFP was measured after release from the 40°C ER block by shifting the cells to 32°C. Surface to total fluorescence was quantified, indicating the relative amount of VSV-G on the plasma membrane at different time points after the shift. Total VSV-G was measured using GFP fluorescence and surface VSV-G was measured by staining the cells with an antibody against the lumenal fragment of VSV-G (I-14). In both, control (diamonds) or p28-depleted (rectangles) HepG2 cells the transport of VSV-G-GFP from the ER to the plasma membrane was comparable. Data show mean values ± SEM (>100 cells per condition and experiment) from 3 independent experiments. (B) Immunofluorescence of control or p28 siRNA transfected cells showed prominent staining for GFP and VSV-G-GFP on the cell surface after 60 min of release from the ER. Bars, 10 μM. (C) Transport of VSV-G-GFP from the ER to the *medial* Golgi in control and p28 siRNA treated HeLa cells. Immunoprecipitated and Endo H digested VSV-G-GFP 40 min after radioactive labeling and chase is presented. In untreated, control or p28 siRNA treated

cells about 45% of the protein acquires Endo H-resistance. Therefore, anterograde transport of VSV-G-GFP to the *medial* Golgi is comparable in control and p28-depleted HeLa cells. Results are mean values ± SD of 3 independent experiments. (D) Additionally, control and p28 siRNA transfected cells were subjected to pulse-chase analysis of total secretion using ^{35}S-methionine. Conditioned media were collected and assayed for incorporated radioactivity after 1 and 3 h. P28 knockdown cells exhibited the same amount of secreted radiolabeled proteins than in control siRNA transfected cells. Results are mean values ± SD of 3 independent experiments.

COPI-mediated retrograde transport is p28-independent

Not only anterograde transport influences membrane flow in the early secretory pathway, but also retrograde traffic from the Golgi to the ER has an impact on Golgi integrity. Moreover p24 proteins were proposed to function in retrograde vesicle generation via the interaction of coatomer with p24 tails and because p23 was shown to act as ARF1 receptor on Golgi membranes (Gommel et al., 2001). Therefore we investigated COPI-dependent retrograde transport of temperature sensitive mutant of VSV-G fused with the KDEL receptor (ts045 VSV-G-KDELr) (Cole et al., 1998). At 32°C the fusion protein localizes to the Golgi apparatus, whereas shifting the cells to 40°C leads to the accumulation of recycled protein in the ER, since the mutant protein cannot exit the ER any more at the restrictive temperature. In both control and p28 knockdown HeLa cells VSV-G-KDELr localized to the Golgi in more than 80% of the cells (Figure 9A and C). Shifting the cells for 1 h to 40°C led to the accumulation of the construct in the ER (Figure 9B and C). Since the number of cells showing ER localization of VSV-G-KDELr was comparable between control and p28-depleted cells we concluded that COPI-mediated retrograde transport was not affected in the absence of p28 protein.

Lack of p28 does not affect the localization of the Golgi matrix protein GM130

It was shown previously, that knockdown of the Golgi matrix protein GM130 leads to Golgi fragmentation in HeLa cells (Puthenveedu et al., 2006). Depletion of GM130, which also reduces GRASP65 levels, inhibits bridging and subsequent fusion of equivalent cisternae. Perhaps GM130 recruits GRASP65 to Golgi membranes, which then tethers equivalent cisternae and primes them for fusion. Similar to p28-depleted cells, knocking down GM130 in HeLa cells does neither affect anterograde transport of VSV-G-GFP to the cell surface nor retrograde transport of Shiga toxin KDEL to the ER. Members of the p24 protein family were found in a complex with the Golgi matrix proteins GM130, GRASP65 and also GRASP55 (Barr et al., 2001). Because of apparent similarities between GM130 and p28 knockdown phenotypes and the interaction of p24

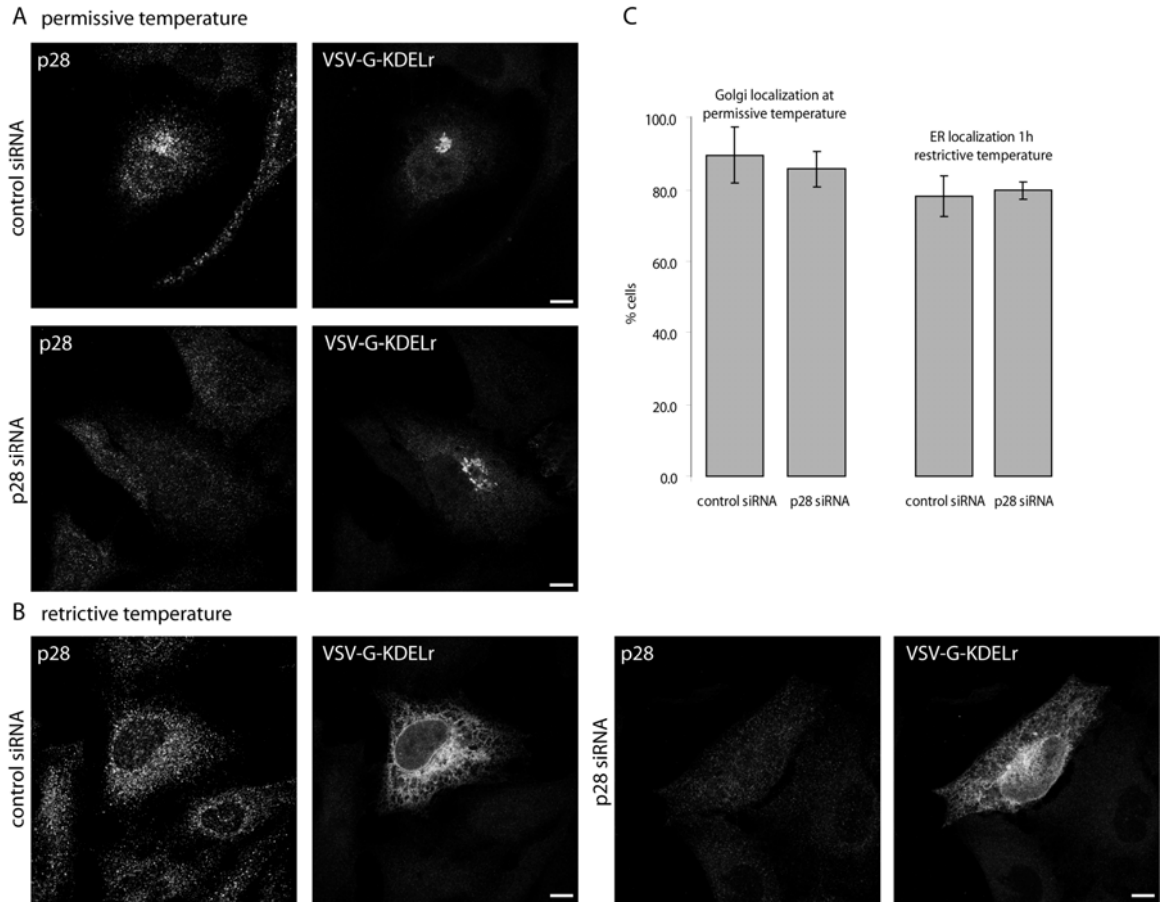

Figure 9: COPI-mediated retrograde transport is p28-independent. (A) VSV-G-KDELr was expressed in control or p28 siRNA transfected HeLa cells. Cells were subjected to immunofluorescence using p28 and myc antibodies. Incubating control cells at the permissive temperature (32°C) led to the localization of the fusion protein to the perinuclear Golgi. The same was observed in p28-depleted cells, where VSV-G-KDELr localized to the fragmented Golgi. (B) Shifting cells for 1 h to 40°C leads to the recycling of the protein to the ER, where it is trapped. Both control and p28 siRNA transfected HeLa cells show an ER pattern for VSV-G-KDELr. Bars, 10 µm. (C) Quantifications of Golgi localization at the permissive temperature and ER localization of the construct at the restrictive temperature revealed that the COPI-dependent recycling of the KDEL receptor construct was unchanged in p28 knockdown cells. Results are mean values in % ± SD of 3 independent experiments.

proteins with Golgi matrix proteins we investigated GM130 localization in p28-silenced cells. GM130 localizes to the *cis*-Golgi in mammalian cells (Nakamura et al., 1995). Control siRNA transfected cells showed GM130 localizing to the Golgi apparatus in immunofluorescence (Figure 10). Likewise, there was apparent GM130 staining associated with the Golgi in p28 knockdown cells (Figure 10). The correct localization of GM130 was not surprising since it is thought that GRASP proteins keep p24 proteins in the Golgi. Thus, the fragmented Golgi phenotype is independent of GM130 in p28-silenced cells.

In p28-depleted cells formation of cisternal connections is perturbed

Since we did not observe any defects in transport nor redistribution of Golgi matrix proteins, known to affect Golgi morphology, we explored whether p28 functions during assembly of the Golgi. We merged Golgi membranes with the endoplasmic reticulum, by treating cells with BFA. Biogenesis of the Golgi from the ER was monitored by washing out the drug. Cells were treated with 5 µg/ml Brefeldin A for 40 min and reformation of the Golgi after washout was quantified. Whereas about 90% of the cells exhibited a normal, compact Golgi 2 h after drug washout in control cells (Figure 11A), p28-depleted cells reformed a fragmented Golgi in 80% of the cells (Figure 11B). Based on these results we conclude that the lack of p28 perturbs Golgi ribbon formation. Already the electron microscopy data showing Golgi ministacks in cells lacking p28 led us to assume that these ministacks were not linked laterally. To test this hypothesis we asked the question whether these ministacks are in continuity with each other or if they remain isolated functional compartments. To account for presence of connecting tubular bridges in non-compact zones FRAP experiments were performed.

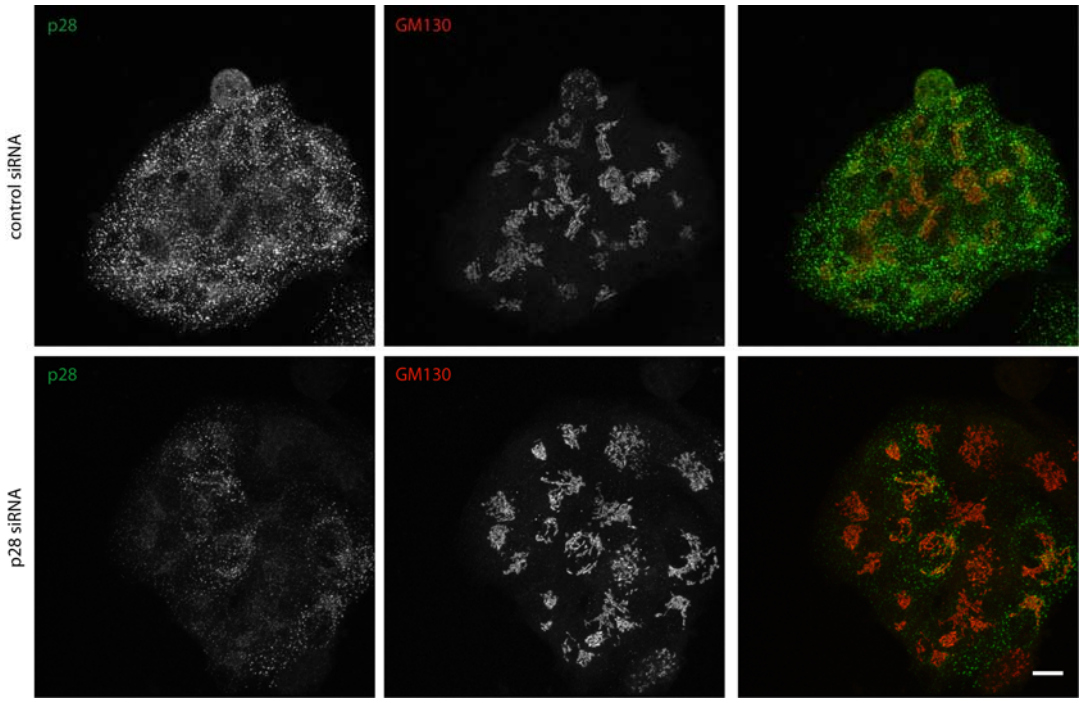

Figure 10: GM130 is still associated with Golgi membranes in p28-depleted cells. HepG2 cells were treated with control or p28 siRNA for 3 days and then subjected to immunofluorescence using GM130 and p28 antibodies. Under both conditions GM130 shows apparent Golgi staining. However, GM130 clearly showed a fragmented Golgi pattern in p28-silenced HepG2 cells. Bar, 10 µm.

We overexpressed GFP tagged β1,4-galacosyltransferase in siRNA transfected HeLa cells. In control and p28-depleted cells a region of the Golgi was bleached and subsequent fluorescence recovery in the bleached area was measured for 150 seconds (Figure 11D). In control cells continuity between fluorescent Golgi objects was demonstrated by rapid recovery of fluorescence in bleached areas of the Golgi apparatus (Figure 11C). Clearly, in p28 siRNA treated cells the bleached Golgi region failed to recover significantly from photobleaching (Figure 11C). These results were quantified for multiple experiments (Figure 11D). Representative movies are present in Supplemental movie S3 and S4. Taken together, in p28 knockdown cells the Golgi is able to assemble cisternae into stacks, but fails to accomplish the last step of Golgi formation, the linkage of stacks into a ribbon.

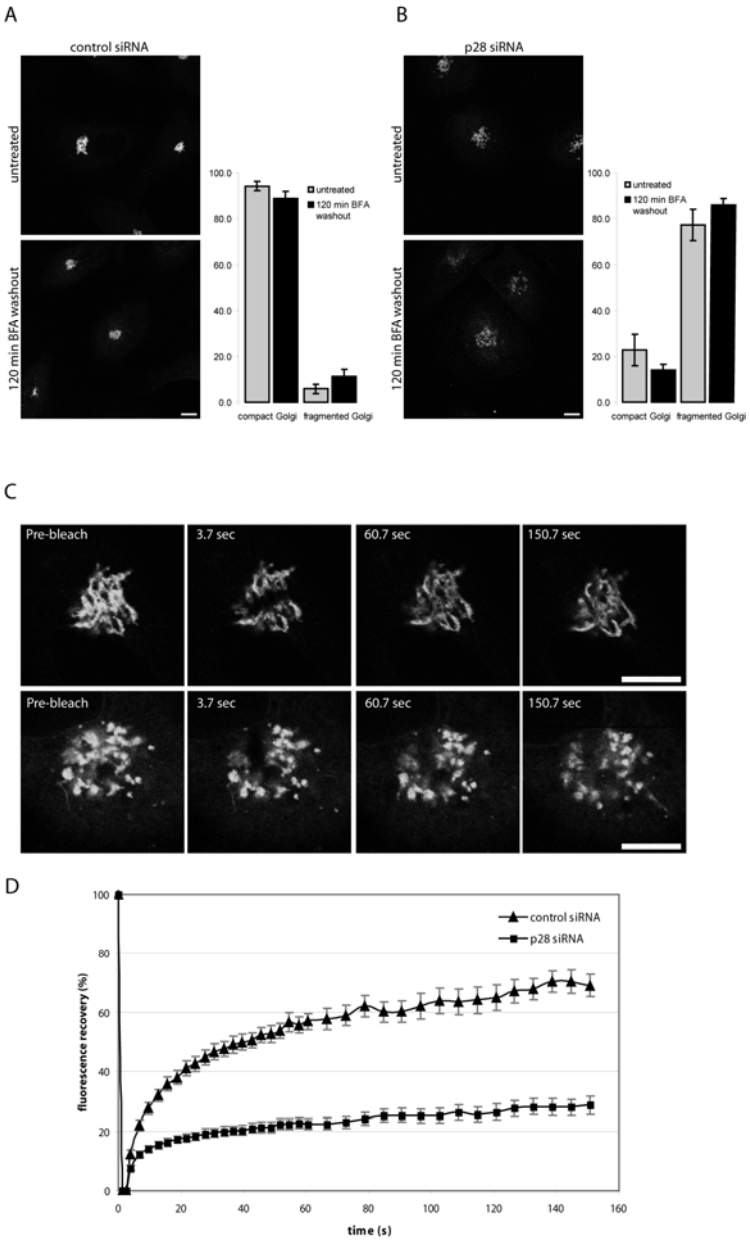

Figure 11: Bridging Golgi-tubules are prevented during assembly of the Golgi in p28-depleted cells. HeLa cells were treated with control or p28 siRNA. 3 days after transfection cells were treated with 5 µg/ml BFA for 40 min. Subsequently the drug was washed out and recovery of the Golgi was investigated 120 min later. Cells were fixed and stained for giantin. Whereas in control cells (A) the Golgi reformed as a compact perinuclear structure, p28-depleted cells recovered a fragmented Golgi (B). For quantifications cells with compact or fragmented Golgi phenotype were counted in more than 100 cells per experiment. Presented are mean values ± SD from 3 independent experiments. Bars, 10 µM. (C) HeLa cells were transfected with control or p28 siRNA, 1 day later they were transfected with GalT-EGFP and subjected to live imaging FRAP experiments two days later. A region within the Golgi was bleached using 2 frames of bleaching with 100% laser power. Representative images of indicated timepoints are shown. Bars, 10 µM. (D) Fluorescence was measured in the bleached area as well as in an adjacent unbleached area. The ratio was calculated and normalized to the initial values. Recovery of fluorescence was observed for 150 sec. Mean fluorescence recovery from 10 cells out of 3 independent experiments is indicated. Whereas in control cells (triangle) the bleached region rapidly recovered to about 70% of the initial fluorescence intensity, p28-depleted (rectangle) HeLa cells did not recover substantially. Shown are mean values ± SEM.

Supplemental movie S3 and S4: Revealing Golgi linkage by FRAP. HeLa cells were transiently transfected with GalT-EGFP as a Golgi marker and treated with control (Supplemental movie S3) or p28 siRNA (Supplemental movie S4). 3 days after knockdown they were imaged with a LeicaSP5 microscope. Bleaching was performed by applying two 100% laser pulses and membrane integrity was assayed by measuring the recovery of fluorescence in the bleached region of interest relative to an adjacent unbleached region.

Discussion

The present work indicates p28, a new γ subfamily member of p24 proteins, as an ERGIC, *cis*-Golgi protein. P28 accumulates in the ERGIC after Brefeldin A treatment indicating its ability to cycle in the early secretory pathway. This is substantially in agreement with our previous study in which p28 was found as component of purified ERGIC membranes in HepG2 cells after BFA treatment (Breuza et al., 2004). Based on our findings ultimately all the p24 members investigated, continuously cycle in the early secretory pathway (Dominguez et al., 1998; Jenne et al., 2002; Nickel et al., 1997; Rojo et al., 1997). Typically, we found p28 to interact with other p24 proteins. Immunoprecipitations revealed interactions with the α subfamily member p25 and the δ subfamily member p23. Overexpressed p28 did accumulate in the ER and required the coexpression of p23 to localize to the ERGIC, *cis*-Golgi. Interestingly in p28-depleted HepG2 cells also p23 protein levels were reduced. Therefore we conclude that p28 interacts with p23, requires p23 for correct localization and leads to reduced p23 protein levels when knocked down. Further, p28 knockdown cells revealed a fragmentation of the Golgi apparatus on the morphological level. This was detected by immunofluorescence for different Golgi marker proteins. On the ultrastructural level it became obvious that Golgi cisternae were stacked, but numerous cisternal stacks were not coaligned. Aiming to understand the mechanism behind the Golgi fragmentation in p28 knockdown cells we investigated the p28-knockdown phenotype in comparison to other conditions known to fragment the Golgi. For example, microtubule disorganization leads to the fragmentation of the Golgi into ministacks, which are dispersed throughout the cytoplasm. Microtubule disorganization as cause of Golgi fragmentation in p28-depleted cells was excluded, because microtubuli were organized normally in p28 siRNA-treated cells and the Golgi ministacks remained close to the nucleus.

Moreover, perturbing traffic has a strong impact on organelle morphology. For instance, perturbing ER exit site organization, which affects anterograde ER to Golgi traffic, by depleting Sec16, leads to the disruption of the Golgi ribbon (Watson et al., 2006). Also the knockdown of Sar1, a GTPase acting in the assembly of COPII-coated vesicles at ER exit sites, causes dispersion of the Golgi complex in cultured neurons (Ye et al., 2007). However, depletion of p28 in human cells did not perturb anterograde vesicular transport. Likewise, yeast cells lacking all eight p24 family members display normal growth (Marzioch et al., 1999; Springer et al., 2000). Furthermore, retrograde

transport affects Golgi maintenance. If KDEL receptor-dependent retrograde transport is prevented by depleting KAP3, the non-motor subunit of kinesin2, the Golgi fragments (Stauber et al., 2006). Further, coatomer, implicated in retrograde vesicle formation, was shown to be necessary for compartmentalizing organelles of the secretory pathway (Styers et al., 2008). Similarly, we reported recently that depleting putative cargo receptors (Surf4 and ERGIC-53 or p25), all showing a classical di-lysine (KKXX) retrieval motif, has an effect on coatomer-association with the Golgi and fragments the Golgi (Mitrovic et al., 2008). Most likely the recruitment of coatomer to Golgi membranes via these molecules is the reason for Golgi fragmentation under these conditions. The Golgi phenotype after depleting p28 cannot be explained by COPI redistribution, because the βCOP staining on Golgi membranes remained normal in p28-depleted cells. This was not surprising since p28 compared to p25, Surf4 and ERGIC-53, does not contain a canonical di-lysine motif (Bethune et al., 2006; Cosson and Letourneur, 1994; Jackson et al., 1990).

Measuring retrograde transport of VSV-G-KDEL receptor from the Golgi to the ER revealed no change of COPI-mediated retrograde transport between control and p28-depleted cells. This indicates that neither retrograde transport per se nor retrograde-acting motors were affected in p28-depleted cells.

Other proteins important for Golgi integrity are tethering proteins. These proteins mediate the first contacts between incoming vesicles and target Golgi membranes. For instance, the depletion of the tether p115 leads to Golgi fragmentation. Compared to p28 knockdown cells the knockdown of p115 in mammalian cells shows diminished anterograde transport. Therefore and because p115 still localizes to the Golgi in p28-depleted cells in immunofluorescence (unpublished observation) we exclude the perturbation of p115-mediated tethering events in p28-depleted cells.

The Golgi phenotype in p28-depleted cells resembles strongly the Golgi-phenotype after GM130/GRASP65 knockdown. GM130-depleted cells show no defects in anterograde or retrograde transport, but the Golgi fragments into ministacks, which are not linked laterally. It was proposed that the Golgi matrix protein GM130 and the stacking proteins GRASP65 and more recently also GRASP55 act directly by cross-bridging adjacent cisternae for fusion (Feinstein and Linstedt, 2008; Puthenveedu et al., 2006). However there is contradictory data showing that depletion of GM130 or GRASP65 does not necessarily lead to Golgi fragmentation but rather affects centrosome morphology (Kodani and Sutterlin, 2008; Sutterlin et al., 2005). Because of the similarities and the known interaction of some p24 proteins with GM130 and GRASP

proteins (Barr et al., 2001), we analyzed the distribution of GM130 in p28-depleted HepG2 cells. We did not see a significant redistribution of GM130 from Golgi membranes in p28-depleted cells. Therefore we conclude that the p28 knockdown phenotype is independent of GM130.

Overall, we can exclude various conditions leading to Golgi fragmentation in p28-silenced cells. We did observe normal anterograde and retrograde transport as well as normal distribution of the Golgi matrix protein GM130 and coatomer. Aiming to understand in more detail the origin of Golgi fragmentation in p28-depleted cells we asked if p28 is involved in the early steps of Golgi biogenesis. Mergence of the Golgi membranes with the ER utilizing BFA and subsequent washout of the drug enabled us to follow Golgi reformation. Golgi reformation experiments showed that in p28-depleted cells the Golgi was incompetent to assembly into a compact Golgi. Conducting FRAP experiments we were able to analyze in more detail, which step was perturbed during Golgi biogenesis in p28 knockdown cells. Golgi ministacks did not possess membrane continuity with each other in p28-depleted cells. Based on these results, we conclude that the presence of p28 is required for ribbon formation during Golgi assembly. Since p28 was shown to localize to ERGIC membranes or Golgi nucleation sites after BFA treatment we propose that it acts in ribbon formation during Golgi assembly. The formation of the ribbon is the last step in Golgi biogenesis. First, Golgi biogenesis requires membrane fusion via the AAA ATPase p97 and its adaptor p37 (Uchiyama et al., 2006). Then the forming cisternae assemble into a stack. Requirements for this process are mostly unknown *in vivo*. In the final step proteins like GM130 and GRASP were reported to be involved. However, one can only speculate how this compaction of the Golgi proceeds. Perhaps, at the rim of a Golgi cisterna a tubule forms. Subsequently it extends along cytoskeletal elements towards the neighbouring Golgi stack. In close proximity tethering with an equivalent cisterna takes place. Finally the tubule fuses with another Golgi cisterna stabilizing the higher-order architecture. Since p28 exposes only a 12 amino acid short tail into the cytoplasm it is rather unlikely that it functions as tethering factor like the long coiled-coil proteins of the golgin family. The fusion step seems also not to be affected in p28-depleted cells, since formation of cisternae would already require fusion of membranes and they were formed and stacked normally. Moreover, breakdown of the Golgi because of a simple imbalance in traffic was excluded. Also the action of molecular motors is rather unlikely to be affected in p28-silenced cells since this would also lead to defects in anterograde or retrograde transport. Currently we can only speculate about the function of p28 during Golgi assembly. One hypothesis

would be that p28 might recruit proteins mediating linkage with the cytoskeleton (Simpson et al., 2006). Under this condition one would expect normal transport and normal distribution of golgins, coatomer and Golgi matrix proteins. However, weakening of these connections between *cis*-Golgi cisternae and the cytoskeleton would lead to reduced proximity of ministacks. Tubules from Golgi rims would still be formed, but would not be able to reach the neighbouring cisterna. The consequence would be a stacked Golgi, which fails to establish a ribbon. Overall we conclude that more than coatomer, Golgi matrix and SNARE proteins are required to form a Golgi ribbon in mammalian cells.

Part II –pH measurements in the early secretory pathway *in vivo*

Introduction

Implications of pH on cellular processes

Eukaryotic cells need to be compartmentalized to execute different cellular processes. The chemical microenvironments of these compartments have to suit their biochemical function. For example the milieu in the cytosol is fundamentally different from the lumen of the ER, where proteins are folded and disulfide bonds are generated in an oxidizing ambience (Agarwal and Auchus, 2005). Lysosomes possess an acidic milieu, which is important for proper functioning of hydrolases. These enzymes are only active in lysosomes and not during their delivery in earlier, less acidic organelles. Thus, organellar biochemical properties have to be carefully controlled and maintained for proper cell functioning. Aberrations in normal organellar pH homeostasis can lead to diseases like cystic fibrosis or Dent`s disease (Weisz, 2003). Amongst other parameters pH has an impact on several cellular processes like **intracellular membrane transport** (Carnell and Moore, 1994; Yilla et al., 1993), **prohormone processing and cleavage** (Carnell and Moore, 1994; Nishi and Forgac, 2002; Schmidt and Moore, 1995; Orci et al., 1987), **ligand receptor dissociation** (Appenzeller-Herzog et al., 2004; Appenzeller et al., 1999; Wilson et al., 1993), **viral entry** (Helenius et al., 1980), **receptor recycling** (Desbuquois et al., 1992), **localization of proteins** (Bachert et al., 2001; Chapman and Munro, 1994; Linstedt et al., 1997; Puri et al., 2002) and **posttranslational processing** (Axelsson et al., 2001; Palokangas et al., 1994).

Historically the first indication that cells have low intracellular pH compartments came from observations by Metchnikoff, who used protozoa to phagocytose litmus paper, which displays colour depending on the pH. Inside the cells the paper changed colour from blue to red indicating an acidic pH (Metchnikoff, 1968). Since then acidic compartments in living cells have been explored extensively using different techniques. Even small pH differences of less than 0.5 units between organelles can be essential for conducting biochemical reactions (Wu et al., 2000). Here I will focus on pH-dependent ligand/receptor dissociation, protein localization, posttranslational processing of secretory proteins, intracellular membrane transport and functions of pH in the endocytic pathway.

Regulation of receptor ligand interactions

Continuous flow of proteins and lipids in the secretory pathway requires efficient regulation. For instance the retrieval of escaped lumenal ER proteins as well as the efficient export and transport of secretory proteins out of the ER has to be tightly regulated.

Cargo receptors like ERGIC-53 or the KDEL receptor interact through motifs on their cytoplasmic tails, with coat proteins (COPII and COPI). The COPII coat mediates budding of vesicles from the ER for anterograde traffic, whereas the COPI coat is necessary to generate vesicles from ERGIC and Golgi membranes, mediating retrograde or intra-Golgi traffic. On the lumenal side the receptors bind to a subset of cargo proteins and thereby enhance their traffic in the early secretory pathway. For example it was shown that the KDEL receptor binds in a pH-dependent manner to peptides bearing a KDEL-signal *in vitro* (Wilson et al., 1993). This receptor ensures the proper retrieval of many ER resident proteins from post ER compartments. Based on *in vitro* data it was postulated that KDEL receptor binds cargo in acidic post-ER compartments and transports them back to the ER, where cargo release is triggered by neutral pH. Not only the retrieval of proteins by the KDEL receptor is pH-regulated but also the forward transport of proteins from the ER to the ERGIC is influences by pH. The transport lectin ERGIC-53 is a receptor for glycoproteins (Appenzeller et al., 1999). Its cargo, cathepsin Z, can be crosslinked with ERGIC-53 in the ER. Inactivation of the carbohydrate recognition domain in ERGIC-53 inhibits binding to cathepsin Z, indicating the interaction via the sugar chains of cathepsin Z. Cathepsin Z acquires the lysosomal-targeting signal mannose-6-phosphate. Only in the presence of BFA, which merges ER and Golgi membranes, phosphorylated protein was cross-linked to ERGIC-53. This indicates that under normal conditions cathepsin Z is released from the lectin ERGIC-53 before reaching the *cis*-Golgi. Further, pH influences binding of purified recombinant ERGIC-53 to immobilized D-mannose *in vitro* (Appenzeller-Herzog et al., 2004). ERGIC-53 binds to D-mannose at neutral pH and physiological ER Ca^{2+}-concentrations and looses binding at acidic pH and reduced Ca^{2+}-concentrations. Treating cells with chloroquine, which rises intracellular pH, reduces the release of cathepsin Z in the ERGIC, arguing for a pH-dependent binding activity of ERGIC-53. The carbohydrate recognition domain of this receptor contains a histidine, which has the hallmarks of a molecular pH sensor. His178 is conserved in ERGIC-53 orthologs and positioned in a characteristic α-helix in the active site of the receptor called histidine ion sensor (HIS)-

loop. A model was proposed in which the cargo is bound in a calcium-dependent manner in the ER at neutral pH. The histidine residue might be considerably protonated at mildly acidic pH in the ERGIC. Upon arrival of the complex in the ERGIC, calcium is lost in a pH-dependent manner. This leads to inactivation of the mannose binding pocket and results in release of the glycoprotein cargo.

Both, KDEL and ERGIC-53 receptor, bind cargo in a pH-dependent manner. Whereas KDEL receptor binds cargo proteins at lower pH in the *cis*-Golgi and releases them in the ER, ERGIC-53 interacts with cargo proteins in the ER and releases them in the ERGIC. Thus, both use the same mechanism but in a reciprocal way. Taken together, pH seems to be a widely used mechanism to control and regulate protein-protein interactions and this implicates the importance of increased acidification along the organelles of the secretory pathway.

Protein localization and correct glycosylation of cargo

Not only binding of receptors to ligands is regulated by pH but also the localization of some proteins. Chapman et al. investigated the pH-dependent localization of the TGN protein TGN28 and the protease furin, which are continuously recycled from the plasma membrane to the Golgi (Chapman and Munro, 1994). In cells where pH is perturbed by chloroquine, these two proteins accumulate in an endosomal compartment. Beyond this other Golgi proteins like GPP130 and GP73 were shown to redistribute to endosomes after perturbation of lumenal pH with monensin (Bachert et al., 2001; Linstedt et al., 1997; Puri et al., 2002). This effect is reversible after drug washout. Moreover, the steady state distribution of glycosyltransferases to the Golgi depends on pH (Axelsson et al., 2001). Altering pH along the secretory pathway with ammonium chloride or bafilomycin A1 causes relocalization of *N*-acetylgalactosaminyltransferase 2, β1,2 *N*-acetylglucosaminyltransferase I and β1,4 galactosyltransferase 1 to vesicles of endosomal type (Ammonium chloride treatment) or to the plasma membrane (bafilomycin A1 treatment). Collectively, these data implicate that several Golgi proteins depend on proper pH regulation to localize correctly along the secretory pathway.

Protein Transport

Studies utilizing pH perturbing agents also gave insight into other pH-dependent processes. The vacuolar H^+-ATPase (V-ATPase) inhibitor concanamycin B significantly impairs intra-Golgi trafficking and Golgi to plasma membrane transport of albumin and

alpha1-antitrypsin in HepG2 cells (Yilla et al., 1993). Furthermore, treatment of semi-intact PC12 cells with nigericin, a protonophore, completely blocks export of secretogranin II from the TGN in a transport reaction assay (Carnell and Moore, 1994). These examples demonstrate that the perturbation of pH throughout all cell compartments leads to defects in protein transport.

pH in the endocytic pathway

Like in the secretory pathway, pH plays also a key role in endosomes. For example, it triggers and ensures the dissociation of internalized receptor-ligand complexes, which allows controlling both the rate of ligand uptake and the density of cell-surface receptors (Brown and Greene, 1991; Ciechanover et al., 1983; Forgac, 1992). In addition, acidification of late endosomes causes the release of lysosomal hydrolases from the mannose 6-phosphate receptor (Distler et al., 1991; Gonzalez-Noriega et al., 1980; Kornfeld, 1987). Penetration of certain viruses also depends on acidification of endosomes (Helenius et al., 1980; Marsh and Helenius, 2006; Smith and Helenius, 2004). Viral fusion factors change their conformation upon pH drop, which results in fusion with the endosomal membrane leading to penetration into the cytosol. Even the generation of vesicles, which requires the recruitment of βCOP protein and ARF1 to the cytoplasmic side of the membrane, appears to be a pH-dependent process (Aniento et al., 1996; Gu and Gruenberg, 2000; Zeuzem et al., 1992). Already years ago it was proposed that the cytosolic βCOP recruitment is regulated by a transmembrane pH sensor. Recently the V-ATPase, which facilitates acidification of organelles and vesicles, was found to serve as sensor (Hurtado-Lorenzo et al., 2006). PH-dependent recruitment of Arf6/ARNO (GEF for Arf6) to endosomes depends on the V-ATPase. Arf6 was shown to interact with the c-subunit and ARNO with the a2-isoform of the V-ATPase, which is targeted to early endosomes. The interaction between the a2 subunit of the V-ATPase and ANRO was shown to be intra-endosomal acidification-dependent. Further, when the interaction is disrupted, endocytosis is inhibited. Hence, the V-ATPase is an essential component of the endosomal pH-sensing machinery.

All these examples of cellular processes depending on pH affirm the importance of different pH in different compartments of the cell. Hence, the cell needs a machinery to generate and maintain unique pH values inside organelles. The next chapter will deal with mechanisms and proteins required to establish different pHs between organelles.

Regulation of organelle acidity

Acidification needs the active transport of protons into the lumen of an organelle. The intra-organellar pH is influenced by other ions, the activity of ion pumps and channels, proton leak, and the buffer capacity of the lumenal matrix (Grabe and Oster, 2001.). Acidified organelles build up a proton motif force (pmf), which opposes further acidification. This pmf has two components:

a) the membrane potential ($\Delta\psi$)
b) the proton concentration gradient (ΔpH)

Together chemical and electrical components of the proton-motive force determine the pH (Demaurex et al., 1998). The V-ATPase actively pumps protons into the lumen of intracellular organelles (Figure 1 (1)). The positively charged protons increase the membrane potential, which inhibits further acidification. However, efflux of cations (Figure 1 (2)), influx of anions (Figure 1 (3)) together with the specific proton leak of the organellar membrane (Figure 1 (4)) regulate acidification.

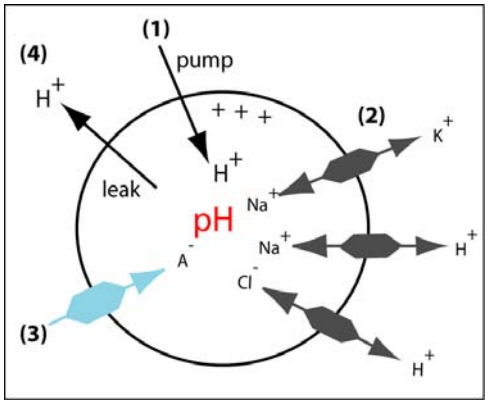

Figure 1: Regulation of lumenal pH. (1) Active proton pumping into the lumen of an organelle via the V-ATPase leads the interior to become acidic and electrically positive. (2) In the Golgi, endosomes and lysosomes several exchangers have an influence on lumenal pH regulation via transporting protons out of the lumen or transporting anions into the lumen. (3) In theory, counterion flow through anion channels would decreases membrane potential and therefore would facilitate acidification. However, it seems to play a minor role in practise. (4) Mainly proton pumping by the V-ATPase together with the proton leak rates of organellar membranes influence intra-lumenal pH.

The V-ATPase

The vacuolar H^+-ATPase resides in endomembranes of eukaryotic cells (endosomes, lysosomes and secretory vesicles) and on the plasma membrane of certain cells (Stevens and Forgac, 1997) as a large multisubunit complex with a molecular mass of nearly 10^6 Da (Weisz, 2003). The V-ATPase carries out ATP-dependent proton transport from the cytoplasmic side to the opposite side of the membrane (lumen or extracellular space (Figure 1)). It is an electrogenic pump, meaning its activity is influenced by the

membrane potential (Paroutis et al., 2004). Two domains form the multisubunit complex (Figure 2) (Nishi and Forgac, 2002; Stevens and Forgac, 1997). The V_1 domain is the peripheral complex composed of eight different subunits, which form a ball-like structure and a stack. This part is responsible for ATP hydrolysis. The V_0 domain is integral to the membrane and composed of five different subunits. It functions in proton translocation through the membrane. The exact subunit composition varies because several subunit isoforms are known (Schoonderwoert and Martens, 2001). For instance the "a" subunit has four isoforms in mammalian cells and targets the V-ATPase to different compartments (Hurtado-Lorenzo et al., 2006; Sun-Wada et al., 2006). Structurally, the V-ATPase resembles the ATP synthase and it operates by a similar rotary mechanism. The AB subunits form a hexameric ball, which hydrolyses ATP by the catalytic site of subunit A. This forces the rotation of a central stalk (D subunit) inside the hexamer. The stalk is linked to a ring of proteolipid subunits and causes rotation of this ring relative to the a subunit. Thereby protons are pumped across the membrane. A second stalk impedes the simultaneous rotation of a, the hexameric ball, the central stalk and the proteolipid ring.

To explore the impact of the V-ATPase on cellular processes the macrolite antibiotics bafilomycins and concanamycins are widely used experimentally to inhibit V-ATPase activity.

How is lumenal pH regulated?

The V-ATPase itself is present in almost all membranes even though there are differences in pH between individual compartments. It might be that pump densities vary among organelles, but there are no systematic studies comparing pump densities along the secretory pathway (Forgac, 1992). What is known is that the activity of the pump under physiological circumstances can be regulated by dynamic disassembly and reassembly of free V_1 and V_0 sectors (Qi et al., 2007). Other regulatory mechanisms involve disulfide bond formation, which inactivates the pump, conformational changes in the c subunits (in acidic environment the pumping capacity is reduced), variable proton-ATP coupling and targeting by different isoforms (Nishi and Forgac, 2002; Qi et al., 2007; Recchi and Chavrier, 2006; Schoonderwoert and Martens, 2001).

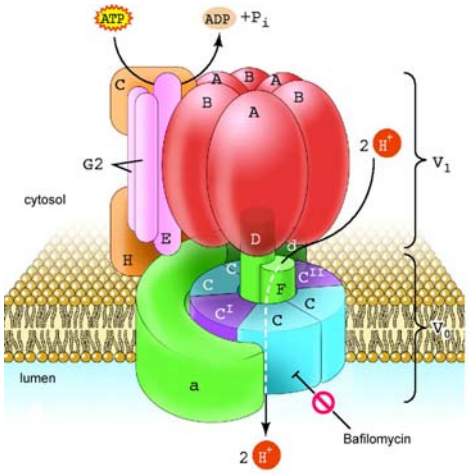

Figure 2: Schematic representation of the V-ATPase. The 10^6 Da V-ATPase is subdivided into the membrane spanning V_0 and the cytosolic V_1 part. Together they assemble the functional V-ATPase, which pumps protons across membranes utilizing a rotary mechanism. Reproduced from (Paroutis et al., 2004).

Intact membrane bilayers are permeable to protons to different extents, but relatively impermeable to other ions (Figure 1). Both proton pumping and proton leak are electrogenic, they require the movement of a compensating charge and are thus limited by the permeability of the organelle to counterions (Figure 1) (Demaurex, 2002). For example the presence of lumenal chloride ions decreases membrane potential and therefore facilitates organelle acidification, by anticipating a large inside-positive voltage that impedes V-ATPase function (Orlowski and Grinstein, 2007). Passive chloride flow is accomplished by the presence of chloride channels. So far effects of chloride channels on pH have only been observed in Golgi and post-Golgi compartments (see chapter: Organelle acidification and disease). In the Golgi, endosomes and lysosomes also cation/proton exchangers, Na^+/K^+ exchangers and Cl^-/H^+ exchangers help to generate optimal pH environments (Figure 1 (2)).

A more general but indirect impact on acidification comes from different proton leaks of organellar membranes. ER membranes have a three times greater proton permeability than Golgi membranes (Figure 3) (Wu et al., 2000). Because the ER is highly permeable to protons, it is susceptible to alterations in the cytosolic pH (Kim et al., 1998). The Golgi is more acidic than the ER because it has an active proton pump and fewer or smaller proton leaks. For the TGN, which is even more acidic than the Golgi, it was also observed that the endogenous proton permeability was quite low (Demaurex et al., 1998). pH heterogeneity of individual compartments of the Golgi are most likely explained by the abundance of pumps or the proton leak and neither buffer capacity nor counterion permeabilities are key determinants (Wu et al., 2000).

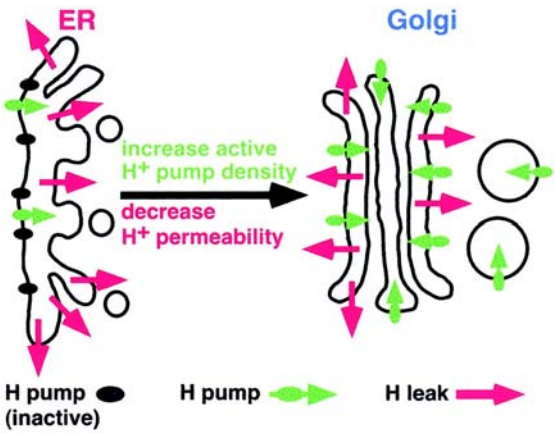

Figure 3: Regulation of lumenal pH. Lumenal pH is a result of mainly two mechanisms. The V-ATPase pumps protons actively into the lumen, whereas the permeability of the organellar membrane assigns the leak of protons back into the cytosol. Increase in active proton pumping combined with a decrease in permeability of the membrane along the early secretory pathway establishes optimal pH in these organelles. Reprodued from (Wu et al., 2001).

Ionophores

The lipid bilayer of eukaryotic membranes is only selectively permeable for inorganic ions. Ionophores, which are mostly synthesized by microorganisms, increase permeability of the membranes for specific ions. Two such compounds were used during this study:

Monensin (Mollenhauer et al., 1990) is synthesized by *Streptomyces cinnamonensis* and is a macrolite antibiotic which facilitates the transmembrane exchange of sodium ions for protons. This compound is freely soluble in the lipid bilayer and diffuses or shuttles through the membranes of the cell. A consequence of this exchange is the neutralization of acidic intracellular compartments such as the Golgi apparatus, lysosomes and endosomes. A secondary effect is cisternal swelling due to osmotic uptake of water to compensate for the inward movement of ions. Monensin acts quite rapidly and changes in the Golgi apparatus may be observed already after a 2-5 min exposure. Late Golgi processing functions such as terminal glycosylation and proteolytic cleavages are most susceptible to inhibition by monensin. Monensin does not affect endocytosis itself, but intracellular degradation of internalized ligands may be prevented.

Nigericin exchanges potassium ions for protons and is derived from *Streptomyces hygroscopicus.* It forms a 1:1 complex with the monovalent cation like monensin does (Stern, 1977).

Methods used to measure pH in situ in different cellular organelles

Several methods have been developed to measure pH inside cells. Microelectrodes can only be used for relatively large cells, whereas small cells can be targeted with pH-dependent dyes. Since the 1970s intracellular pH measurements were routinely carried out using pH-dependent dyes like fluorescein or the derivate BCECF. These dyes were popular because of their resistance to organellar enzymes, stability and nontoxicity (Demaurex, 2002). Adding fluorescein-labeled dextran to cells leads to pinocytosis and targeting of the probe to the endocytic system (Yamashiro and Maxfield, 1987a; Yamashiro and Maxfield, 1987b).

These pH probes require proper calibration, which was either done *in vitro* or *in vivo* with diverse methods. Szatkowski and Thomas (Szatkowski and Thomas, 1986) exposed dye-loaded cells to a weak acid or a weak base and calculated the original pH from the resulting pH change. This method can only be applied if the pH probe possesses linear pH sensitivity. Later this method was developed further to a so called null point method also suitable for indicators with non-linear pH-dependent fluorescence change (Eisner et al., 1989). Cells were incubated with several different weak acid/base mixtures of a given pH to narrow down the actual pH in the cell. In such a way cytosolic pH measurements were possible, but individual organelles could not be targeted at that time. The probe could just be localized to the cytosol and lysosomes, via endocytosis of dextran (Ohkuma and Poole, 1978). Other techniques were needed to target dyes selectively to intracellular compartments.

In the mid 1980s it was shown that the *trans*-Golgi is an acidic compartment. Anderson et al. loaded cells with DAMP, a weak base and congener of dinitrophenol, which diffuses into cells and accumulates in the lumen of acidic organelles (Anderson et al., 1984; Anderson and Pathak, 1985). There it can be fixed and processed for detection by an antibody followed by electron microscopical analysis. The authors found DAMP to accumulate specifically in multivesicular bodies, lysosomes, endosomes, forming secretory vesicles, and the *trans*-Golgi cisternae. Following this study several groups applied ingenious strategies to target dyes to the Golgi apparatus to measure pH *in situ*. For example liposomes, which fuse selectively with the Golgi, were used (Seksek et al., 1995). Although a great achievement, the disadvantage of this method is the dilution of the Golgi content by the liposomes, which might alter the buffering capacity of the organelle. Additionally the dye is rapidly transported out of the Golgi and the

measurements have to be carried out in a relatively small time window. Another group utilized the retrograde transport of verotoxin receptor to the Golgi and ER (Kim et al., 1996). Enhanced delivery to the endoplasmic reticulum was achieved by adding the C-terminal ER retrieval signal KDEL to the B subunit of the toxin. Yet another approach to access the Golgi was to take advantage of chimeric proteins and fluoresceinated antibodies using furin and TGN38, which continuously cycle from the plasma membrane to the TGN (Demaurex et al., 1998). The extracellular domain was replaced by CD25 for which highly specific fluoresceinated antibodies are available. Labeling of these chimeric proteins with the fluoresceinated antibodies from the outside of the cell leads to internalization of the antigen/antibody complexes and hence to the targeting of the pH indicator to the TGN. Alternatively, it is possible to use ER- and Golgi-targeted avidin, followed by the addition of membrane-permeable fluorescein-biotin as a pH indicator (Wu et al., 2000). Another technique is to express an antibody and then to incubate with cell-permeable ligand-fluorophore conjugates permitting measurements in ER and Golgi (Farinas and Verkman, 1999).

In the late 1990s genetically encoded indicators, which can be selectively expressed in defined intracellular compartments by addition of organelle-specific targeting signals, became available. Miesenboeck et al. performed structure-directed combinatorial mutagenesis of wildtype green fluorescent protein (GFP), which displays pH-dependent fluorescence (Miesenbock et al., 1998). Two classes of pH-sensitive fluorescent proteins (pHluorins) were generated, termed “ratiometric” and “ecliptic”. Wildtype GFP shows two excitation peaks at about 395 and 475 nm. Ratiometric pHluorin shows a pH-dependent shift in the excitation spectra. For quantitative measurements the fluorescence ratio of pHluorin excited at 410 and 470 nm is calculated. The lower the pH the higher is the fluorescence at 470nm, whereas the fluorescence at 410 nm is decreasing.

Other GFP mutants were also shown to have pH-dependent absorbance and fluorescence (Bokman and Ward, 1981; Kneen et al., 1998; Llopis et al., 1998). They exhibit acidification-dependent decreases in excitation- and fluorescence emission spectra (Figure 4). Overall fluorescence is quenched when pH is decreased. Especially EGFP and EYFP mutants are suitable as physiological pH indicators. The main advantage of using EGFP/EYFP is the potential to generate fusion constructs with mammalian proteins. Their targetability and the non-invasive manner of measuring denoted a big step in the field of intracellular pH measurements.

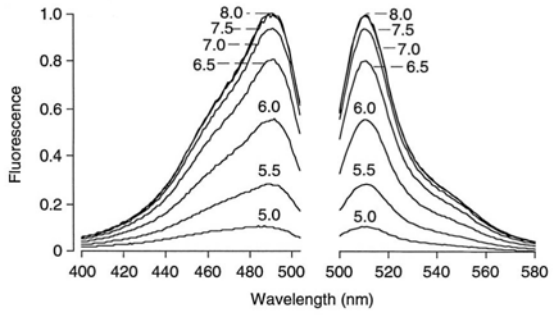

Figure 4: pH-dependent excitation- (left) and emission- spectra (right) of EGFP. Decreasing pH leads to decreased fluorescence excitation as well as fluorescence emission of EGFP. Reproduced from (Kneen et al., 1998).

pH in the cytosol, ER, Golgi, mitochondria, endosomes and lysosomes

With the different methods available several studies on intra-organellar pH were performed. The endocytic system was the first target of pH measurements. Especially the convenient accessibility to these compartments via pinocytosis was an advantage. Already in 1978 Ohkuma et al. estimated **lysosomal pH** in macrophages to be 4.7 - 4.8 (Ohkuma and Poole, 1978). They added FITC-dextran to cells for 24 h and showed, that after subcellular fractionation the probe localized to the lysosomal compartments. Treating cells with chloroquine led to a substantial increase in intra-lysosomal pH. These results supported the idea of an acidic pH in lysosomes. Four years later fluorescein-α_2-macroglobulin was targeted to **endocytic vesicles**, which did not colocalize with acid phosphatase, and calculated the pH to be 5.0 ± 0.2 (Tycko and Maxfield, 1982). The DAMP approach confirmed data about lysosomes and endosomes and in addition revealed the **Golgi** to be acidic (Anderson and Pathak, 1985). This new finding started people to be interested in Golgi pH. Ten years later numerous publications about Golgi pH were published. Different strategies to target pH-dependent fluorescent dyes to the Golgi apparatus were developed and applied to measure **intra-Golgi** pH. Values ranged between 5.95 (Demaurex et al., 1998) and 6.47 (Schapiro and Grinstein, 2000) and were in good agreement with the notion that the Golgi is mildly acidic. The pH of the **TGN** was shown to be between 6.17 (Seksek et al., 1995) and 6.34 (Machen et al., 2003), which is very close to the average Golgi pH. At the same time, with the development of these new targeting techniques and the availability of GFP, endosomal pH was reinvestigated with these methods and **endosomal pH** was measured to lie between 5.51 (Miesenbock et al., 1998) to 6.77 (D'Souza et al., 1998).

In contrast the **ER** was found to have a neutral milieu ranging around 7.1-7.4 (Kim et al., 1998; Wu et al., 2001). Since **secretory granules** need an acidic lumen for correct processing of prohormones their pH was also worth knowing. VAMP2-pHluorin was

targeted to secretory granules and their pH was found to be 5.67 (Miesenbock et al., 1998). Using pHluorin Jankowski et al. targeted **peroxisomes** and measured their pH to be between 6.90 and 7.1, resembling the cytosolic pH (Jankowski et al., 2001). By fusing the 12 N-terminal residues of the presequence of cytochrome c subunit IV with EYFP, **mitochondrial pH** was investigated to be 7.98 ± 0.07 in HeLa cells (Llopis et al., 1998). Figure 5 shows a summary of the exocytic and endocytic pathway compartments with their corresponding pHs.

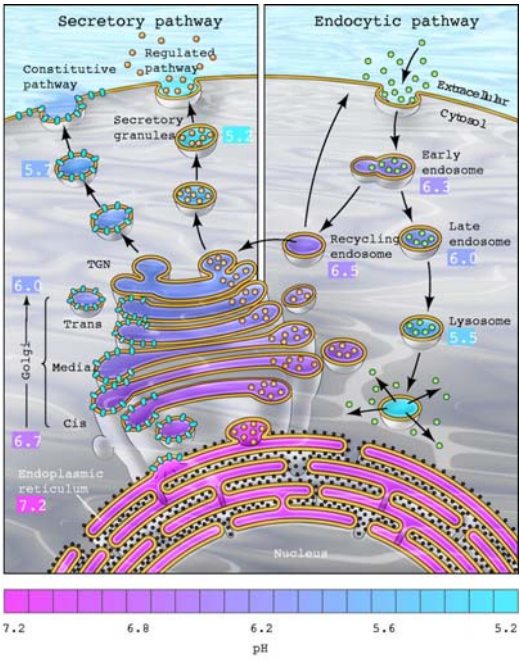

Figure 5: pH along the exocytic and endocytic pathway. Endosomes show gradual acidification from early to late endosomes. The pH of lysosomes is even more acidic. Along the exocytic pathway there is also a gradual acidification starting at neutral pH in the ER to acidic pH of about 5.2 in secretory granules. Reproduced from (Paroutis et al., 2004).

Organelle acidification and disease

Misregulation of organellar pH is associated with the progression of **cancer**, **Dent`s disease**, and **cystic fibrosis** (Weisz, 2003). Transformation of cells correlates with a higher cytosolic pH. In many tumour cell lines the V-ATPase resides in the plasma membrane, which might lead first to an elevated cytosolic pH (Gillies et al., 1990) and second to an acidic extracellular environment (Griffiths, 1991). The acidification of the extracellular surrounding is necessary for invasion and the metastatic potential is correlated with the level of V-ATPase activity on the plasma membrane (Martinez-Zaguilan et al., 1993). 3T3 cells expressing the yeast plasma membrane H^+-ATPase were shown to grow serum-independent and are tumorigenic when injected into nude mice. Further, it was proposed that altered cytosolic pH plays a role in multi drug resistance. Treating drug-resistant cells with bafilomycin A1, leads to the intracellular accumulation of drugs and renders the cells sensitive again (Marquardt and Center, 1991).

Dent`s disease is an X-linked renal disorder caused by mutations in the CLC5 gene encoding a chloride channel. The protein is highest expressed in kidney, but also found in liver, brain, intestine and testis. Patients suffer from proteinuria, excess urinary secretion of phosphate and calcium, kidney stones, rickets and nephrocalcinosis (Wrong et al., 1994). CLC5 is thought to supply the counterion conductance required for renal acidification (Weisz, 2003). Impaired acidification of intracellular vesicles causes altered endocytosis, but might not be the only CLC5-dependent mechanism (Devuyst et al., 2005; Veizis and Cotton, 2007).

Another disease linked to altered intracellular pH is cystic fibrosis. It occurs with an incidence of about 1 in 2000 live births. Patients suffer from pulmonary accumulation of viscous mucus, chronic airway infection, pancreatic dysfunction, high levels of sweat chloride and infertility in males (Weisz, 2003). The affected gene encodes a cAMP-regulated chloride channel (CFTR, cystic fibrosis transmembrane conductance regulator). Based on the acidification hypothesis postulated by Barasch and coworkers *trans*-Golgi, TGN, prelysosomes and endosomes of cystic fibrosis cells show a defect in acidification which is a result of diminished chloride conductance (Barasch and al-Awqati, 1993; Barasch et al., 1991). Sialyation of lipids and proteins is reduced, which leads to an altered glycosylation of mucins. In contrast other studies showed that TGN pH in cystic fibrosis cells is hyperacidified in comparison with control cells (Chandy et al., 2001; Machen et al., 2001). However, a small difference of 0.2 pH units was stated to be unlikely to be of physiological relevance. However, Poschet et al. measured a more pronounced TGN pH difference in cystic fibrosis cells of 0.6-0.7 pH units (Poschet et al., 2001). In addition endosomes were hyperacidified and Transferrin receptor recycling was altered (Poschet et al., 2002). There is some uncertainly about these data since other groups were unable to observe a change in pH in TGN and endosomes, when CFTR was transfected into CHO, 3T3 and L cells (Biwersi et al., 1996; Dho et al., 1993; Seksek et al., 1996). Taken together, the exact mechanism by which CFTR regulates organelle pH remains to be elucidated.

Aim of the project

pH measurements in the early secretory pathway *in vivo*

Organelles of the secretory and endocytic pathways display characteristic chemical properties. Among other processes compartmental pH changes are essential for cargo binding to and subsequent cargo release from transport receptors. The pH of the ER, Golgi and endosomes has been investigated in different studies. There is only rudimentary knowledge about the lumenal pH in the early secretory pathway, particularly the ERGIC. I*n vitro* data showed that the organelles of the early secretory pathway may exhibit a gradient of decreasing pH. For the ERGIC, it was postulated that pH changes are involved in anterograde and retrograde cargo delivery by ERGIC-53 and KDEL receptor (Appenzeller-Herzog et al., 2004; Wilson et al., 1993). Further evidence comes from studies of the rat homolog of ERGIC-53, which accumulates in tubules after inhibition of the V-ATPase with Bafilomycin A1 (Palokangas et al., 1998). A combined treatment with Bafilomycin A1 and Brefeldin A leads to the inhibition of mannosidase II redistribution to the ER which indicates a role of pH and in particular the V-ATPase in retrograde trafficking. Biochemically it was shown that the c-subunit of the V-ATPase is enriched in the intermediate compartment fraction (Ying et al., 2000). These data together with the evidence of early V-ATPase assembly in the ER in yeast suggest a pH change already from the ER to the ERGIC in mammalian cells.

Material and Methods

Recombinant DNA

Standard molecular biology protocols including PCR amplifications and ligations were used. Oligonucleotides were from Microsynth (Switzerland) and enzymes from New England BioLabs. Throughout this study, GFP refers to the enhanced version of GFP. All constructs were verified by sequencing. To clone ER-targeted EGFP, the calreticulin signal sequence was introduced 5' of EGFP, which was modified with a KDEL signal at the 3' end. The following primers were used for DNA amplifications: 5' TCGGGATCCGGTGAGCAAGGGCGAGGAGCTG 3' (containing a *BamHI* site), 5' TCGTCTAGATTACAGCTCATCCTTGCCGAGAGTGATC 3' (containing a *XbaI* site); PCR constructs were digested with *BamHI* and *XbaI* and cloned into pcDNA3SScal vector. To target GFP to the Golgi, the first 61 amino acids of β1,4-galactosyltransferase were amplified and cloned into the pEGFP-N1 (Clontech) vector. The following primers were used for DNA amplifications: 5' CTGATAGATCTATGAGGCTTCGGGAGC 3' (containing a *BglII* site) and 5' AGGCGGAATTCTGAGCTGCAGCGGTGTGGAGAC 3' (containing an *EcoRI* site). For the analysis of ERGIC-targeted EGFP a stable HeLa cell line was used (Ben-Tekaya et al., 2005).

Reagents and antibodies

The following antibodies were used: mouse mAb A1-82 against BAP31 (Klumperman et al., 1998) (ALX-804-602; Alexis, Lausen, Switzerland), mouse mAb against giantin (G1/133/34) (Linstedt and Hauri, 1993), rabbit Ab against Sec31 (Shugrue et al., 1999) (kind gift from F. Gorelick, Yale University); As secondary antibodies Alexa 488- and Alexa 568- (Molecular Probes Europe BV, Leiden, Netherlands) were used. To equilibrate pH throughout the cells 10 μM monensin (Calbiochem, Monensin sodium salt, high purity, 475895) and 10 μM nigericin (Sigma, sodium salt, N7143) were used. Further chemicals used: Hepes (Applichem, A3268), NaCl (Merck), MES (Applichem, A1074), KCl (Fluka), $CaCl_2$ (Fluka) and $MgCl_2$ (Fluka) were used.

Live cell imaging

HeLa cells stably expressing EGFP-ERGIC-53 (treated with sodium butyrate for 8-12 h followed by incubation without sodium butyrate for at least 5 h) or transiently expressing ER- and Golgi-targeted EGFP were cultured on 18 mm round glass coverslips. They were then transferred into a Ludin chamber (Life Imaging Services GmbH, Switzerland, www.lis.ch) and imaged with a x100 1.4 NA Plan-Apochromat oil objective on a Zeiss Axiovert 135M microscope at 37°C. Images were taken with a three-CCD camera (Hamamatsu 3 CCD Cooled Digital Color Camera C7780) using a filter wheel to switch between excitation and emission wavelengths. The excitation/emission combination used was at 480/525nm for GFP (Chroma Technology). ImagePro® Plus software (Media Cybernetics®) was used for both recording and for image processing and the MatLab plugin Qu (written by A. Ponti, FMI Basel) was used for quantitative data analysis. Cells were kept in "outside buffer" (10mM Hepes, 10mM MES, 0.5mM $MgCl_2$, 0.5mM $CaCl_2$, 120mM NaCl and 2.5mM KCl pH 7.40 at 37°C) or incubated with different "pH buffers" (125mM KCl, 20mM NaCl, 10mM Hepes, 10mM MES, 0.5mM $CaCl_2$, 0.5mM $MgCl_2$ pH ranging from 4.0 to 7.7 at 37°C) (Kim et al., 1996).

Qu – Data analysis

Qu is a MATLAB toolbox for the visualization and analysis of N-dimensional datasets targeted to the field of biomedical imaging. It supports several microscopy image formats and offers a plugin mechanism and a consistent API for easy extension. One of its advantages compared to similar tools is that it makes use of the power of MATLAB and can use its innumerable tools and functions. Qu is open source and was written by Aaron Ponti (aaron.ponti@fmi.ch). It is distributed under the terms of the Mozilla Public License Version 1.1 and can be obtained from http://qum.sourceforge.net. The pH measurement functions were written as a plugin for Qu. Area based measurements were either performed automatically by "unsupervised fitting of mixture models" as described (Jain, 2002) or by drawing regions of interest by the user. Particle extraction for ERGIC measurements were performed by Qu as described (Meister et al., 2007). Here, no VOIs were extracted, but instead whole images were used at once. Particle tracking was performed by Qu as described (Ponti et al., 2005).

Immunofluorescence microscopy

Cells were cultured on 18 mm round glass coverslips. They were fixed with 3% paraformaldehyde and permeabilized with 0.1% saponin, 10 mM glycine in PBS (solution 1). Non-specific binding was blocked by 30-minute incubation in solution 1. Cells were then incubated with primary antibodies diluted in solution 1 followed by appropriate secondary antibodies for 60 minutes (solution 2). After several washes in 0.1% saponine in PBS (solution 2), the cells were embedded in Mowiol 4-88 (Calbiochem) supplemented with 1.3 mg/ml DABCO (Sigma-Aldrich). Images were obtained using a Leica TCS NT confocal laser-scanning microscope, with a 63x 1.32 NA or a 100x 1.4 NA lens, a pinhole diameter of 1 Airy unit and 488 nm laser excitation for GFP and 568 nm for Alexa568.

Results

Targeting EGFP to the organelles of the early secretory pathway

EGFP was targeted to the organelles of the early secretory pathway by generating fusion constructs targeting EGFP to the ER (Figure 1A), ERGIC (Figure 1B) and Golgi (Figure 1C). Expression of these constructs in HeLa cells in combination with co-stainings with endogenous organellar markers was used to test for the correct targeting. To target EGFP to the ER I cloned it into a pcDNA3 vector containing the calreticulin signal sequence. To assure retrieval of the protein back to the ER I modified the very C-terminal MDEL of EGFP to KDEL, which works as signal to bind to the KDEL receptor. Hence, recycling of escaped EGFP is assured. ER-targeted EGFP showed a reticular staining pattern, which entirely co-localized with the ER marker BAP31 (Figure 2A).

For ERGIC pH measurements I made use of a stable HeLa cell line expressing EGFP-ERGIC-53 (Ben-Tekaya et al., 2005). Whereas ER-background fluorescence was often observed with transient transfections this was not the case in this cell line. Further this construct was shown to behave like the endogenous protein. Immunofluorescence showed partial overlap of the COPII coat component Sec31 with EGFP-ERGIC-53 positive elements, which indicates the correct localization of the construct to the intermediate compartment (Figure 2B).

Golgi experiments were performed with HeLa cells expressing β1,4-galactosyltransferase GalT-EGFP already described (Cole et al., 1996). Transiently transfected HeLa cells expressing the GalT-EGFP showed bright juxtanuclear staining, coinciding with the Golgi apparatus. There was apparent colocalization between overexpressed GalT-EGFP and the *cis*-Golgi marker giantin (Figure 2C).

Since all three constructs were targeted correctly and showed minimal background fluorescence these fusion proteins were used for pH measurements in the early secretory pathway in living HeLa cells.

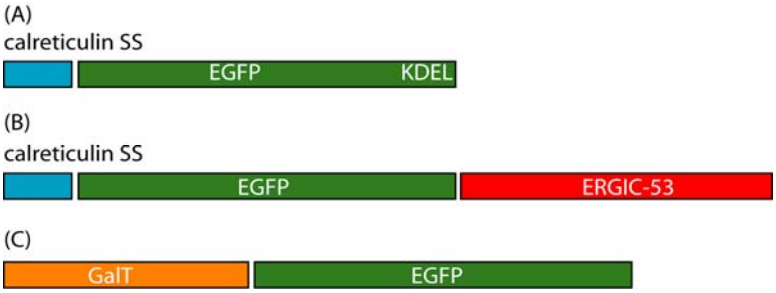

Figure 1: Schematic representation of the EGFP-fusion proteins. To target EGFP to the ER and ERGIC, a calreticulin signal sequence (blue) was introduced at the N-terminus followed by either EGFP(KDEL) (A, green) or EGFP-ERGIC-53 (B, green and red), respectively. To target the Golgi apparatus a fusion construct consisting of the first 61 amino acids of β1,4-galactosyltransferase (orange) and EGFP (green) was constructed (C).

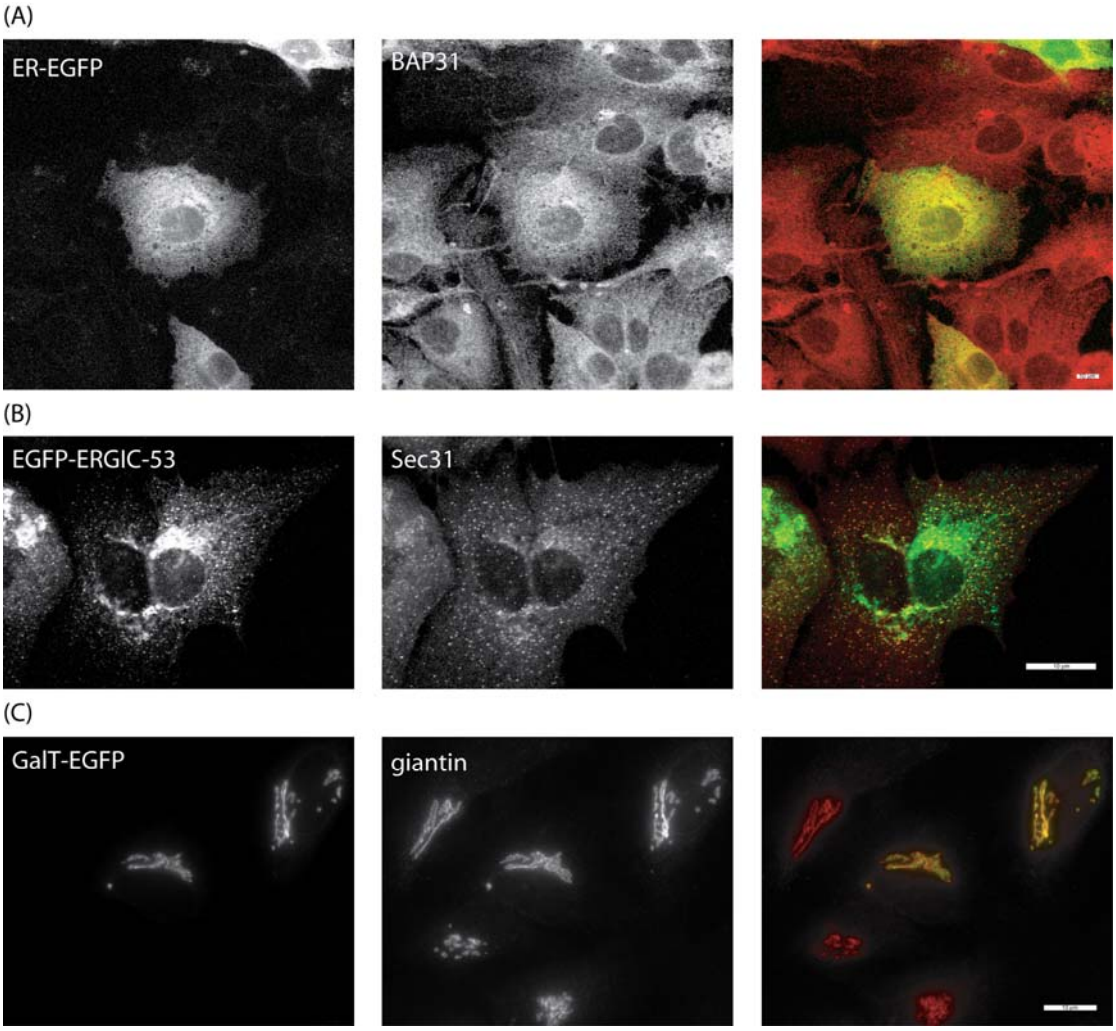

Figure 2: Localization of EGFP-fusion proteins in HeLa cells. (A) HeLa cells transfected with EGFP targeted to the endoplasmic reticulum (green) show reticular EGFP fluorescence 2 days after transfection, which significantly overlaps with the ER transmembrane protein BAP31 (red). (B) EGFP-ERGIC-53 (green) accumulates in the juxtanuclear region additionally to the presence in small peripheral punctate elements distributed throughout the cell. There is partial overlap with the COPII component Sec31 (red). (C) GalT-EGFP (green) distributes to the juxtanuclear Golgi apparatus, which was co-labeled with the *cis*-Golgi marker protein giantin (red). Bars, 10 µm.

EGFP responds to changes in pH in vivo

To confirm that EGFP can be used as reliable pH sensor I conducted titration experiments in the ER and Golgi *in vivo*. Cells expressing EGFP in the lumen of the ER or the Golgi were exposed to buffers with pH 7.7 in the presence of ionophores followed by incubation with another buffer solution of lower pH (Figure 3). For the ER, incubations with nine different pH buffers were done in one experiment sequentially, whereas for the Golgi only tandem incubations were possible. Otherwise osmotic swelling disturbed the measurements. Several of these tandem incubations were carried out down to a pH of 4.0. Since EGFP is pH-dependent its fluorescence decreases progressively upon lowering pH (Figure 3). Using buffers ranging from 7.7 down to 4.0 in multiple experiments, I obtained a best-fit titration curve for EGFP in the ER and Golgi, which is similar to previous findings (Figure 3) (Kneen et al., 1998; Llopis et al., 1998). At pH 5.8 and 6.1 EGFP showed 50% of its maximal fluorescence at pH 7.7 in ER and Golgi, respectively. The pH range of the titration curve was in total 3.7 pH units. The linear region of the curve was between 5.0 and 6.5 (ΔpH = 1.5, fluorescence change = 60%). This would mean that a pH change of about 0.5 pH units (in the linear range) corresponds to ~20% fluorescence change. Whereas in the upper, non-linear region of the titration curve a pH change of 1.5 units (from pH 7.0 down to pH 6.5) would only result in about 14% fluorescence decrease.

To test if EGFP in the ERGIC also shows pH-dependent fluorescence increases and decreases I incubated HeLa cells stably expressing EGFP-ERGIC-53 sequentially with buffers of different pH (Figure 4 and movie1). As expected EGFP-ERGIC-53 fluorescence was pH-dependent. Taken together, the pH probe reacted upon pH changes in all three organelles. However, a titration curve in the ERGIC would have looked different from ER and Golgi curves, since small ERGIC structures lost their fluorescence completely already at pH 6.0 (Figure 4). Since the ERGIC pH cannot be derived from ER and Golgi titration curves, I had to employ another way of pH calculation. Therefore I utilized a “balancing method” to analyze pH in the ERGIC. This method allowed us to estimate pH without knowing an exact ERGIC titration curve.

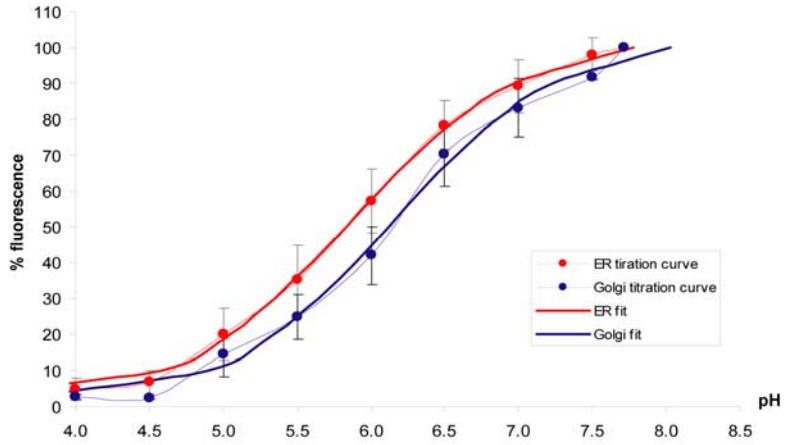

Figure 3: Best-fit ER and Golgi titration curves. Cells were incubated with pH 7.7 followed by buffers with lower pH. Fluorescence at pH 7.7 was set to 100% and changes in fluorescence are indicated in percent. It became clear that Golgi (n=2-7 per pH, blue) and ER titration curve (n=10, red) are quite similar. At about pH 6.0 in both organelles EGFP showed 50% of its fluorescence at pH 7.7. Values are means ± SD.

Figure 4: GFP in the ERGIC shows pH-dependent fluorescence changes. A HeLa cell stably expressing EGFP-ERGIC-53 was sequentially exposed to buffers with different pH. Bright dotty ERGIC elements were visible at pH 7.7 (left), whereas at pH 6.0 (middle) fluorescence decreased significantly. Re-incubation at pH 7.7 (right) increased the fluorescence signal in the ERGIC again, indicating that ERGIC-targeted EGFP responds to pH.

Balancing method to measure pH in the ER, ERGIC and Golgi

Clearly EGFP can be used as non-ratiometric pH sensor in living cells. This was already shown previously for ER, cytosol, mitochondria and Golgi (Llopis et al., 1998). From titration experiments in living cells it is possible to calculate EGFP fluorescence intensities back to cellular pH. Due to limitations encountered with ERGIC titrations I used a method termed "balancing method" deduced from Szatkowski (Szatkowski and Thomas, 1986). Sequential incubation of snail neurons or crab muscle with a mixture of membrane-permeable weak acid and base changes the intracellular pH. From these changes the initial pH can be calculated. I adapted this method to estimate pH in different cellular organelles independent of titration curves using EGFP as pH probe. Instead of

using cell-permeable mixtures of weak acid and base I added ionophores to the buffers, which equilibrate pH throughout the cell. A cell expressing EGFP in one of the organelles of interest was imaged for a certain time and the fluorescence signal was recorded (Figure 5A). The intensity of the fluorescence signal depends on the pH in this compartment. Subsequently the cell was exposed to a buffer solution with known pH, supplemented with ionophores (10 μM nigericin and 10 μM monensin) to equilibrate the pH throughout all organelles (Figure 5B). After equilibration of about 2.5 minutes and a break in imaging, the fluorescence signal was followed again. At that time point the fluorescence of EGFP had changed according to the pH of the buffer incubated with. The higher the pH the brighter the EGFP fluorescence was. This can be seen nicely by eye if pH differences are big (movie2). Depending whether the signal was lower, higher or equal to the starting fluorescence, conclusions about the original pH in the organelle were drawn (Figure 5C). After conducting several experiments I narrowed down the initial pH. The advantage of this approach is the fast and simple way to narrow down organellar pH. The amount of fluorescence difference from the start to the value after equilibration indicates how far the questioned pH lies from the known value. Theoretically, with the knowledge of titration experiments definite pH numbers can be calculated.

Data analysis – How to quantify fluorescence in small and mobile ERGIC structures?

The working protocol presented in the previous section yielded fluorescence images acquired over time. To obtain pH values, the data had to be processed and analyzed. Experiments with ER- and Golgi-targeted probes were analyzed manually with image processing tools provided by the Image Pro or Qu software. Regions of interest were drawn around the fluorescent organelle. Mean intensities were collected and normalized to pH 7.7. The pattern of the ERGIC raised some difficulties for data analysis. Since ERGIC elements are vesicular-tubular clusters scattered throughout the cell with accumulations in the juxtanuclear region, it is impossible to draw regions of interest around all these structures. To identify and highlight discrete ERGIC elements I required customized software. Therefore Aaron Ponti (FMI, Basel) programmed a plug-in for MatLab, termed Qu, for custom analysis. Qu automatically identifies individual ERGIC elements throughout the cell and collects the intensity values in a 2x2 pixel area (Figure 6). Yet, the nature of the ERGIC makes the analysis even more complicated because ERGIC elements are not stable (Ben-Tekaya et al., 2005). Over time elements move around, fuse with one another or split, which explains the need to track these structures

for pH measurements. The software Qu is capable of tracking individual spots over several time frames. Finally fluorescence data is displayed as plot of the mean fluorescence intensity against time of all tracks or individual fluorescence tracks over time (Figure 7). In addition a background subtraction tool was implemented. For ERGIC measurements I accessorily wanted to exclude the fluorescence signal from the juxtanuclear region. Accumulating ERGIC structures cannot be identified as single entities in that area as they appear as big blob on fluorescence images. I decided to avoid including imprecise data by drawing masking areas around juxtanuclear regions and focused primarily on the peripheral ERGIC spots.

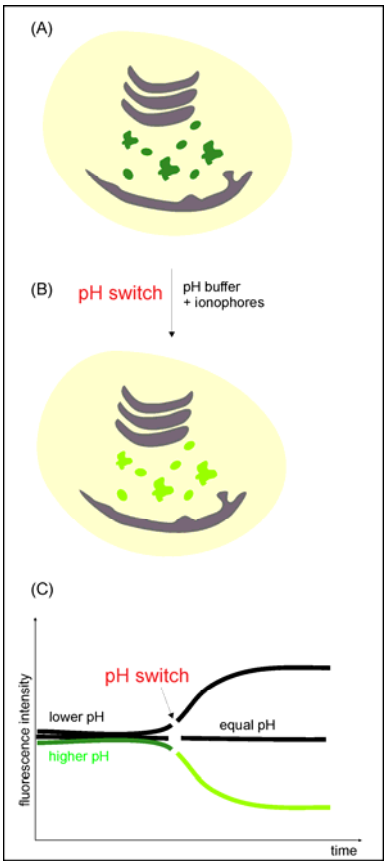

Figure 5: The balancing method. (A) A cell expressing EGFP in one of the organelles (e.g.: ERGIC, green) of the early secretory pathway is imaged for several frames. Other organelles like ER and Golgi are indicated in grey. First EGFP fluorescence is recorded in the unperturbed cell. (B) Subsequently the cell is bathed in buffer solution of given pH, containing ionophores. This results in pH equilibration throughout the cell including the ERGIC. Meanwhile the fluorescence intensity changes according to the pH (indicated by a different shade of green). (C) From the recorded fluorescence curve conclusions about the starting pH can be drawn. In the graph shown, the starting pH of the ERGIC would have been higher than the pH of the equilibrated buffer (dark green curve) because the fluorescence dropped after equilibration (light green curve).

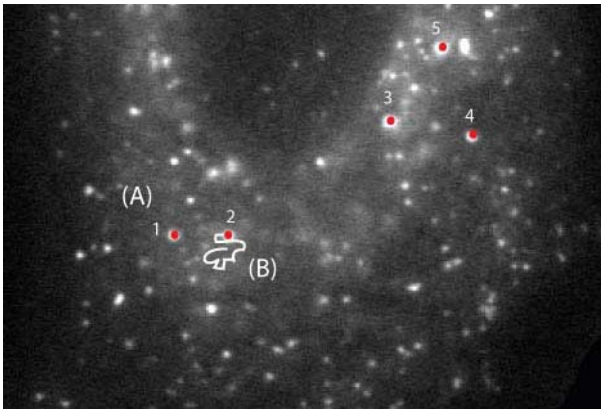

Figure 6: The software Qu. The MatLab plug-in called Qu identifies individual small ERGIC elements (A), marks them and tracks them over time (B). The tracked data points are numbered and fluorescence data can be assigned to single ERGIC structures in the movie. Additionally the software is supplemented with a background subtraction tool, which allows the drawing of a region of interest, from which an average grey value is obtained and subtracted at each frame.

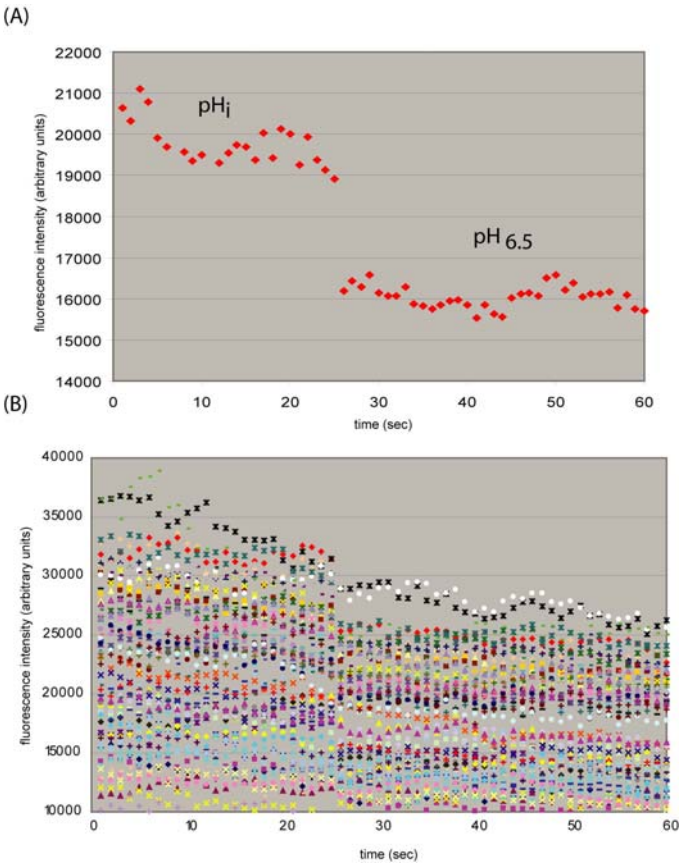

Figure 7: pH balancing experiment in the ERGIC with pH 6.5. (A) A HeLa cell expressing EGFP-ERGIC-53 was imaged for 25 frames (unperturbed, pH_i = intracellular) before the pH of the bathing solution was switched to pH 6.5. After an equilibration break the cell's fluorescence was recorded again. According to the result the pH in the ERGIC was higher that 6.5 in this example because the fluorescence signal decreased. The data can either be plotted as an average fluorescence intensity of all the tracked structures over time (A) or as fluorescence intensity of individual ERGIC elements followed over time (B). Based on the course of the fluorescence intensity the % fluorescence change can be calculated.

pH measurements in the early secretory pathway

For each organelle several balancing experiments were carried out at multiple pH values. Fluorescence intensity curves over time where obtained and analyzed for their progression. For cells expressing EGFP in the reticular network of the ER an outline around the borders of this network was drawn manually and the average intensity over the whole cell was analyzed in each experiment. Based on an average standard deviation of the titration curve in the ER and Golgi of ±6% this value was set as Δfluorescence threshold, which defines a significant change. Accordingly, data displaying fluorescence changes within this range were treated as revealing equal pH to the original pH in the organelle. Fluorescence changes were calculated as follows: ΔF (in %) = F_{pHi} -F_{pHx} (pH_x – known pH, pH_i – pH of the organelle); ΔF is positive when pH_i is higher than the pH of the buffer incubated with, whereas ΔF is negative when pH_i is lower than the pH of the buffer incubated with. An example can be seen in Figure 8A, where a cell expressing EGFP in the ER was recorded and incubated with different pH buffers. Whereas at pH 7.7 the fluorescence was increasing compared to the starting fluorescence it was about the same at pH 7.0 and decreased at pH 6.0 and 5.5. Nine independent experiments in the ER gave results that matched the pH incubated with (Figure 8B and 9A). Combining all the

data from the balancing experiments gave an estimate of the ER pH to be in the range of 6.9 to 7.5. Note, that three ER experiments balanced with buffers lower than pH 7.0 resulted in positive ΔF indicating that pH_i was higher than pH 7.0 (Figure 8 B, triangles in the yellow region). The same way of analysis and data processing was applied for the Golgi (Figure 8B and 9B). Various balancing experiments of GalT-EGFP expressing HeLa cells yielded ten experiments where the fluorescence at the indicated pHs corresponded to the original fluorescence. Finally, a Golgi pH range of 6.4 to 7.0 was revealed. This is concordant with other studies using EGFP (Kim et al., 1996; Llopis et al., 1998; Schapiro and Grinstein, 2000; Wu et al., 2000). Next, pH data in the ERGIC were acquired from several ERGIC balancing experiments. Like for the other two organelles I applied a ±6% fluorescence change as threshold. Conducting 15 experiments in the range of pH 6.4 to pH 7.4 I found the ERGIC pH to lie between 6.5 and 7.2 (Figure 8B and 9C). These borders were set because three experiments at pH 6.4 revealed fluorescence changes >6% indicating the ERGIC pH to be higher (Figure 8B, green rectangles). The upper boarder was set to pH 7.2 since at that pH one experiment revealed a lower ERGIC pH (Figure 8B, green rectangle). The ER pH was found to be between pH 6.9 and 7.5 and the Golgi pH between 6.4 and 7.0. Thus, the ERGIC pH is in between ER and Golgi. Collectively, these ranges highlight a sequential acidification in the early secretory pathway.

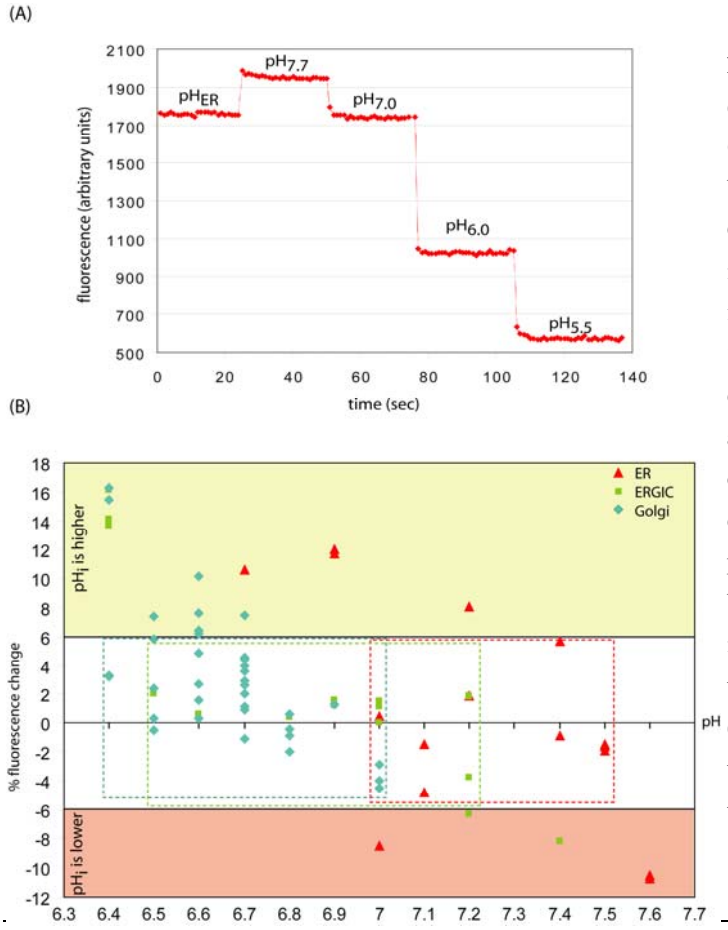

Figure 8: Summary of the balancing data obtained for ER, ERGIC and Golgi. Shown is an example of a pH balancing experiment in the ER (A). Clearly, the original EGFP fluorescence in the ER is about the same as the fluorescence of EGFP at pH 7.0. (B) Summary of all pH balancing experiment performed for ER, ERGIC and Golgi. Plotted are %fluorescence changes against the pH at which the experiment was performed. Each data point represents one single live imaging balancing experiment. Positive values indicate that the pH in that experiment was higher than the one incubated with (x-axes). Negative values were obtained when the pH in the organelle was lower than the pH balanced with (x-axes). All

experiments inside the ±6% boarder (y-axes) are counted as experiments where the original organellar pH fitted the equilibrated pH in that experiment. ER data points (red triangles) show a pH range between 7.5 and 6.9. There was one outlier present at pH 7.0, which showed ΔF about -8%. ERGIC experiments (green rectangles) indicate a quite broad pH present throughout the experiments from pH 6.5 up to 7.2. Golgi measurements (blue diamonds) suggest the pH of the Golgi to lie between 6.4 and 7.0.

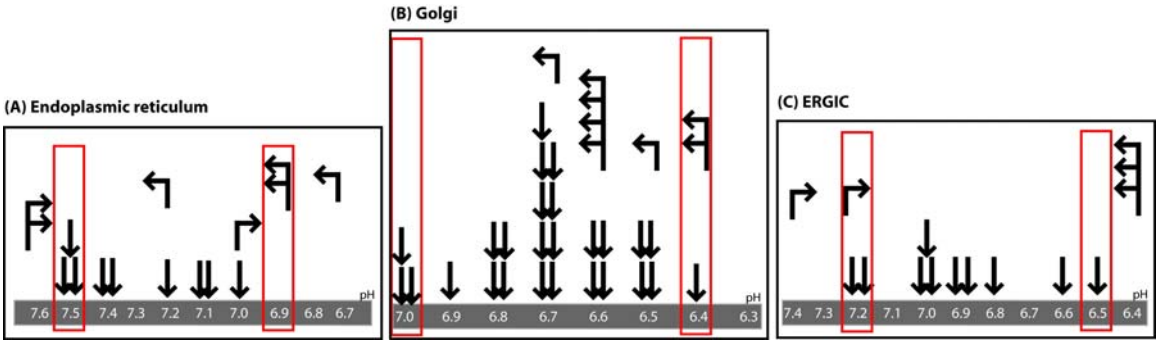

Figure 9: Summary of pH balancing experiments in the ER, Golgi and ERGIC. Each arrow indicates an individual experiment. Depending on the direction the arrow is pointing to the result of the experiment was an equal pH (arrow points down), the pH in the organelles was higher than the pH incubated with (arrow points to the left) or the pH was lower (arrow points to the right). The red boxes mark the pH ranges fixed for each organelle after applying a ± 6% threshold (range in which results were set to equal). Hence, the pH range of the ER is 7.5 to 6.9, Golgi 7.0 to 6.4 and ERGIC 7.2 to 6.5.

Discussion and Perspectives

Over the past three decades the pH was delineated in lysosomes, endosomes, cytosol, mitochondria, ER, Golgi and peroxisomes (D'Souza et al., 1998; Demaurex et al., 1998; Jankowski et al., 2001; Kim et al., 1998; Machen et al., 2003; Miesenbock et al., 1998; Ohkuma and Poole, 1978; Schapiro and Grinstein, 2000; Seksek et al., 1995; Tycko and Maxfield, 1982; Wu et al., 2001). Only recently, the utilization of EGFP as pH-dependent probe was established (Kneen et al., 1998; Llopis et al., 1998; Miesenbock et al., 1998). In contrast to other probes its easy targetability and the availability of different spectral mutants was a great break through for intracellular pH measurements. Here, I used EGFP to investigate the pH in the organelles of the early secretory pathway. EGFP was successfully targeted to the ER, ERGIC and Golgi, which enabled me to explore the pH along the early secretory pathway. In this study I focused on the ERGIC, since its pH has not been established. Performing titration experiments in the ER, ERGIC and Golgi I confirmed the pH-dependent decrease of EGFP fluorescence upon lowering the pH. Establishing pH titration curves in the ERGIC was met with difficulties. Hence, I established a new method to narrow down the pH in different organelles with an approach termed “balancing method”. This approach uses the equilibration of intracellular compartments with buffers of different pH. Depending on the fluorescence change conclusions about the original pH can be drawn. It was not known so far if there is acidification from ER to ERGIC *in vivo*, which might control receptor ligand association/dissociation processes, protein localization and trafficking. Therefore I was interested in exploring the chemical properties of that organelle in more detail.

In summary, I observed near neutral pH in the ER (pH 6.9-7.5) and mildly acidic pH in the Golgi (pH 6.4-7.0). In the ERGIC a pH range of 6.5 to 7.2 was measured. Thus, the pH of the ERGIC lies between the pH of ER and Golgi. Altogether, I provide evidence for a gradient of decreasing pH from the ER to the Golgi in the early secretory pathway.

It seems that *in vitro* pH data sculptured our current view of intracellular pH. For example the low pH of endosomes was first mentioned by Helenius et al. in 1980 (Helenius et al., 1980). They studied the entry of Semliki forest virus into BHK cells. Addition of chloroquine, which rises lysosomal pH, inhibited early steps in infection. At pH 6.0 or lower efficient fusion of viral and liposomal membranes occurred. Strikingly, the first *in vivo* pH measurements in endosomes appeared in 1982, where the pH of endocytic vesicles was calculated to be 5.0 ± 0.2 (Tycko and Maxfield, 1982). Two other

studies investigating endosomal pH were performed sixteen years later. Miesenbock's data confirmed the pH of endosomes to be around pH 5.5 (Miesenbock et al., 1998), whereas estimated pH of recycling endosomes lies between 6.77 (D'Souza et al., 1998) and 6.37 (Machen et al., 2003). At the same time heterogeneity amongst recycling endosomes was observed (Teter et al., 1998). Their calculated pH ranged between pH 5.2-7.2. These findings highlight the difficulty to obtain a clear pH value for an organelle *in vivo*. The results of *in vivo* pH measurements depend upon the method used.

Here I present the development of customized software to analyze pH experiments in different organelles. Previous studies using pH-dependent fluorescence probes did not use any specialized software to process and analyze the raw data. Since simple region of interest selections were not sufficient for all organelles I had to develop a MatLab plug-in to analyze data from small, vesicular ERGIC elements. Unlike ER and Golgi that are extended organelles with defined morphology and location inside the cell, the ERGIC is distributed as vesicular-tubular clusters throughout the cytoplasm. Additionally, these structures are not static and move around in time (Appenzeller-Herzog and Hauri, 2006; Ben-Tekaya et al., 2005). This particular morphology and behaviour demands sophisticated software tools to perform proper data processing and analysis. With the MatLab plug-in Qu I developed a tool to extract fluorescence intensity data over time. Individual ERGIC elements were identified, tracked and average fluorescence intensities and individual fluorescence intensities were plotted against time. This made it possible to visualize the variation of pH-dependent EGFP-fluorescence over time of single ERGIC elements. Individual ERGIC tracks showed a heterogeneous distribution of fluorescence changes upon pH variation (Figure 7B). Therefore I asked the question of whether individual ERGIC elements indeed have different pH. An alternative possibility is that the heterogeneity of fluorescence changes might have been caused by the imaging system and data processing. To test if the imaging system itself and data processing led to these results, I performed control experiments to assess if the system is constant and linear. Constance and linearity would implicate that EGFP in different regions of an organelle shows the same response everywhere independent of the original fluorescence intensity. This is what would be expected for the continuous lumen of the ER. When analyzing different subregions of the ER, I saw that the pH change was different depending on the initial fluorescence (Figure 10A and B). Close to the nucleus, where the signal was brightest, decreasing pH from 7.4 to 6.5 gave a 30% decrease in fluorescence (Figure 10A). However analyzing the periphery in the same cell gave only a slight reduction of 16% (Figure 10 A). Whereas in the core region the difference between raw data (30%)

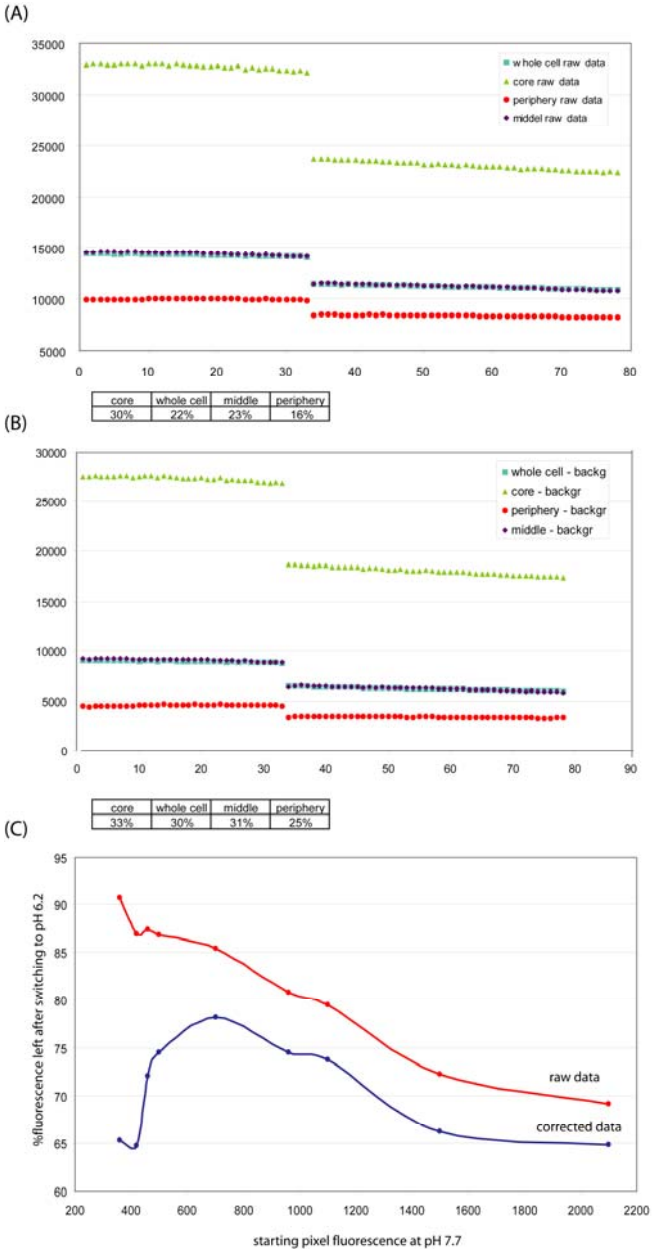

Figure 10: Region-dependent heterogeneity of EGFP fluorescence changes in different regions of the ER. Four different regions where analyzed: whole cell analysis indicates the selection of the whole endoplasmic reticulum for analysis (blue rectangle), core regions represent perinuclear endoplasmic reticulum areas (green triangle), analysis in the periphery of the cell close to the plasma membrane (red circle) and in an intermediate region closer to the center of the cell (violet diamond) is also indicated. Both raw data (A) and processed data (B) after background subtraction are presented for all the different regions. From these data fluorescence changes in percent were calculated and compared with each other (boxes below graphs). Depending on the initial fluorescence the fluorescence decrease, upon a pH drop, was stronger for more intense regions (compare core with periphery in A). A single pixel analysis with ER-targeted EGFP revealed that after a change from pH 7.7 down to 6.2, fluorescence changed in distinct regions of the ER differently (C). High fluorescence pixel values were found in the centre of the cell and low intensity pixels were from peripheral regions (starting pixel fluorescence, x-axes). The red curve represents raw data, whereas the blue curve represents data after processing (background subtraction). Low intensity pixels are very sensitive to background subtractions, which results in strong differences between original data (red) and processed data (blue). In contrast high intensity pixels show similar fluorescence changes in raw and processed data. This analysis points to the importance of high starting fluorescence signals. With the imaging system used herein a minimal fluorescence intensity of about 2000 would be needed to give reliable results.

and processed data (33%; subtraction of background) is negligible this is not the case in the periphery (16% compared to 25%; Figure 10B). This indicates that the low data points from the periphery are more sensitive against background subtraction. This can also be seen when analyzing single pixels, which was done to simulate the ERGIC analysis (Figure 10C). Choosing single pixel grey values with different starting fluorescence revealed that after switching pH from 7.7 to 6.2 the corresponding grey value dropped to

different extents. Note that highest intensity values at the x-axes showed a more constant change (curve gets linear). Moreover, when background was subtracted from pixels with low starting fluorescence the resulting fluorescence change increased from 10% in raw data to 35% in processed data (Figure 10C). Taken together, fluorescence signals should be above a minimal value to ensure that pH changes result in equal fluorescence changes and that these high values additionally guarantee reduced sensitivity against background subtraction (high signal to noise ratio). Overall, the ER data consisted of so many pixels that it was more stable against low intensity signals. However for the ERGIC, which consists of isolated tiny vesicular compartments, this is not the case. Based on control experiments I suggest that individual ERGIC elements do not have different pH but rather this is a consequence of their small size and low content of fluorescent material. Consequently, the average ERGIC fluorescence change varies from experiment to experiment depending on the original intensity distribution of individual ERGIC elements. Taken together, I conclude that the imaging system has limitations. The system is not linear and ERGIC elements displayed too low fluorescence to obtain ERGIC titration curves. The ERGIC elements displayed a kind of pH-dependent on/off fluorescence. When decreasing pH ERGIC structures decreased in fluorescence often leading to loss of detection, whereas they reappeared after shifting to high pH (Figure 4).

One solution would be to use another microscope setup, which is equipped with an ultra-sensitive camera for low intensity detection which would increase signal to noise ratio. Further, utilization of a ratiometric probe (pHluorin) would be an advantage because then the presence of a reference channel would allow the detection of all ERGIC elements throughout the experiment. Additionally, errors by alterations in the focal plane or based on photobleaching would be diminished using a ratiometric method allowing for increased precision. The disappearance of ERGIC elements also contributed to changes in average fluorescence values. I tried to express pHluorin-ERGIC-53, but failed to obtain satisfying fluorescence signal.

The pH ranges in ER and Golgi support published data. Published data about measurements performed in the Golgi of mammalian cells gave pH values between 5.95 (Demaurex et al., 1998) and 6.47 (Schapiro and Grinstein, 2000). In another study a Golgi pH range of 6.4-6.81 was defined (Llopis et al., 1998). Likewise, I obtained a similar pH range for the Golgi (6.4-7.0).

When pH values, obtained from different studies, are compared one has to be aware, that temperature can influence the results. For the Golgi pH it was shown that room temperature measurements gave lower pH values compared to measuring at 37°C (Kim et

al., 1996). Hence, it is important to keep the measurement settings as close to the *in vivo* situation as possible which requires utilization of pre-heated buffer solutions and incubations at 37°C on the microscope stage. Llopis et al. performed their experiment at 22°C in comparison to the data herein which were acquired at 37°C. Accordingly, it is possible that the Golgi pH range measured in my study is shifted to higher values.

My study expanded the knowledge about the pH in the early secretory pathway. The data are in line with *in vitro* data showing that a drop in pH and calcium in the ERGIC leads to the release of cargo from the cargo receptor ERGIC-53 (Appenzeller-Herzog et al., 2004; Appenzeller et al., 1999). Changes from pH 7.4 to 6.5 in the presence of 0.5mM $CaCl_2$ *in vitro* slightly reduce binding of ERGIC-53 to immobilized mannose. However, combining low pH and low calcium concentrations (0.2mM) significantly decreases binding of the lectin (Appenzeller-Herzog et al., 2004). Thus, a combination of low pH and low calcium concentration may regulate the interactions between the lectin ERGIC-53 and its cargoes. My current data support this hypothesis since the change from ER to ERGIC is small and would not suffice by itself to promote cargo dissociation.

The functional importance of a pH change in the early secretory pathway is also supported by data showing binding of the ER-resident receptor associated protein (RAP) to LDL-receptor-related protein (LRP) (Bu et al., 1995). RAP might function as a molecular chaperone for LRP, regulating its ligand binding activity along the secretory pathway. Dissociation of RAP from LRP happens at lowered pH in the early secretory pathway.

A drop in pH in the early secretory pathway is further supported by work on ARF1 (Zeuzem et al., 1992). These authors found ARF1 to be recruited in a pH-dependent manner to membranes and speculated about an unknown pH sensor. Recently their hypothesis was confirmed for endosomes. On endosomes the V-ATPase was found as a pH sensing unit (Gu and Gruenberg, 2000; Hurtado-Lorenzo et al., 2006). The V-ATPase possibly undergoes a conformational change, when the pH in the endosome is acidic leading to the interaction of the Arf6-GEF ARNO with the a2 subunit. Therefore pH-dependent recruitment of a cytosolic coat to the organelle is regulated.

I propose a model of gradual acidification along the early secretory pathway (Figure 11), which is necessary for proper trafficking (Palokangas et al., 1998). In light of my finding it is tempting to think about a pH sensor in the ERGIC. V-ATPase, which seems to be assembled already in the ER, might be a good candidate to fulfil this function (Myers and Forgac, 1993). This sensor might mediate pH-dependent COPI recruitment to the ERGIC, form where COPI-coated vesicles bud (Zeuzem et al., 1992). Further,

acidification along the organelles of the secretory pathway is very likely a prerequisite for proper interactions of ERGIC-53 and KDEL receptor with their cargoes. Other parameters, like calcium concentrations, might work in concert to regulate this essential mechanism.

My data supports the idea of analogy between endosomes and ERGIC. Similarly to ligand receptor dissociation processes in endosomes the same mechanism seems to work in the compartments of the early secretory pathway. Moreover, acidification along the endocytic compartments is fundamental for the invasion of viruses and toxins. After entering the cells viruses replicate, asssemble and are secreted. For example for the Hepatitis B virus it is widely accepted that subviral particles self-assemble in the ERGIC (Patient et al., 2007). Importantly, comparable to the pH-dependent invasion of viruses and toxins into cells my data presumably is crucial for ongoing research concerning virus assembly in the early secretory pathway, which might be envisioned to be pH-dependent.

In future experiments one could study directly the dissociation of cargo from the receptor in the ERGIC by using EYFP-ERGIC-53 in combination with an ECFP-tagged cargo protein. A combined expression of both constructs in the same cells and measuring of fluorescence resonance energy transfer (FRET) between the two molecules would visualize the interaction of the receptor with the cargo. Additionally, while manipulating ERGIC pH, which can be measured directly with EYFP, and manipulating calcium concentrations inside the cell one could define the pH at which cargo and receptor dissociate *in vivo*.

To find out more about the mechanism of acidification in the ERGIC it would be interesting to test for the localization of the V-ATPase in the ERGIC (Ying et al., 2000). Since different isoforms of the a subunit locate the pump to different organelles one could test subunit-specific antibodies in immunofluorescence for their localization in the ERGIC.

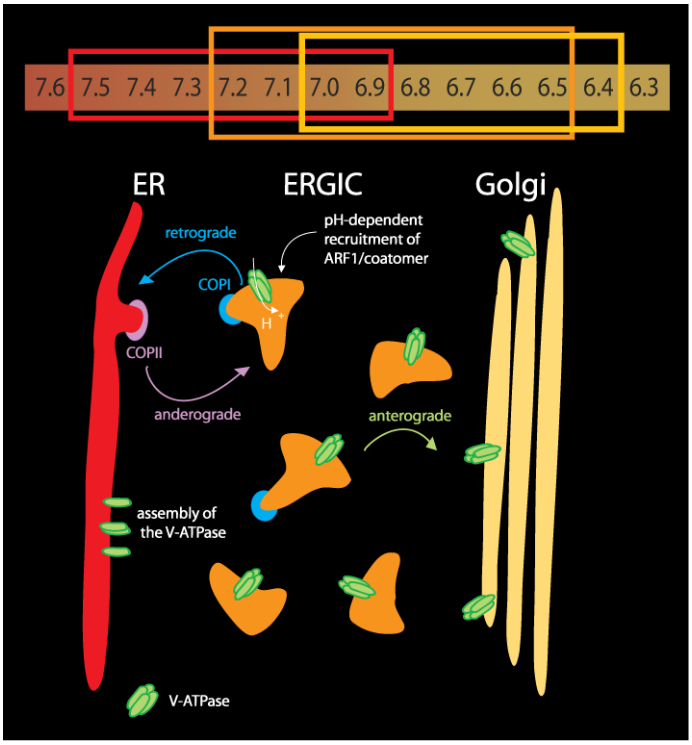

Figure 11: Model of pH in the early secretory pathway. From the ER COPII-coated vesicles bud off to transport proteins along the secretory pathway. The transport receptor ERGIC-53 would accumulate lumenal cargo into these vesicles. Arriving at the ERGIC cargo would be released because of a drop in pH and calcium. ERGIC-53 recycles back to the ER via COPI-coated vesicles. Other proteins head anterograde further to the Golgi apparatus, which displays an even more acidic pH. I speculate that the continuous acidification along the early secretory pathway could be sensed like in endosomes. Acidification might be facilitated by the presence of assembled V-ATPase molecules in the ERGIC and Golgi. I found the pH of the ER in the neutral range (red box), the ERGIC pH in between ER and Golgi (orange box), and the Golgi pH was mildly acidic (yellow box).

References

Agarwal, A.K., and R.J. Auchus. 2005. Minireview: cellular redox state regulates hydroxysteroid dehydrogenase activity and intracellular hormone potency. *Endocrinology*. 146:2531-8.

Aguilera-Romero, A., J. Kaminska, A. Spang, H. Riezman, and M. Muniz. 2008. The yeast p24 complex is required for the formation of COPI retrograde transport vesicles from the Golgi apparatus. *J Cell Biol*. 180:713-20.

Alberts, J., Lewis, Raff, Robert, Walter. 2002. Molecular Biology of the Cell. Garland Science.

Allan, B.B., B.D. Moyer, and W.E. Balch. 2000. Rab1 recruitment of p115 into a cis-SNARE complex: programming budding COPII vesicles for fusion. *Science*. 289:444-8.

Altan-Bonnet, N., R. Sougrat, and J. Lippincott-Schwartz. 2004. Molecular basis for Golgi maintenance and biogenesis. *Curr Opin Cell Biol*. 16:364-72.

Alvarez, C., H. Fujita, A. Hubbard, and E. Sztul. 1999. ER to Golgi transport: Requirement for p115 at a pre-Golgi VTC stage. *J Cell Biol*. 147:1205-22.

Anantharaman, V., and L. Aravind. 2002. The GOLD domain, a novel protein module involved in Golgi function and secretion. *Genome Biol*. 3:research0023.

Anderson, R.G., J.R. Falck, J.L. Goldstein, and M.S. Brown. 1984. Visualization of acidic organelles in intact cells by electron microscopy. *Proc Natl Acad Sci U S A*. 81:4838-42.

Anderson, R.G., and R.K. Pathak. 1985. Vesicles and cisternae in the trans Golgi apparatus of human fibroblasts are acidic compartments. *Cell*. 40:635-43.

Aniento, F., F. Gu, R.G. Parton, and J. Gruenberg. 1996. An endosomal beta COP is involved in the pH-dependent formation of transport vesicles destined for late endosomes. *J Cell Biol*. 133:29-41.

Appenzeller-Herzog, C., and H.P. Hauri. 2006. The ER-Golgi intermediate compartment (ERGIC): in search of its identity and function. *J Cell Sci*. 119:2173-83.

Appenzeller-Herzog, C., A.C. Roche, O. Nufer, and H.P. Hauri. 2004. pH-induced conversion of the transport lectin ERGIC-53 triggers glycoprotein release. *J Biol Chem*. 279:12943-50.

Appenzeller, C., H. Andersson, F. Kappeler, and H.P. Hauri. 1999. The lectin ERGIC-53 is a cargo transport receptor for glycoproteins. *Nat Cell Biol*. 1:330-4.

Aridor, M., S.I. Bannykh, T. Rowe, and W.E. Balch. 1995. Sequential coupling between COPII and COPI vesicle coats in endoplasmic reticulum to Golgi transport. *J Cell Biol*. 131:875-93.

Aridor, M., K.N. Fish, S. Bannykh, J. Weissman, T.H. Roberts, J. Lippincott-Schwartz, and W.E. Balch. 2001. The Sar1 GTPase coordinates biosynthetic cargo selection with endoplasmic reticulum export site assembly. *J Cell Biol*. 152:213-29.

Axelsson, M.A., N.G. Karlsson, D.M. Steel, J. Ouwendijk, T. Nilsson, and G.C. Hansson. 2001. Neutralization of pH in the Golgi apparatus causes redistribution of glycosyltransferases and changes in the O-glycosylation of mucins. *Glycobiology*. 11:633-44.

Bachert, C., T.H. Lee, and A.D. Linstedt. 2001. Lumenal endosomal and Golgi-retrieval determinants involved in pH-sensitive targeting of an early Golgi protein. *Mol Biol Cell*. 12:3152-60.

Baines, A.C., and B. Zhang. 2007. Receptor-mediated protein transport in the early secretory pathway. *Trends Biochem Sci*. 32:381-8.

Baker, D., L. Hicke, M. Rexach, M. Schleyer, and R. Schekman. 1988. Reconstitution of SEC gene product-dependent intercompartmental protein transport. *Cell*. 54:335-44.

Balch, W.E., W.G. Dunphy, W.A. Braell, and J.E. Rothman. 1984. Reconstitution of the transport of protein between successive compartments of the Golgi measured by the coupled incorporation of N-acetylglucosamine. *Cell*. 39:405-16.

Bannykh, S.I., T. Rowe, and W.E. Balch. 1996. The organization of endoplasmic reticulum export complexes. *J Cell Biol*. 135:19-35.

Barasch, J., and Q. al-Awqati. 1993. Defective acidification of the biosynthetic pathway in cystic fibrosis. *J Cell Sci Suppl*. 17:229-33.

Barasch, J., B. Kiss, A. Prince, L. Saiman, D. Gruenert, and Q. al-Awqati. 1991. Defective acidification of intracellular organelles in cystic fibrosis. *Nature*. 352:70-3.

Barlowe, C., L. Orci, T. Yeung, M. Hosobuchi, S. Hamamoto, N. Salama, M.F. Rexach, M. Ravazzola, M. Amherdt, and R. Schekman. 1994. COPII: a membrane coat formed by Sec proteins that drive vesicle budding from the endoplasmic reticulum. *Cell*. 77:895-907.

Barr, F.A., C. Preisinger, R. Kopajtich, and R. Korner. 2001. Golgi matrix proteins interact with p24 cargo receptors and aid their efficient retention in the Golgi apparatus. *J Cell Biol*. 155:885-91.

Barr, F.A., and B. Short. 2003. Golgins in the structure and dynamics of the Golgi apparatus. *Curr Opin Cell Biol*. 15:405-13.

Barroso, M., D.S. Nelson, and E. Sztul. 1995. Transcytosis-associated protein (TAP)/p115 is a general fusion factor required for binding of vesicles to acceptor membranes. *Proc Natl Acad Sci U S A*. 92:527-31.

Bartoszewski, S., S. Luschnig, I. Desjeux, J. Grosshans, and C. Nusslein-Volhard. 2004. Drosophila p24 homologues eclair and baiser are necessary for the activity of the maternally expressed Tkv receptor during early embryogenesis. *Mech Dev*. 121:1259-73.

Bascom, R.A., S. Srinivasan, and R.L. Nussbaum. 1999. Identification and characterization of golgin-84, a novel Golgi integral membrane protein with a cytoplasmic coiled-coil domain. *J Biol Chem*. 274:2953-62.

Belden, W.J., and C. Barlowe. 1996. Erv25p, a component of COPII-coated vesicles, forms a complex with Emp24p that is required for efficient endoplasmic reticulum to Golgi transport. *J Biol Chem*. 271:26939-46.

Belden, W.J., and C. Barlowe. 2001. Role of Erv29p in collecting soluble secretory proteins into ER-derived transport vesicles. *Science*. 294:1528-31.

Ben-Tekaya, H., K. Miura, R. Pepperkok, and H.P. Hauri. 2005. Live imaging of bidirectional traffic from the ERGIC. *J Cell Sci*. 118:357-67.

Bentley, M., Y. Liang, K. Mullen, D. Xu, E. Sztul, and J.C. Hay. 2006. SNARE status regulates tether recruitment and function in homotypic COPII vesicle fusion. *J Biol Chem*. 281:38825-33.

Bethune, J., M. Kol, J. Hoffmann, I. Reckmann, B. Brugger, and F. Wieland. 2006. Coatomer, the coat protein of COPI transport vesicles, discriminates endoplasmic reticulum residents from p24 proteins. *Mol Cell Biol*. 26:8011-21.

Biwersi, J., N. Emans, and A.S. Verkman. 1996. Cystic fibrosis transmembrane conductance regulator activation stimulates endosome fusion in vivo. *Proc Natl Acad Sci U S A*. 93:12484-9.

Blobel, G., and V.R. Potter. 1967. Studies on free and membrane-bound ribosomes in rat liver. II. Interaction of ribosomes and membranes. *J Mol Biol*. 26:293-301.

Blum, R., P. Feick, M. Puype, J. Vandekerckhove, R. Klengel, W. Nastainczyk, and I. Schulz. 1996. Tmp21 and p24A, two type I proteins enriched in pancreatic microsomal membranes, are members of a protein family involved in vesicular trafficking. *J Biol Chem*. 271:17183-9.

Blum, R., F. Pfeiffer, P. Feick, W. Nastainczyk, B. Kohler, K.H. Schafer, and I. Schulz. 1999. Intracellular localization and in vivo trafficking of p24A and p23. *J Cell Sci*. 112 (Pt 4):537-48.

Bokman, S.H., and W.W. Ward. 1981. Renaturation of Aequorea gree-fluorescent protein. *Biochem Biophys Res Commun*. 101:1372-80.

Boltz, K.A., L.L. Ellis, and G.E. Carney. 2007. Drosophila melanogaster p24 genes have developmental, tissue-specific, and sex-specific expression patterns and functions. *Dev Dyn*. 236:544-55.

Bonfanti, L., A.A. Mironov, Jr., J.A. Martinez-Menarguez, O. Martella, A. Fusella, M. Baldassarre, R. Buccione, H.J. Geuze, A.A. Mironov, and A. Luini. 1998. Procollagen traverses the Golgi stack without leaving the lumen of cisternae: evidence for cisternal maturation. *Cell*. 95:993-1003.

Bonifacino, J.S., and B.S. Glick. 2004. The mechanisms of vesicle budding and fusion. *Cell*. 116:153-66.

Bremser, M., W. Nickel, M. Schweikert, M. Ravazzola, M. Amherdt, C.A. Hughes, T.H. Sollner, J.E. Rothman, and F.T. Wieland. 1999. Coupling of coat assembly and vesicle budding to packaging of putative cargo receptors. *Cell*. 96:495-506.

Breuza, L., R. Halbeisen, P. Jeno, S. Otte, C. Barlowe, W. Hong, and H.P. Hauri. 2004. Proteomics of endoplasmic reticulum-Golgi intermediate compartment (ERGIC) membranes from brefeldin A-treated HepG2 cells identifies ERGIC-32, a new cycling protein that interacts with human Erv46. *J Biol Chem*. 279:47242-53.

Brown, V.I., and M.I. Greene. 1991. Molecular and cellular mechanisms of receptor-mediated endocytosis. *DNA Cell Biol*. 10:399-409.

Bu, G., H.J. Geuze, G.J. Strous, and A.L. Schwartz. 1995. 39 kDa receptor-associated protein is an ER resident protein and molecular chaperone for LDL receptor-related protein. *Embo J*. 14:2269-80.

Burkhardt, J.K., C.J. Echeverri, T. Nilsson, and R.B. Vallee. 1997. Overexpression of the dynamitin (p50) subunit of the dynactin complex disrupts dynein-dependent maintenance of membrane organelle distribution. *J Cell Biol*. 139:469-84.

Cabrera, M., M. Muniz, J. Hidalgo, L. Vega, M.E. Martin, and A. Velasco. 2003. The retrieval function of the KDEL receptor requires PKA phosphorylation of its C-terminus. *Mol Biol Cell*. 14:4114-25.

Cai, H., S. Yu, S. Menon, Y. Cai, D. Lazarova, C. Fu, K. Reinisch, J.C. Hay, and S. Ferro-Novick. 2007. TRAPPI tethers COPII vesicles by binding the coat subunit Sec23. *Nature*. 445:941-4.

Carnell, L., and H.P. Moore. 1994. Transport via the regulated secretory pathway in semi-intact PC12 cells: role of intra-cisternal calcium and pH in the transport and sorting of secretogranin II. *J Cell Biol*. 127:693-705.

Carney, G.E., and B.J. Taylor. 2003. Logjam encodes a predicted EMP24/GP25 protein that is required for Drosophila oviposition behavior. *Genetics*. 164:173-86.

Caro, L.G., and G.E. Palade. 1964. Protein Synthesis, Storage, and Discharge in the Pancreatic Exocrine Cell. an Autoradiographic Study. *J Cell Biol*. 20:473-95.

Chandy, G., M. Grabe, H.P. Moore, and T.E. Machen. 2001. Proton leak and CFTR in regulation of Golgi pH in respiratory epithelial cells. *Am J Physiol Cell Physiol*. 281:C908-21.

Chapman, R.E., and S. Munro. 1994. Retrieval of TGN proteins from the cell surface requires endosomal acidification. *Embo J*. 13:2305-12.

Chen, F., H. Hasegawa, G. Schmitt-Ulms, T. Kawarai, C. Bohm, T. Katayama, Y. Gu, N. Sanjo, M. Glista, E. Rogaeva, Y. Wakutani, R. Pardossi-Piquard, X. Ruan, A. Tandon, F. Checler, P. Marambaud, K. Hansen, D. Westaway, P. St George-Hyslop, and P. Fraser. 2006. TMP21 is a presenilin complex component that modulates gamma-secretase but not epsilon-secretase activity. *Nature*. 440:1208-12.

Ciechanover, A., A.L. Schwartz, and H.F. Lodish. 1983. Sorting and recycling of cell surface receptors and endocytosed ligands: the asialoglycoprotein and transferrin receptors. *J Cell Biochem*. 23:107-30.

Ciufo, L.F., and A. Boyd. 2000. Identification of a lumenal sequence specifying the assembly of Emp24p into p24 complexes in the yeast secretory pathway. *J Biol Chem*. 275:8382-8.

Cole, N.B., J. Ellenberg, J. Song, D. DiEuliis, and J. Lippincott-Schwartz. 1998. Retrograde transport of Golgi-localized proteins to the ER. *J Cell Biol*. 140:1-15.

Cole, N.B., C.L. Smith, N. Sciaky, M. Terasaki, M. Edidin, and J. Lippincott-Schwartz. 1996. Diffusional mobility of Golgi proteins in membranes of living cells. *Science*. 273:797-801.

Contreras, I., E. Ortiz-Zapater, and F. Aniento. 2004. Sorting signals in the cytosolic tail of membrane proteins involved in the interaction with plant ARF1 and coatomer. *Plant J*. 38:685-98.

Cosson, P., and F. Letourneur. 1994. Coatomer interaction with di-lysine endoplasmic reticulum retention motifs. *Science*. 263:1629-31.

D'Souza, S., A. Garcia-Cabado, F. Yu, K. Teter, G. Lukacs, K. Skorecki, H.P. Moore, J. Orlowski, and S. Grinstein. 1998. The epithelial sodium-hydrogen antiporter Na+/H+ exchanger 3 accumulates and is functional in recycling endosomes. *J Biol Chem*. 273:2035-43.

Demaurex, N. 2002. pH Homeostasis of cellular organelles. *News Physiol Sci*. 17:1-5.

Demaurex, N., W. Furuya, S. D'Souza, J.S. Bonifacino, and S. Grinstein. 1998. Mechanism of acidification of the trans-Golgi network (TGN). In situ measurements of pH using retrieval of TGN38 and furin from the cell surface. *J Biol Chem*. 273:2044-51.

Denzel, A., F. Otto, A. Girod, R. Pepperkok, R. Watson, I. Rosewell, J.J. Bergeron, R.C. Solari, and M.J. Owen. 2000. The p24 family member p23 is required for early embryonic development. *Curr Biol*. 10:55-8.

Desbuquois, B., S. Lopez, M. Janicot, H. Burlet, B. de Galle, and F. Fouque. 1992. Role of acidic subcellular compartments in the degradation of internalized insulin and in the recycling of the internalized insulin receptor in liver cells: in vivo and in vitro studies. *Diabete Metab*. 18:104-12.

Devuyst, O., F. Jouret, C. Auzanneau, and P.J. Courtoy. 2005. Chloride channels and endocytosis: new insights from Dent's disease and ClC-5 knockout mice. *Nephron Physiol*. 99:p69-73.

Dho, S., S. Grinstein, and J.K. Foskett. 1993. Plasma membrane recycling in CFTR-expressing CHO cells. *Biochim Biophys Acta*. 1225:78-82.

Diao, A., D. Rahman, D.J. Pappin, J. Lucocq, and M. Lowe. 2003. The coiled-coil membrane protein golgin-84 is a novel rab effector required for Golgi ribbon formation. *J Cell Biol*. 160:201-12.

Distler, J.J., J.F. Guo, G.W. Jourdian, O.P. Srivastava, and O. Hindsgaul. 1991. The binding specificity of high and low molecular weight phosphomannosyl receptors from bovine testes. Inhibition studies with chemically synthesized 6-O-phosphorylated oligomannosides. *J Biol Chem*. 266:21687-92.

Dominguez, M., K. Dejgaard, J. Fullekrug, S. Dahan, A. Fazel, J.P. Paccaud, D.Y. Thomas, J.J. Bergeron, and T. Nilsson. 1998. gp25L/emp24/p24 protein family members of the cis-Golgi network bind both COP I and II coatomer. *J Cell Biol*. 140:751-65.

Eisner, D.A., N.A. Kenning, S.C. O'Neill, G. Pocock, C.D. Richards, and M. Valdeolmillos. 1989. A novel method for absolute calibration of intracellular pH indicators. *Pflugers Arch*. 413:553-8.

Emery, G., R.G. Parton, M. Rojo, and J. Gruenberg. 2003. The trans-membrane protein p25 forms highly specialized domains that regulate membrane composition and dynamics. *J Cell Sci*. 116:4821-32.

Emery, G., M. Rojo, and J. Gruenberg. 2000. Coupled transport of p24 family members. *J Cell Sci*. 113 (Pt 13):2507-16.

Eugster, A., G. Frigerio, M. Dale, and R. Duden. 2004. The alpha- and beta'-COP WD40 domains mediate cargo-selective interactions with distinct di-lysine motifs. *Mol Biol Cell*. 15:1011-23.

Fan, J.Y., J. Roth, and C. Zuber. 2003. Ultrastructural analysis of transitional endoplasmic reticulum and pre-Golgi intermediates: a highway for cars and trucks. *Histochem Cell Biol*. 120:455-63.

Farhan, H., V. Reiterer, V.M. Korkhov, J.A. Schmid, M. Freissmuth, and H.H. Sitte. 2007. Concentrative export from the endoplasmic reticulum of the gamma-aminobutyric acid transporter 1 requires binding to SEC24D. *J Biol Chem*. 282:7679-89.

Farinas, J., and A.S. Verkman. 1999. Receptor-mediated targeting of fluorescent probes in living cells. *J Biol Chem*. 274:7603-6.

Fasshauer, D., D. Bruns, B. Shen, R. Jahn, and A.T. Brunger. 1997. A structural change occurs upon binding of syntaxin to SNAP-25. *J Biol Chem*. 272:4582-90.

Feiguin, F., A. Ferreira, K.S. Kosik, and A. Caceres. 1994. Kinesin-mediated organelle translocation revealed by specific cellular manipulations. *J Cell Biol*. 127:1021-39.

Feinstein, T.N., and A.D. Linstedt. 2008. GRASP55 Regulates Golgi Ribbon Formation. *Mol Biol Cell*. 19:2696-707.

Fiedler, K., and J.E. Rothman. 1997. Sorting determinants in the transmembrane domain of p24 proteins. *J Biol Chem*. 272:24739-42.

Fiedler, K., M. Veit, M.A. Stamnes, and J.E. Rothman. 1996. Bimodal interaction of coatomer with the p24 family of putative cargo receptors. *Science*. 273:1396-9.

Forgac, M. 1992. Structure, function and regulation of the coated vesicle V-ATPase. *J Exp Biol*. 172:155-69.

Fromme, J.C., and R. Schekman. 2005. COPII-coated vesicles: flexible enough for large cargo? *Curr Opin Cell Biol*. 17:345-52.

Fullekrug, J., B. Sonnichsen, U. Schafer, P. Nguyen Van, H.D. Soling, and G. Mieskes. 1997. Characterization of brefeldin A induced vesicular structures containing cycling proteins of the intermediate compartment/cis-Golgi network. *FEBS Lett*. 404:75-81.

Fullekrug, J., T. Suganuma, B.L. Tang, W. Hong, B. Storrie, and T. Nilsson. 1999. Localization and recycling of gp27 (hp24gamma3): complex formation with other p24 family members. *Mol Biol Cell*. 10:1939-55.

Gallwitz, D., C. Donath, and C. Sander. 1983. A yeast gene encoding a protein homologous to the human c-has/bas proto-oncogene product. *Nature*. 306:704-7.

Gayle, M.A., J.L. Slack, T.P. Bonnert, B.R. Renshaw, G. Sonoda, T. Taguchi, J.R. Testa, S.K. Dower, and J.E. Sims. 1996. Cloning of a putative ligand for the T1/ST2 receptor. *J Biol Chem*. 271:5784-9.

Gillies, R.J., R. Martinez-Zaguilan, G.M. Martinez, R. Serrano, and R. Perona. 1990. Tumorigenic 3T3 cells maintain an alkaline intracellular pH under physiological conditions. *Proc Natl Acad Sci U S A*. 87:7414-8.

Gillingham, A.K., A.C. Pfeifer, and S. Munro. 2002. CASP, the alternatively spliced product of the gene encoding the CCAAT-displacement protein transcription factor, is a Golgi membrane protein related to giantin. *Mol Biol Cell*. 13:3761-74.

Girod, A., B. Storrie, J.C. Simpson, L. Johannes, B. Goud, L.M. Roberts, J.M. Lord, T. Nilsson, and R. Pepperkok. 1999. Evidence for a COP-I-independent transport route from the Golgi complex to the endoplasmic reticulum. *Nat Cell Biol*. 1:423-30.

Goldberg, J. 1999. Structural and functional analysis of the ARF1-ARFGAP complex reveals a role for coatomer in GTP hydrolysis. *Cell*. 96:893-902.

Goldberg, J. 2000. Decoding of sorting signals by coatomer through a GTPase switch in the COPI coat complex. *Cell*. 100:671-9.

Gommel, D., L. Orci, E.M. Emig, M.J. Hannah, M. Ravazzola, W. Nickel, J.B. Helms, F.T. Wieland, and K. Sohn. 1999. p24 and p23, the major transmembrane proteins of COPI-coated transport vesicles, form hetero-oligomeric complexes and cycle between the organelles of the early secretory pathway. *FEBS Lett*. 447:179-85.

Gommel, D.U., A.R. Memon, A. Heiss, F. Lottspeich, J. Pfannstiel, J. Lechner, C. Reinhard, J.B. Helms, W. Nickel, and F.T. Wieland. 2001. Recruitment to Golgi membranes of ADP-ribosylation factor 1 is mediated by the cytoplasmic domain of p23. *Embo J*. 20:6751-60.

Gonzalez-Noriega, A., J.H. Grubb, V. Talkad, and W.S. Sly. 1980. Chloroquine inhibits lysosomal enzyme pinocytosis and enhances lysosomal enzyme secretion by impairing receptor recycling. *J Cell Biol*. 85:839-52.

Grabe, M., and G. Oster. 2001. Regulation of organelle acidity. *J Gen Physiol*. 117:329-44.

Grasse, P.P. 1957. [Ultrastructure, polarity and reproduction of Golgi apparatus.]. *C R Hebd Seances Acad Sci*. 245:1278-81.

Griffiths, J.R. 1991. Are cancer cells acidic? *Br J Cancer*. 64:425-7.

Gu, F., and J. Gruenberg. 2000. ARF1 regulates pH-dependent COP functions in the early endocytic pathway. *J Biol Chem*. 275:8154-60.

Gupta, V., and G. Swarup. 2006. Evidence for a role of transmembrane protein p25 in localization of protein tyrosine phosphatase TC48 to the ER. *J Cell Sci*. 119:1703-14.

Hardwick, K.G., M.J. Lewis, J. Semenza, N. Dean, and H.R. Pelham. 1990. ERD1, a yeast gene required for the retention of luminal endoplasmic reticulum proteins, affects glycoprotein processing in the Golgi apparatus. *Embo J*. 9:623-30.

Harter, C., and F.T. Wieland. 1998. A single binding site for dilysine retrieval motifs and p23 within the gamma subunit of coatomer. *Proc Natl Acad Sci U S A*. 95:11649-54.

Helenius, A., J. Kartenbeck, K. Simons, and E. Fries. 1980. On the entry of Semliki forest virus into BHK-21 cells. *J Cell Biol*. 84:404-20.

Holthuis, J.C., M.C. van Riel, and G.J. Martens. 1995. Translocon-associated protein TRAP delta and a novel TRAP-like protein are coordinately expressed with pro-opiomelanocortin in Xenopus intermediate pituitary. *Biochem J*. 312 (Pt 1):205-13.

Hong, W. 2005. SNAREs and traffic. *Biochim Biophys Acta*. 1744:493-517.

Hurtado-Lorenzo, A., M. Skinner, J. El Annan, M. Futai, G.H. Sun-Wada, S. Bourgoin, J. Casanova, A. Wildeman, S. Bechoua, D.A. Ausiello, D. Brown, and V. Marshansky. 2006. V-ATPase interacts with ARNO and Arf6 in early endosomes and regulates the protein degradative pathway. *Nat Cell Biol*. 8:124-36.

Jackson, M.R., T. Nilsson, and P.A. Peterson. 1990. Identification of a consensus motif for retention of transmembrane proteins in the endoplasmic reticulum. *Embo J*. 9:3153-62.

Jain, M.F.a.A.K. 2002. "Unsupervised learning of finite mixture models" *IEEE Transactions on Pattern Analysis and Machine Intelligence - PAMI*. 24:381-396.

Jamieson, J.D., and G.E. Palade. 1966. Role of the Golgi complex in the intracellular transport of secretory proteins. *Proc Natl Acad Sci U S A*. 55:424-31.

Jamieson, J.D., and G.E. Palade. 1967. Intracellular transport of secretory proteins in the pancreatic exocrine cell. I. Role of the peripheral elements of the Golgi complex. *J Cell Biol*. 34:577-96.

Jankowski, A., J.H. Kim, R.F. Collins, R. Daneman, P. Walton, and S. Grinstein. 2001. In situ measurements of the pH of mammalian peroxisomes using the fluorescent protein pHluorin. *J Biol Chem*. 276:48748-53.

Jenne, N., K. Frey, B. Brugger, and F.T. Wieland. 2002. Oligomeric state and stoichiometry of p24 proteins in the early secretory pathway. *J Biol Chem*. 277:46504-11.

Kappeler, F., D.R. Klopfenstein, M. Foguet, J.P. Paccaud, and H.P. Hauri. 1997. The recycling of ERGIC-53 in the early secretory pathway. ERGIC-53 carries a cytosolic endoplasmic reticulum-exit determinant interacting with COPII. *J Biol Chem*. 272:31801-8.

Kasap, M., S. Thomas, E. Danaher, V. Holton, S. Jiang, and B. Storrie. 2004. Dynamic nucleation of Golgi apparatus assembly from the endoplasmic reticulum in interphase hela cells. *Traffic*. 5:595-605.

Kelly, R.B. 1990. Microtubules, membrane traffic, and cell organization. *Cell*. 61:5-7.

Kim, J.H., L. Johannes, B. Goud, C. Antony, C.A. Lingwood, R. Daneman, and S. Grinstein. 1998. Noninvasive measurement of the pH of the endoplasmic reticulum at rest and during calcium release. *Proc Natl Acad Sci U S A*. 95:2997-3002.

Kim, J.H., C.A. Lingwood, D.B. Williams, W. Furuya, M.F. Manolson, and S. Grinstein. 1996. Dynamic measurement of the pH of the Golgi complex in living cells using retrograde transport of the verotoxin receptor. *J Cell Biol*. 134:1387-99.

Kirchhausen, T. 2000. Three ways to make a vesicle. *Nat Rev Mol Cell Biol*. 1:187-98.

Klumperman, J., A. Schweizer, H. Clausen, B.L. Tang, W. Hong, V. Oorschot, and H.P. Hauri. 1998. The recycling pathway of protein ERGIC-53 and dynamics of the ER-Golgi intermediate compartment. *J Cell Sci*. 111 (Pt 22):3411-25.

Kneen, M., J. Farinas, Y. Li, and A.S. Verkman. 1998. Green fluorescent protein as a noninvasive intracellular pH indicator. *Biophys J*. 74:1591-9.

Kodani, A., and C. Sutterlin. 2008. The Golgi Protein GM130 Regulates Centrosome Morphology and Function. *Mol Biol Cell*. 19:745-53.

Kornfeld, S. 1987. Trafficking of lysosomal enzymes. *Faseb J*. 1:462-8.

Kuehn, M.J., and R. Schekman. 1997. COPII and secretory cargo capture into transport vesicles. *Curr Opin Cell Biol*. 9:477-83.

Kuiper, R.P., G. Bouw, K.P. Janssen, J. Rotter, F. van Herp, and G.J. Martens. 2001. Localization of p24 putative cargo receptors in the early secretory pathway depends on the biosynthetic activity of the cell. *Biochem J*. 360:421-9.

Ladinsky, M.S., D.N. Mastronarde, J.R. McIntosh, K.E. Howell, and L.A. Staehelin. 1999. Golgi structure in three dimensions: functional insights from the normal rat kidney cell. *J Cell Biol*. 144:1135-49.

Lahtinen, U., U. Hellman, C. Wernstedt, J. Saraste, and R.F. Pettersson. 1996. Molecular cloning and expression of a 58-kDa cis-Golgi and intermediate compartment protein. *J Biol Chem*. 271:4031-7.

Langhans, M., M.J. Marcote, P. Pimpl, G. Virgili-Lopez, D.G. Robinson, and F. Aniento. 2008. In vivo Trafficking and Localization of p24 Proteins in Plant Cells. *Traffic*.

Lanoix, J., J. Ouwendijk, A. Stark, E. Szafer, D. Cassel, K. Dejgaard, M. Weiss, and T. Nilsson. 2001. Sorting of Golgi resident proteins into different subpopulations of COPI vesicles: a role for ArfGAP1. *J Cell Biol*. 155:1199-212.

Lee, M.C., and E.A. Miller. 2007. Molecular mechanisms of COPII vesicle formation. *Semin Cell Dev Biol*. 18:424-34.

Letourneur, F., E.C. Gaynor, S. Hennecke, C. Demolliere, R. Duden, S.D. Emr, H. Riezman, and P. Cosson. 1994. Coatomer is essential for retrieval of dilysine-tagged proteins to the endoplasmic reticulum. *Cell*. 79:1199-207.

Linstedt, A.D., and H.P. Hauri. 1993. Giantin, a novel conserved Golgi membrane protein containing a cytoplasmic domain of at least 350 kDa. *Mol Biol Cell*. 4:679-93.

Linstedt, A.D., A. Mehta, J. Suhan, H. Reggio, and H.P. Hauri. 1997. Sequence and overexpression of GPP130/GIMPc: evidence for saturable pH-sensitive targeting of a type II early Golgi membrane protein. *Mol Biol Cell*. 8:1073-87.

Lippincott-Schwartz, J., and N.B. Cole. 1995. Roles for microtubules and kinesin in membrane traffic between the endoplasmic reticulum and the Golgi complex. *Biochem Soc Trans*. 23:544-8.

Lippincott-Schwartz, J., N.B. Cole, A. Marotta, P.A. Conrad, and G.S. Bloom. 1995. Kinesin is the motor for microtubule-mediated Golgi-to-ER membrane traffic. *J Cell Biol*. 128:293-306.

Lippincott-Schwartz, J., J.G. Donaldson, A. Schweizer, E.G. Berger, H.P. Hauri, L.C. Yuan, and R.D. Klausner. 1990. Microtubule-dependent retrograde transport of proteins into the ER in the presence of brefeldin A suggests an ER recycling pathway. *Cell*. 60:821-36.

Lippincott-Schwartz, J., L.C. Yuan, J.S. Bonifacino, and R.D. Klausner. 1989. Rapid redistribution of Golgi proteins into the ER in cells treated with brefeldin A: evidence for membrane cycling from Golgi to ER. *Cell*. 56:801-13.

Llopis, J., J.M. McCaffery, A. Miyawaki, M.G. Farquhar, and R.Y. Tsien. 1998. Measurement of cytosolic, mitochondrial, and Golgi pH in single living cells with green fluorescent proteins. *Proc Natl Acad Sci U S A*. 95:6803-8.

Lotti, L.V., M.R. Torrisi, M.C. Pascale, and S. Bonatti. 1992. Immunocytochemical analysis of the transfer of vesicular stomatitis virus G glycoprotein from the intermediate compartment to the Golgi complex. *J Cell Biol*. 118:43-50.

Lucocq, J.M., and G. Warren. 1987. Fragmentation and partitioning of the Golgi apparatus during mitosis in HeLa cells. *Embo J*. 6:3239-46.

Luo, W., Y. Wang, and G. Reiser. 2007. p24A, a type I transmembrane protein, controls ARF1-dependent resensitization of protease-activated receptor-2 by influence on receptor trafficking. *J Biol Chem*. 282:30246-55.

Ma, D., N. Zerangue, Y.F. Lin, A. Collins, M. Yu, Y.N. Jan, and L.Y. Jan. 2001. Role of ER export signals in controlling surface potassium channel numbers. *Science*. 291:316-9.

Machen, T.E., G. Chandy, M. Wu, M. Grabe, and H.P. Moore. 2001. Cystic fibrosis transmembrane conductance regulator and H+ permeability in regulation of Golgi pH. *Jop*. 2:229-36.

Machen, T.E., M.J. Leigh, C. Taylor, T. Kimura, S. Asano, and H.P. Moore. 2003. pH of TGN and recycling endosomes of H+/K+-ATPase-transfected HEK-293 cells: implications for pH regulation in the secretory pathway. *Am J Physiol Cell Physiol*. 285:C205-14.

Majoul, I., K. Sohn, F.T. Wieland, R. Pepperkok, M. Pizza, J. Hillemann, and H.D. Soling. 1998. KDEL receptor (Erd2p)-mediated retrograde transport of the cholera toxin A subunit from the Golgi involves COPI, p23, and the COOH terminus of Erd2p. *J Cell Biol*. 143:601-12.

Majoul, I., M. Straub, S.W. Hell, R. Duden, and H.D. Soling. 2001. KDEL-cargo regulates interactions between proteins involved in COPI vesicle traffic: measurements in living cells using FRET. *Dev Cell*. 1:139-53.

Malhotra, V., and S. Mayor. 2006. Cell biology: the Golgi grows up. *Nature*. 441:939-40.

Malkus, P., F. Jiang, and R. Schekman. 2002. Concentrative sorting of secretory cargo proteins into COPII-coated vesicles. *J Cell Biol*. 159:915-21.

Malsam, J., A. Satoh, L. Pelletier, and G. Warren. 2005. Golgin tethers define subpopulations of COPI vesicles. *Science*. 307:1095-8.

Marquardt, D., and M.S. Center. 1991. Involvement of vacuolar H(+)-adenosine triphosphatase activity in multidrug resistance in HL60 cells. *J Natl Cancer Inst*. 83:1098-102.

Marsh, B.J., N. Volkmann, J.R. McIntosh, and K.E. Howell. 2004. Direct continuities between cisternae at different levels of the Golgi complex in glucose-stimulated mouse islet beta cells. *Proc Natl Acad Sci U S A*. 101:5565-70.

Marsh, M., and A. Helenius. 2006. Virus entry: open sesame. *Cell*. 124:729-40.
Martinez-Menarguez, J.A., H.J. Geuze, J.W. Slot, and J. Klumperman. 1999. Vesicular tubular clusters between the ER and Golgi mediate concentration of soluble secretory proteins by exclusion from COPI-coated vesicles. *Cell*. 98:81-90.
Martinez-Zaguilan, R., R.M. Lynch, G.M. Martinez, and R.J. Gillies. 1993. Vacuolar-type H(+)-ATPases are functionally expressed in plasma membranes of human tumor cells. *Am J Physiol*. 265:C1015-29.
Marzioch, M., D.C. Henthorn, J.M. Herrmann, R. Wilson, D.Y. Thomas, J.J. Bergeron, R.C. Solari, and A. Rowley. 1999. Erp1p and Erp2p, partners for Emp24p and Erv25p in a yeast p24 complex. *Mol Biol Cell*. 10:1923-38.
Matanis, T., A. Akhmanova, P. Wulf, E. Del Nery, T. Weide, T. Stepanova, N. Galjart, F. Grosveld, B. Goud, C.I. De Zeeuw, A. Barnekow, and C.C. Hoogenraad. 2002. Bicaudal-D regulates COPI-independent Golgi-ER transport by recruiting the dynein-dynactin motor complex. *Nat Cell Biol*. 4:986-92.
Matsuoka, K., L. Orci, M. Amherdt, S.Y. Bednarek, S. Hamamoto, R. Schekman, and T. Yeung. 1998. COPII-coated vesicle formation reconstituted with purified coat proteins and chemically defined liposomes. *Cell*. 93:263-75.
Meister, P., A. Taddei, A. Ponti, G. Baldacci, and S.M. Gasser. 2007. Replication foci dynamics: replication patterns are modulated by S-phase checkpoint kinases in fission yeast. *Embo J*. 26:1315-26.
Metchnikoff, E. 1968. Lectures on the comparative pathology of inflammation Dover Publications Inc.
Miesenbock, G., D.A. De Angelis, and J.E. Rothman. 1998. Visualizing secretion and synaptic transmission with pH-sensitive green fluorescent proteins. *Nature*. 394:192-5.
Miller, E., B. Antonny, S. Hamamoto, and R. Schekman. 2002. Cargo selection into COPII vesicles is driven by the Sec24p subunit. *Embo J*. 21:6105-13.
Miller, E.A., T.H. Beilharz, P.N. Malkus, M.C. Lee, S. Hamamoto, L. Orci, and R. Schekman. 2003. Multiple cargo binding sites on the COPII subunit Sec24p ensure capture of diverse membrane proteins into transport vesicles. *Cell*. 114:497-509.
Mironov, A.A., A.A. Mironov, Jr., G.V. Beznoussenko, A. Trucco, P. Lupetti, J.D. Smith, W.J. Geerts, A.J. Koster, K.N. Burger, M.E. Martone, T.J. Deerinck, M.H. Ellisman, and A. Luini. 2003. ER-to-Golgi carriers arise through direct en bloc protrusion and multistage maturation of specialized ER exit domains. *Dev Cell*. 5:583-94.
Mitrovic, S., H. Ben-Tekaya, E. Koegler, J. Gruenberg, and H.P. Hauri. 2008. The Cargo Receptors Surf4, ERGIC-53 and p25 are Required to Maintain the Architecture of ERGIC and Golgi. *Mol Biol Cell*.
Mollenhauer, H.H., D.J. Morre, and L.D. Rowe. 1990. Alteration of intracellular traffic by monensin; mechanism, specificity and relationship to toxicity. *Biochim Biophys Acta*. 1031:225-46.
Mossessova, E., L.C. Bickford, and J. Goldberg. 2003. SNARE selectivity of the COPII coat. *Cell*. 114:483-95.
Moyer, B.D., B.B. Allan, and W.E. Balch. 2001. Rab1 interaction with a GM130 effector complex regulates COPII vesicle cis--Golgi tethering. *Traffic*. 2:268-76.

Muniz, M., C. Nuoffer, H.P. Hauri, and H. Riezman. 2000. The Emp24 complex recruits a specific cargo molecule into endoplasmic reticulum-derived vesicles. *J Cell Biol*. 148:925-30.

Myers, M., and M. Forgac. 1993. Assembly of the peripheral domain of the bovine vacuolar H(+)-adenosine triphosphatase. *J Cell Physiol*. 156:35-42.

Nakamura, N., C. Rabouille, R. Watson, T. Nilsson, N. Hui, P. Slusarewicz, T.E. Kreis, and G. Warren. 1995. Characterization of a cis-Golgi matrix protein, GM130. *J Cell Biol*. 131:1715-26.

Nelson, D.S., C. Alvarez, Y.S. Gao, R. Garcia-Mata, E. Fialkowski, and E. Sztul. 1998. The membrane transport factor TAP/p115 cycles between the Golgi and earlier secretory compartments and contains distinct domains required for its localization and function. *J Cell Biol*. 143:319-31.

Nichols, W.C., U. Seligsohn, A. Zivelin, V.H. Terry, C.E. Hertel, M.A. Wheatley, M.J. Moussalli, H.P. Hauri, N. Ciavarella, R.J. Kaufman, and D. Ginsburg. 1998. Mutations in the ER-Golgi intermediate compartment protein ERGIC-53 cause combined deficiency of coagulation factors V and VIII. *Cell*. 93:61-70.

Nickel, W., K. Sohn, C. Bunning, and F.T. Wieland. 1997. p23, a major COPI-vesicle membrane protein, constitutively cycles through the early secretory pathway. *Proc Natl Acad Sci U S A*. 94:11393-8.

Nishi, T., and M. Forgac. 2002. The vacuolar (H+)-ATPases--nature's most versatile proton pumps. *Nat Rev Mol Cell Biol*. 3:94-103.

Nishimura, N., and W.E. Balch. 1997. A di-acidic signal required for selective export from the endoplasmic reticulum. *Science*. 277:556-8.

Nishimura, N., S. Bannykh, S. Slabough, J. Matteson, Y. Altschuler, K. Hahn, and W.E. Balch. 1999. A di-acidic (DXE) code directs concentration of cargo during export from the endoplasmic reticulum. *J Biol Chem*. 274:15937-46.

Novick, P., S. Ferro, and R. Schekman. 1981. Order of events in the yeast secretory pathway. *Cell*. 25:461-9.

Novick, P., C. Field, and R. Schekman. 1980. Identification of 23 complementation groups required for post-translational events in the yeast secretory pathway. *Cell*. 21:205-15.

Nufer, O., S. Guldbrandsen, M. Degen, F. Kappeler, J.P. Paccaud, K. Tani, and H.P. Hauri. 2002. Role of cytoplasmic C-terminal amino acids of membrane proteins in ER export. *J Cell Sci*. 115:619-28.

Nyfeler, B., V. Reiterer, M.W. Wendeler, E. Stefan, B. Zhang, S.W. Michnick, and H.P. Hauri. 2008. Identification of ERGIC-53 as an intracellular transport receptor of alpha1-antitrypsin. *J Cell Biol*. 180:705-12.

Ohkuma, S., and B. Poole. 1978. Fluorescence probe measurement of the intralysosomal pH in living cells and the perturbation of pH by various agents. *Proc Natl Acad Sci U S A*. 75:3327-31.

Orci, L., B.S. Glick, and J.E. Rothman. 1986. A new type of coated vesicular carrier that appears not to contain clathrin: its possible role in protein transport within the Golgi stack. *Cell*. 46:171-84.

Orci, L., M. Ravazzola, M.J. Storch, R.G. Anderson, J.D. Vassalli, and A. Perrelet. 1987. Proteolytic maturation of insulin is a post-Golgi event which occurs in acidifying clathrin-coated secretory vesicles. *Cell*. 49:865-8.

Orlowski, J., and S. Grinstein. 2007. Emerging roles of alkali cation/proton exchangers in organellar homeostasis. *Curr Opin Cell Biol*. 19:483-92.

Otte, S., and C. Barlowe. 2004. Sorting signals can direct receptor-mediated export of soluble proteins into COPII vesicles. *Nat Cell Biol*. 6:1189-94.

Palade, G. 1975. Intracellular aspects of the process of protein synthesis. *Science*. 189:347-58.

Palmer, K.J., P. Watson, and D.J. Stephens. 2005. The role of microtubules in transport between the endoplasmic reticulum and Golgi apparatus in mammalian cells. *Biochem Soc Symp*:1-13.

Palokangas, H., K. Metsikko, and K. Vaananen. 1994. Active vacuolar H+ATPase is required for both endocytic and exocytic processes during viral infection of BHK-21 cells. *J Biol Chem*. 269:17577-85.

Palokangas, H., M. Ying, K. Vaananen, and J. Saraste. 1998. Retrograde transport from the pre-Golgi intermediate compartment and the Golgi complex is affected by the vacuolar H+-ATPase inhibitor bafilomycin A1. *Mol Biol Cell*. 9:3561-78.

Paroutis, P., N. Touret, and S. Grinstein. 2004. The pH of the secretory pathway: measurement, determinants, and regulation. *Physiology (Bethesda)*. 19:207-15.

Patient, R., C. Hourioux, P.Y. Sizaret, S. Trassard, C. Sureau, and P. Roingeard. 2007. Hepatitis B virus subviral envelope particle morphogenesis and intracellular trafficking. *J Virol*. 81:3842-51.

Patterson, G.H., K. Hirschberg, R.S. Polishchuk, D. Gerlich, R.D. Phair, and J. Lippincott-Schwartz. 2008. Transport through the Golgi apparatus by rapid partitioning within a two-phase membrane system. *Cell*. 133:1055-67.

Paulhe, F., B.A. Imhof, and B. Wehrle-Haller. 2004. A specific endoplasmic reticulum export signal drives transport of stem cell factor (Kitl) to the cell surface. *J Biol Chem*. 279:55545-55.

Pepperkok, R., J. Scheel, H. Horstmann, H.P. Hauri, G. Griffiths, and T.E. Kreis. 1993. Beta-COP is essential for biosynthetic membrane transport from the endoplasmic reticulum to the Golgi complex in vivo. *Cell*. 74:71-82.

Ponti, A., A. Matov, M. Adams, S. Gupton, C.M. Waterman-Storer, and G. Danuser. 2005. Periodic patterns of actin turnover in lamellipodia and lamellae of migrating epithelial cells analyzed by quantitative Fluorescent Speckle Microscopy. *Biophys J*. 89:3456-69.

Poschet, J.F., J.C. Boucher, L. Tatterson, J. Skidmore, R.W. Van Dyke, and V. Deretic. 2001. Molecular basis for defective glycosylation and Pseudomonas pathogenesis in cystic fibrosis lung. *Proc Natl Acad Sci U S A*. 98:13972-7.

Poschet, J.F., J. Skidmore, J.C. Boucher, A.M. Firoved, R.W. Van Dyke, and V. Deretic. 2002. Hyperacidification of cellubrevin endocytic compartments and defective endosomal recycling in cystic fibrosis respiratory epithelial cells. *J Biol Chem*. 277:13959-65.

Presley, J.F., N.B. Cole, T.A. Schroer, K. Hirschberg, K.J. Zaal, and J. Lippincott-Schwartz. 1997. ER-to-Golgi transport visualized in living cells. *Nature*. 389:81-5.

Puri, S., C. Bachert, C.J. Fimmel, and A.D. Linstedt. 2002. Cycling of early Golgi proteins via the cell surface and endosomes upon lumenal pH disruption. *Traffic*. 3:641-53.

Puri, S., and A.D. Linstedt. 2003. Capacity of the golgi apparatus for biogenesis from the endoplasmic reticulum. *Mol Biol Cell*. 14:5011-8.

Puthenveedu, M.A., C. Bachert, S. Puri, F. Lanni, and A.D. Linstedt. 2006. GM130 and GRASP65-dependent lateral cisternal fusion allows uniform Golgi-enzyme distribution. *Nat Cell Biol*. 8:238-48.

Puthenveedu, M.A., and A.D. Linstedt. 2004. Gene replacement reveals that p115/SNARE interactions are essential for Golgi biogenesis. *Proc Natl Acad Sci U S A*. 101:1253-6.

Qi, J., Y. Wang, and M. Forgac. 2007. The vacuolar (H(+))-ATPase: subunit arrangement and in vivo regulation. *J Bioenerg Biomembr*.

Recchi, C., and P. Chavrier. 2006. V-ATPase: a potential pH sensor. *Nat Cell Biol*. 8:107-9.

Reinhard, C., C. Harter, M. Bremser, B. Brugger, K. Sohn, J.B. Helms, and F. Wieland. 1999. Receptor-induced polymerization of coatomer. *Proc Natl Acad Sci U S A*. 96:1224-8.

Rojo, M., G. Emery, V. Marjomaki, A.W. McDowall, R.G. Parton, and J. Gruenberg. 2000. The transmembrane protein p23 contributes to the organization of the Golgi apparatus. *J Cell Sci*. 113 (Pt 6):1043-57.

Rojo, M., R. Pepperkok, G. Emery, R. Kellner, E. Stang, R.G. Parton, and J. Gruenberg. 1997. Involvement of the transmembrane protein p23 in biosynthetic protein transport. *J Cell Biol*. 139:1119-35.

Rosing, M., E. Ossendorf, A. Rak, and A. Barnekow. 2007. Giantin interacts with both the small GTPase Rab6 and Rab1. *Exp Cell Res*. 313:2318-25.

Rothman, J.E. 1994. Mechanisms of intracellular protein transport. *Nature*. 372:55-63.

Sacher, M., Y. Jiang, J. Barrowman, A. Scarpa, J. Burston, L. Zhang, D. Schieltz, J.R. Yates, 3rd, H. Abeliovich, and S. Ferro-Novick. 1998. TRAPP, a highly conserved novel complex on the cis-Golgi that mediates vesicle docking and fusion. *Embo J*. 17:2494-503.

Saraste, J., and E. Kuismanen. 1984. Pre- and post-Golgi vacuoles operate in the transport of Semliki Forest virus membrane glycoproteins to the cell surface. *Cell*. 38:535-49.

Saraste, J., and K. Svensson. 1991. Distribution of the intermediate elements operating in ER to Golgi transport. *J Cell Sci*. 100 (Pt 3):415-30.

Sato, K., and A. Nakano. 2007. Mechanisms of COPII vesicle formation and protein sorting. *FEBS Lett*. 581:2076-82.

Scales, S.J., R. Pepperkok, and T.E. Kreis. 1997. Visualization of ER-to-Golgi transport in living cells reveals a sequential mode of action for COPII and COPI. *Cell*. 90:1137-48.

Schapiro, F.B., and S. Grinstein. 2000. Determinants of the pH of the Golgi complex. *J Biol Chem*. 275:21025-32.

Schekman, R. 2002. Lasker Basic Medical Research Award. SEC mutants and the secretory apparatus. *Nat Med*. 8:1055-8.

Schimmoller, F., B. Singer-Kruger, S. Schroder, U. Kruger, C. Barlowe, and H. Riezman. 1995. The absence of Emp24p, a component of ER-derived COPII-coated vesicles, causes a defect in transport of selected proteins to the Golgi. *Embo J*. 14:1329-39.

Schindler, R., C. Itin, M. Zerial, F. Lottspeich, and H.P. Hauri. 1993. ERGIC-53, a membrane protein of the ER-Golgi intermediate compartment, carries an ER retention motif. *Eur J Cell Biol*. 61:1-9.

Schmidt, W.K., and H.P. Moore. 1995. Ionic milieu controls the compartment-specific activation of pro-opiomelanocortin processing in AtT-20 cells. *Mol Biol Cell*. 6:1271-85.

Schoonderwoert, V.T., and G.J. Martens. 2001. Proton pumping in the secretory pathway. *J Membr Biol*. 182:159-69.

Schweizer, A., J.A. Fransen, T. Bachi, L. Ginsel, and H.P. Hauri. 1988. Identification, by a monoclonal antibody, of a 53-kD protein associated with a tubulo-vesicular compartment at the cis-side of the Golgi apparatus. *J Cell Biol*. 107:1643-53.

Schweizer, A., J.A. Fransen, K. Matter, T.E. Kreis, L. Ginsel, and H.P. Hauri. 1990. Identification of an intermediate compartment involved in protein transport from endoplasmic reticulum to Golgi apparatus. *Eur J Cell Biol*. 53:185-96.

Seksek, O., J. Biwersi, and A.S. Verkman. 1995. Direct measurement of trans-Golgi pH in living cells and regulation by second messengers. *J Biol Chem*. 270:4967-70.

Seksek, O., J. Biwersi, and A.S. Verkman. 1996. Evidence against defective trans-Golgi acidification in cystic fibrosis. *J Biol Chem*. 271:15542-8.

Semenza, J.C., K.G. Hardwick, N. Dean, and H.R. Pelham. 1990. ERD2, a yeast gene required for the receptor-mediated retrieval of luminal ER proteins from the secretory pathway. *Cell*. 61:1349-57.

Serafini, T., L. Orci, M. Amherdt, M. Brunner, R.A. Kahn, and J.E. Rothman. 1991. ADP-ribosylation factor is a subunit of the coat of Golgi-derived COP-coated vesicles: a novel role for a GTP-binding protein. *Cell*. 67:239-53.

Sesso, A., F.P. de Faria, E.S. Iwamura, and H. Correa. 1994. A three-dimensional reconstruction study of the rough ER-Golgi interface in serial thin sections of the pancreatic acinar cell of the rat. *J Cell Sci*. 107 (Pt 3):517-28.

Shestakova, A., E. Suvorova, O. Pavliv, G. Khaidakova, and V. Lupashin. 2007. Interaction of the conserved oligomeric Golgi complex with t-SNARE Syntaxin5a/Sed5 enhances intra-Golgi SNARE complex stability. *J Cell Biol*. 179:1179-92.

Shima, D.T., S.J. Scales, T.E. Kreis, and R. Pepperkok. 1999. Segregation of COPI-rich and anterograde-cargo-rich domains in endoplasmic-reticulum-to-Golgi transport complexes. *Curr Biol*. 9:821-4.

Short, B., A. Haas, and F.A. Barr. 2005. Golgins and GTPases, giving identity and structure to the Golgi apparatus. *Biochim Biophys Acta*. 1744:383-95.

Short, B., C. Preisinger, R. Korner, R. Kopajtich, O. Byron, and F.A. Barr. 2001. A GRASP55-rab2 effector complex linking Golgi structure to membrane traffic. *J Cell Biol*. 155:877-83.

Shugrue, C.A., E.R. Kolen, H. Peters, A. Czernik, C. Kaiser, L. Matovcik, A.L. Hubbard, and F. Gorelick. 1999. Identification of the putative mammalian orthologue of Sec31P, a component of the COPII coat. *J Cell Sci*. 112 (Pt 24):4547-56.

Simpson, J.C., T. Nilsson, and R. Pepperkok. 2006. Biogenesis of tubular ER-to-Golgi transport intermediates. *Mol Biol Cell*. 17:723-37.

Singer-Kruger, B., R. Frank, F. Crausaz, and H. Riezman. 1993. Partial purification and characterization of early and late endosomes from yeast. Identification of four novel proteins. *J Biol Chem*. 268:14376-86.

Smith, A.E., and A. Helenius. 2004. How viruses enter animal cells. *Science*. 304:237-42.

Smith, R.F., and T.F. Smith. 1990. Automatic generation of primary sequence patterns from sets of related protein sequences. *Proc Natl Acad Sci U S A*. 87:118-22.

Sohda, M., Y. Misumi, S. Yoshimura, N. Nakamura, T. Fusano, S. Sakisaka, S. Ogata, J. Fujimoto, N. Kiyokawa, and Y. Ikehara. 2005. Depletion of vesicle-tethering factor p115 causes mini-stacked Golgi fragments with delayed protein transport. *Biochem Biophys Res Commun*. 338:1268-74.

Sohn, K., L. Orci, M. Ravazzola, M. Amherdt, M. Bremser, F. Lottspeich, K. Fiedler, J.B. Helms, and F.T. Wieland. 1996. A major transmembrane protein of Golgi-derived COPI-coated vesicles involved in coatomer binding. *J Cell Biol*. 135:1239-48.

Sollner, T., S.W. Whiteheart, M. Brunner, H. Erdjument-Bromage, S. Geromanos, P. Tempst, and J.E. Rothman. 1993. SNAP receptors implicated in vesicle targeting and fusion. *Nature*. 362:318-24.

Sonnichsen, B., M. Lowe, T. Levine, E. Jamsa, B. Dirac-Svejstrup, and G. Warren. 1998. A role for giantin in docking COPI vesicles to Golgi membranes. *J Cell Biol*. 140:1013-21.

Springer, S., E. Chen, R. Duden, M. Marzioch, A. Rowley, S. Hamamoto, S. Merchant, and R. Schekman. 2000. The p24 proteins are not essential for vesicular transport in Saccharomyces cerevisiae. *Proc Natl Acad Sci U S A*. 97:4034-9.

Springer, S., A. Spang, and R. Schekman. 1999. A primer on vesicle budding. *Cell*. 97:145-8.

Stagg, S.M., C. Gurkan, D.M. Fowler, P. LaPointe, T.R. Foss, C.S. Potter, B. Carragher, and W.E. Balch. 2006. Structure of the Sec13/31 COPII coat cage. *Nature*. 439:234-8.

Stamnes, M.A., M.W. Craighead, M.H. Hoe, N. Lampen, S. Geromanos, P. Tempst, and J.E. Rothman. 1995. An integral membrane component of coatomer-coated transport vesicles defines a family of proteins involved in budding. *Proc Natl Acad Sci U S A*. 92:8011-5.

Stauber, T., J.C. Simpson, R. Pepperkok, and I. Vernos. 2006. A role for kinesin-2 in COPI-dependent recycling between the ER and the Golgi complex. *Curr Biol*. 16:2245-51.

Stephens, D.J., N. Lin-Marq, A. Pagano, R. Pepperkok, and J.P. Paccaud. 2000. COPI-coated ER-to-Golgi transport complexes segregate from COPII in close proximity to ER exit sites. *J Cell Sci*. 113 (Pt 12):2177-85.

Stephens, D.J., and R. Pepperkok. 2001. Illuminating the secretory pathway: when do we need vesicles? *J Cell Sci*. 114:1053-9.

Stern, P.H. 1977. Ionophores. Chemistry, physiology and potential applications to bone biology. *Clin Orthop Relat Res*:273-98.

Stevens, T.H., and M. Forgac. 1997. Structure, function and regulation of the vacuolar (H+)-ATPase. *Annu Rev Cell Dev Biol*. 13:779-808.

Strating, J.R., G. Bouw, T.G. Hafmans, and G.J. Martens. 2007. Disparate effects of p24alpha and p24delta on secretory protein transport and processing. *PLoS ONE*. 2:e704.

Styers, M.L., A.K. O'Connor, R. Grabski, E. Cormet-Boyaka, and E. Sztul. 2008. Depletion of beta-COP reveals a role for COP-I in compartmentalization of secretory compartments and in biosynthetic transport of caveolin-1. *Am J Physiol Cell Physiol*. 294:C1485-98.

Sun-Wada, G.H., T. Toyomura, Y. Murata, A. Yamamoto, M. Futai, and Y. Wada. 2006. The a3 isoform of V-ATPase regulates insulin secretion from pancreatic beta-cells. *J Cell Sci*. 119:4531-40.

Sutterlin, C., R. Polishchuk, M. Pecot, and V. Malhotra. 2005. The Golgi-associated protein GRASP65 regulates spindle dynamics and is essential for cell division. *Mol Biol Cell*. 16:3211-22.

Sutton, R.B., D. Fasshauer, R. Jahn, and A.T. Brunger. 1998. Crystal structure of a SNARE complex involved in synaptic exocytosis at 2.4 A resolution. *Nature*. 395:347-53.

Szatkowski, M.S., and R.C. Thomas. 1986. New method for calculating pHi from accurately measured changes in pHi induced by a weak acid and base. *Pflugers Arch*. 407:59-63.

Sztul, E., and V. Lupashin. 2006. Role of tethering factors in secretory membrane traffic. *Am J Physiol Cell Physiol*. 290:C11-26.

Teter, K., G. Chandy, B. Quinones, K. Pereyra, T. Machen, and H.P. Moore. 1998. Cellubrevin-targeted fluorescence uncovers heterogeneity in the recycling endosomes. *J Biol Chem*. 273:19625-33.

Touchot, N., P. Chardin, and A. Tavitian. 1987. Four additional members of the ras gene superfamily isolated by an oligonucleotide strategy: molecular cloning of YPT-related cDNAs from a rat brain library. *Proc Natl Acad Sci U S A*. 84:8210-4.

Trucco, A., R.S. Polishchuk, O. Martella, A. Di Pentima, A. Fusella, D. Di Giandomenico, E. San Pietro, G.V. Beznoussenko, E.V. Polishchuk, M. Baldassarre, R. Buccione, W.J. Geerts, A.J. Koster, K.N. Burger, A.A. Mironov, and A. Luini. 2004. Secretory traffic triggers the formation of tubular continuities across Golgi sub-compartments. *Nat Cell Biol*. 6:1071-81.

Tycko, B., and F.R. Maxfield. 1982. Rapid acidification of endocytic vesicles containing alpha 2-macroglobulin. *Cell*. 28:643-51.

Uchiyama, K., G. Totsukawa, M. Puhka, Y. Kaneko, E. Jokitalo, I. Dreveny, F. Beuron, X. Zhang, P. Freemont, and H. Kondo. 2006. p37 is a p97 adaptor required for Golgi and ER biogenesis in interphase and at the end of mitosis. *Dev Cell*. 11:803-16.

Vaisberg, E.A., P.M. Grissom, and J.R. McIntosh. 1996. Mammalian cells express three distinct dynein heavy chains that are localized to different cytoplasmic organelles. *J Cell Biol*. 133:831-42.

Veizis, I.E., and C.U. Cotton. 2007. Role of kidney chloride channels in health and disease. *Pediatr Nephrol*. 22:770-7.

Vetrivel, K.S., P. Gong, J.W. Bowen, H. Cheng, Y. Chen, M. Carter, P.D. Nguyen, L. Placanica, F.T. Wieland, Y.M. Li, M.Z. Kounnas, and G. Thinakaran. 2007. Dual roles of the transmembrane protein p23/TMP21 in the modulation of amyloid precursor protein metabolism. *Mol Neurodegener*. 2:4.

Vollenweider, F., F. Kappeler, C. Itin, and H.P. Hauri. 1998. Mistargeting of the lectin ERGIC-53 to the endoplasmic reticulum of HeLa cells impairs the secretion of a lysosomal enzyme. *J Cell Biol*. 142:377-89.

Votsmeier, C., and D. Gallwitz. 2001. An acidic sequence of a putative yeast Golgi membrane protein binds COPII and facilitates ER export. *Embo J*. 20:6742-50.

Wada, I., D. Rindress, P.H. Cameron, W.J. Ou, J.J. Doherty, 2nd, D. Louvard, A.W. Bell, D. Dignard, D.Y. Thomas, and J.J. Bergeron. 1991. SSR alpha and associated calnexin are major calcium binding proteins of the endoplasmic reticulum membrane. *J Biol Chem*. 266:19599-610.

Walch-Solimena, C., R. Jahn, and T.C. Sudhof. 1993. Synaptic vesicle proteins in exocytosis: what do we know? *Curr Opin Neurobiol*. 3:329-36.

Walter, P., and G. Blobel. 1981. Translocation of proteins across the endoplasmic reticulum III. Signal recognition protein (SRP) causes signal sequence-dependent and site-specific arrest of chain elongation that is released by microsomal membranes. *J Cell Biol*. 91:557-61.

Wang, H., and M.G. Kazanietz. 2002. Chimaerins, novel non-protein kinase C phorbol ester receptors, associate with Tmp21-I (p23): evidence for a novel anchoring mechanism involving the chimaerin C1 domain. *J Biol Chem*. 277:4541-50.

Warren, G., and I. Mellman. 1999. Bulk flow redux? *Cell*. 98:125-7.

Waterman-Storer, C.M., and E.D. Salmon. 1998. Endoplasmic reticulum membrane tubules are distributed by microtubules in living cells using three distinct mechanisms. *Curr Biol*. 8:798-806.

Waters, M.G., D.O. Clary, and J.E. Rothman. 1992. A novel 115-kD peripheral membrane protein is required for intercisternal transport in the Golgi stack. *J Cell Biol*. 118:1015-26.

Waters, M.G., and S.R. Pfeffer. 1999. Membrane tethering in intracellular transport. *Curr Opin Cell Biol*. 11:453-9.

Watson, P., R. Forster, K.J. Palmer, R. Pepperkok, and D.J. Stephens. 2005. Coupling of ER exit to microtubules through direct interaction of COPII with dynactin. *Nat Cell Biol*. 7:48-55.

Watson, P., A.K. Townley, P. Koka, K.J. Palmer, and D.J. Stephens. 2006. Sec16 defines endoplasmic reticulum exit sites and is required for secretory cargo export in mammalian cells. *Traffic*. 7:1678-87.

Weisz, O.A. 2003. Organelle acidification and disease. *Traffic*. 4:57-64.

Wen, C., and I. Greenwald. 1999. p24 proteins and quality control of LIN-12 and GLP-1 trafficking in Caenorhabditis elegans. *J Cell Biol*. 145:1165-75.

Wendeler, M.W., O. Nufer, and H.P. Hauri. 2007a. Improved maturation of CFTR by an ER export signal. *Faseb J*. 21:2352-8.

Wendeler, M.W., J.P. Paccaud, and H.P. Hauri. 2007b. Role of Sec24 isoforms in selective export of membrane proteins from the endoplasmic reticulum. *EMBO Rep*. 8:258-64.

White, J., L. Johannes, F. Mallard, A. Girod, S. Grill, S. Reinsch, P. Keller, B. Tzschaschel, A. Echard, B. Goud, and E.H. Stelzer. 1999. Rab6 coordinates a novel Golgi to ER retrograde transport pathway in live cells. *J Cell Biol*. 147:743-60.

Wieland, F.T., M.L. Gleason, T.A. Serafini, and J.E. Rothman. 1987. The rate of bulk flow from the endoplasmic reticulum to the cell surface. *Cell*. 50:289-300.

Wilson, D.W., M.J. Lewis, and H.R. Pelham. 1993. pH-dependent binding of KDEL to its receptor in vitro. *J Biol Chem*. 268:7465-8.

Wrong, O.M., A.G. Norden, and T.G. Feest. 1994. Dent's disease; a familial proximal renal tubular syndrome with low-molecular-weight proteinuria, hypercalciuria, nephrocalcinosis, metabolic bone disease, progressive renal failure and a marked male predominance. *Qjm*. 87:473-93.

Wu, M.M., M. Grabe, S. Adams, R.Y. Tsien, H.P. Moore, and T.E. Machen. 2001. Mechanisms of pH regulation in the regulated secretory pathway. *J Biol Chem*. 276:33027-35.

Wu, M.M., J. Llopis, S. Adams, J.M. McCaffery, M.S. Kulomaa, T.E. Machen, H.P. Moore, and R.Y. Tsien. 2000. Organelle pH studies using targeted avidin and fluorescein-biotin. *Chem Biol*. 7:197-209.

Yamashiro, D.J., and F.R. Maxfield. 1987a. Acidification of morphologically distinct endosomes in mutant and wild-type Chinese hamster ovary cells. *J Cell Biol*. 105:2723-33.

Yamashiro, D.J., and F.R. Maxfield. 1987b. Kinetics of endosome acidification in mutant and wild-type Chinese hamster ovary cells. *J Cell Biol*. 105:2713-21.

Ye, B., Y. Zhang, W. Song, S.H. Younger, L.Y. Jan, and Y.N. Jan. 2007. Growing dendrites and axons differ in their reliance on the secretory pathway. *Cell*. 130:717-29.

Yilla, M., A. Tan, K. Ito, K. Miwa, and H.L. Ploegh. 1993. Involvement of the vacuolar H(+)-ATPases in the secretory pathway of HepG2 cells. *J Biol Chem*. 268:19092-100.

Ying, M., T. Flatmark, and J. Saraste. 2000. The p58-positive pre-golgi intermediates consist of distinct subpopulations of particles that show differential binding of COPI and COPII coats and contain vacuolar H(+)-ATPase. *J Cell Sci*. 113 (Pt 20):3623-38.

Zerangue, N., M.J. Malan, S.R. Fried, P.F. Dazin, Y.N. Jan, L.Y. Jan, and B. Schwappach. 2001. Analysis of endoplasmic reticulum trafficking signals by combinatorial screening in mammalian cells. *Proc Natl Acad Sci U S A*. 98:2431-6.

Zeuschner, D., W.J. Geerts, E. van Donselaar, B.M. Humbel, J.W. Slot, A.J. Koster, and J. Klumperman. 2006. Immuno-electron tomography of ER exit sites reveals the existence of free COPII-coated transport carriers. *Nat Cell Biol*. 8:377-83.

Zeuzem, S., P. Feick, P. Zimmermann, W. Haase, R.A. Kahn, and I. Schulz. 1992. Intravesicular acidification correlates with binding of ADP-ribosylation factor to microsomal membranes. *Proc Natl Acad Sci U S A*. 89:6619-23.

Zolov, S.N., and V.V. Lupashin. 2005. Cog3p depletion blocks vesicle-mediated Golgi retrograde trafficking in HeLa cells. *J Cell Biol*. 168:747-59.

Zuker, M. 2003. Mfold web server for nucleic acid folding and hybridization prediction. *Nucleic Acids Res*. 31:3406-15.